Probabilistic analysis of typhoon induced hydraulic boundary conditions for Suo-nada Bay

by

Elwyn N. Klaver

Graduation committee:

Prof.drs.ir. J.K. Vrijling   (DUT, Chairman)
Dr.ir. P.H.A.J.M. van Gelder (DUT)
Dr.ir. L.H. Holthuijsen   (DUT)
Ir. S.N. Jonkman   (DUT, MTPWWM)
Dr. S. Takahashi   (PARI)
Mr. H. Kawai   (PARI)

Student:

Student: E.N. Klaver
Address: Visstraat 54a
              2611 JX, Delft
Phone: 0641215151
Email: enklaver@gmail.com
Student no.: 1005014

Cooperative research

Cover: Typhoon Jelawat (august 2000) above the Chinese Sea with Suo-nada Bay in the northeast corner
(www.gsfc.nasa.gov)

Preface

This thesis is done in completion of my study Civil Engineering at the Faculty of Civil Engineering and Geosciences, Delft University of Technology. The thesis is written for the section of Hydraulic and Geotechnical Engineering, specialisation Structural Hydraulic Engineering and Probabilistic Design.

The thesis is a result of a cooperative research of Delft University of Technology, the Port and Airport research Institute in Japan and the Dutch Ministry of Transport, Public Works and Water Management. It describes a method to determine the probabilistic properties of the hydraulic boundary conditions for a bay in Japan. These hydraulic boundary conditions consist of the typhoon related high water levels and waves. The research was carried out at the Dutch Ministry of Transport, Public Works and Water Management.

I would like to thank members of my graduation committee for their support and advice during the realisation of this thesis:

Prof.drs.ir. J.K. Vrijling	(Delft University of Technology)
Dr.ir. P.H.A.J.M. van Gelder	(Delft University of Technology)
Dr.ir. L.H. Holthuijsen	(Delft University of Technology)
Ir. S.N. Jonkman	(Delft University of Technology; Ministry of Transport, Public Works and Water Management)
Dr. S. Takahashi	(Port and Airport Research Institute)
Mr. H. Kawai	(Port and Airport Research Institute)

Further, I would like to thank my colleague students at the Dutch Ministry of Transport, Public Works and Water Management, my family and my friends for their help and support during the past months.

Elwyn Klaver
Delft, November 2005

Executive summary

Introduction
The 18th typhoon in the year 1999 struck western Japan, resulting in the flooding of a number of areas and killing 12 people. Not since the Ise Bay typhoon of 1959 had such a major typhoon-related disaster occurred in Japan. The disaster is the motive to review the current design of the Japanese coastal defence system.
The current design of the coastal defence system is based on a deterministic analysis of the water level and the wave characteristics. The determination of the water level is based on the maximum total water level ever recorded or on the sum of the design meteorological tide level and design astronomical tide level. In the first case the return period is not clear. In the second case, the meteorological tide is determined with typhoon modelling, but criteria for the determination of the typhoon parameters lack. The design wave conditions are based on a statistical analysis of extreme events. The simultaneous occurrence of high water level and high waves is not taken into account. The objective of the research is to obtain the marginal and joint probability distributions of the hydraulic variables based on the joint occurrence of the tidal water level, the typhoon induced storm surge level and the typhoon induced wave characteristics.

Approach
Extrapolating the observed data and their correlations into regions of low probability of occurrence where observations are not available can be done based on fully statistical methods and on a method that combines physics and statistics. The last method is used in this research, because a small amount of observations of the hydraulic variables is available and more reliable statistics of physical variables related to the hydraulic variables can be used in this method. Further, the physical boundaries are taken into account in the extrapolation and global knowledge of the physical behaviour of hydraulic variables is included. A Monte Carlo simulation is used in this research to derive the extreme hydraulic boundary conditions with low probabilities of exceedance, since a number of input variables can be included in the method easily. Numerical models are not used because of the increase in calculation time due to the number of simulations used in a Monte Carlo analysis. With respect to the combined method the insight in the basic relations between the physical variables could be lost if numerical models are used. The relevant physical phenomena are therefore described with simple analytical formulae. This approach will only result in a first order approximation of the values of the hydraulic boundary conditions. Refinement of these models is possible.

Relevant physical phenomena and their models
Since the physical origin of all typhoon-related phenomena can be found in the atmospheric pressure and the (resulting) wind field of the typhoon, the description of the typhoon field is necessary. Besides, the input distributions of the typhoon characteristics are based on a relatively long period of observations compared to the hydraulic variables. The high water levels are the result of typhoon induced storm surges and the tidal water level. The pressure set-up and the wind set-up are the main contributions to the storm surge phenomenon. The locally wind-generated waves are important during a typhoon event. Swell is not taken into account separately.
There are several analytical models that describe the physical phenomena. Some of the models are reviewed and a choice is made which models are used in the research. The pressure set-up is proportional to the central pressure depth of the typhoon field. The gradient and surface wind speed can be derived from the pressure

distribution and the forward movement of the typhoon field. The wind set-up, applicable to water bodies with limited water depth, is described with a model using the quadratic wind speed. The wave height and the wave period are calculated with the Sverdrupp Munk and Brettschneider model. The wave period is also determined with a wave steepness model. The total model with the mutual relations is given in Figure 1-1. The model is applied in deterministic and probabilistic analyses of typhoons.
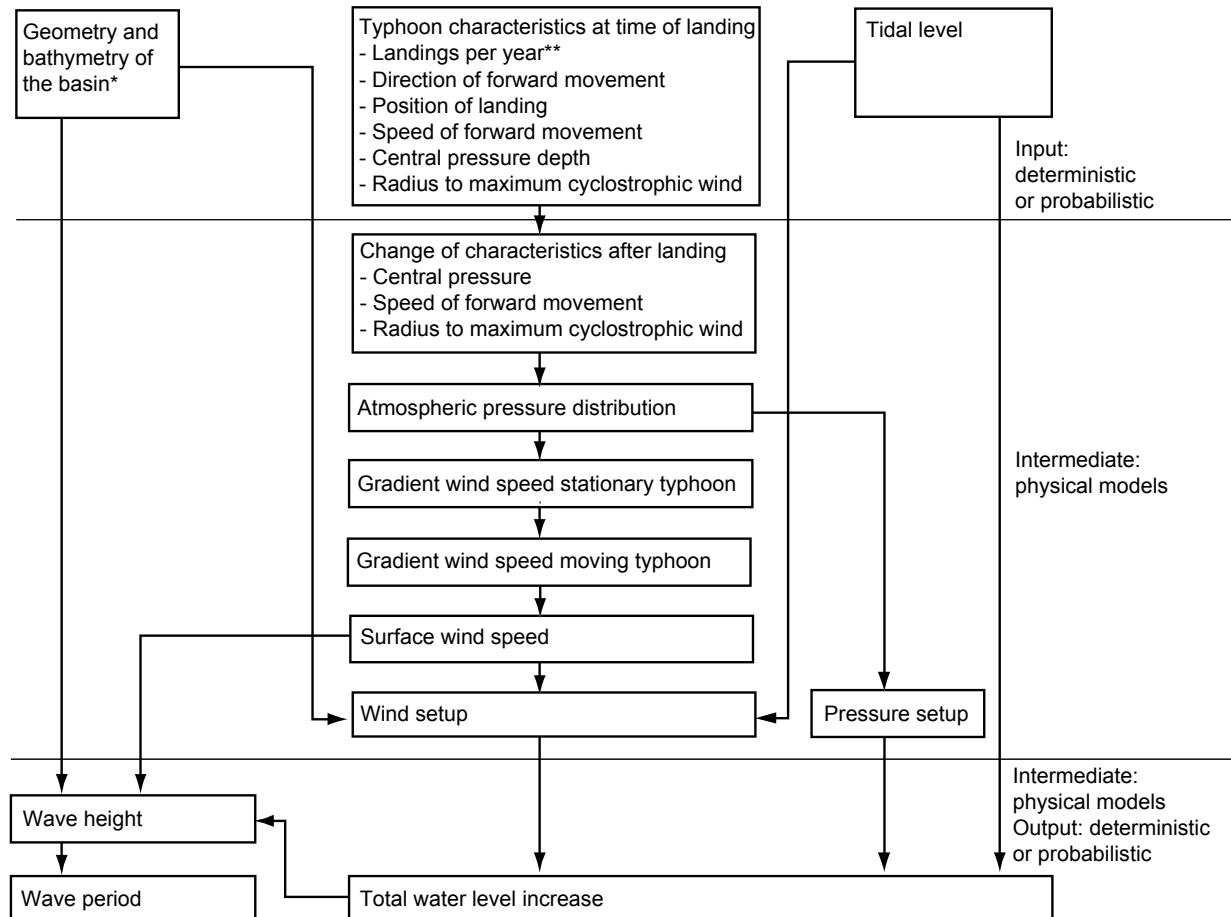

Figure 1-1: Model used for deterministic and probabilistic modelling of typhoons
* In both cases only deterministic values used; ** Only used in probabilistic modelling

<u>Deterministic calibration of the combined model</u>
The storm surge, the wave height and the wave period models are calibrated for a case site in Suo-nada Bay, since various values for constants of different formulae are given in literature and several assumptions in modelling have been done. The Port of Kanda at the west end of the bay is used as case site, since water levels and waves are only observed at this point in the bay. The maximum computed values are calibrated with respect to the maximum observed values. This is because the model does not predict the hourly values correctly due to schematisations and the extreme values are important for the statistical analysis. An exception is made for the calibration of the storm surge level since both the wind set-up and the pressure set-up have to be calibrated with the same series of observations. The average relative and absolute deviations (above and under) from the observations are determined for the hydraulic variables (Table 1-1). The calibrated values are indicative values for the error. Validation of the models should be done to obtain an objective insight in the model uncertainties. In the probabilistic analysis, the calibrated model constants are included in the total model.

Table 1-1: Calibrated model constants and model error relative to observations

Hydraulic variable	Fit constant	Error relative	Error absolute
Pressure set-up	c_1 of 0.03	25%	0.3m
Wind set-up	c_2 of $0.5*10^{-6}$		
Wave height SMB	fit parameter 0.9	20%	0.3m
Wave period SMB	fit parameter 1.0	5%	0.3s
Wave period via steepness	steepness 3.16%	5%	0.3s

<u>Probabilistic analysis of hydraulic boundary conditions</u>

The probabilistic analysis is done with the same model as derived for the deterministic calibration, only now statistical input distributions for typhoon characteristics and the distribution of the tidal water level are used as input variables instead of deterministic values. The deterministic geometry and bathymetry of the bay are also used in the probabilistic analysis. Over 6000 typhoons and their induced hydraulic variables are the result of simulating a period of 10000 years. The marginal probability density functions of the hydraulic variables are derived from the simulated dataset. The tails of the datasets however deviate from the overall marginal probability density functions and are therefore fitted separately. The return periods of the hydraulic variables are given in Table 1-2.

Table 1-2: Hydraulic variables for different return periods according to the derived probability density functions

Return period [1/year]	Dimension	10^{-3}	10^{-4}	10^{-5}
Total water level	[m]	5.5	5.7	6.3
Significant wave height	[m]	2.9	3.4	3.9
Peak wave period	[s]	8.3	9.4	10.8

If physical variables are independent and related to the hydraulic variables, their marginal probability density functions can be used in the analysis of the joint probability density functions. The independence between the wave height and the wave steepness is used to derive the joint probability density function of the wave height and the wave period. The independence between the tidal water level and the storm surge level is used to derive the joint probability density function between total water level and the wave height and the wave period. The physical relations between the storm surge level, the wave height and the wave period are derived via the wind speed and fitted to the simulated dataset. A statistical validation of the marginal and joint probability density functions is done. To illustrate the implementation of the joint probability density functions in the design of a flood defence, a failure mode is analysed.

<u>Conclusions</u>

The analysis of the probability density functions of the hydraulic variables with a limited amount of data available is possible with a method that combines statistics and physical relations. Knowledge of the physical behaviour of hydraulic variables all over the world is included in this method and physical boundaries are taken into account properly in the extrapolation. Input parameters are based on a broader statistical basis than would be the case if the statistics were derived solely from the hydraulic variables.

The deterministic model seems to hindcast the maxima of hydraulic variables induced by historical typhoons reasonably. The probability density functions have been statistically validated and seem to be in line with observations. The number of observations however is far too small to confirm the probability density functions in the regions of low probabilities of exceedance. The dependence structure of the hydraulic variables should be included in the assessment of failure probability of failure modes in the flood defence design.

Contents

List of figures

List of tables

List of symbols

Variable	Description	Unit[I]
a	Constant to determine pressure set-up	cm/hPa
a	Parameter of Generalized Pareto Distribution	-
a	Parameter of Weibull distribution	-
a_c	Change rate of forward movement	km/h^2
a_d	Change rate of direction of forward movement	º/h
a_p	Change rate of pressure depth	1/h
a_r	Change rate of radius to maximum wind	km/h
b	Constant to determine wind set-up	cm/m^2/s^2
b	Parameter of Weibull distribution	-
c_1	Constant of pressure set-up formula	m/hPa
c_2	Constant of wind set-up formula	-
C_{fm}	Forward movement of typhoon	m/s
$C_{fm}(t)$	Forward movement of typhoon after typhoon landing in time	km
C_{fm0}	Forward movement of typhoon at time of landing	km/h
d	Water depth	m
d_{eff}	Effective depth	m
$deltah$	Total water level (increase)	m
dh	Total water level (increase)	m
$dhtide$	Tidal water level	m
dh_{tot}	Height of total water level increase	m
$dhwp$	Strom surge level	m
d_i	Average depth in direction i	m
f	Coriolis parameter	1/s
F_{eff}	Effective fetch length	km
F_i	Fetch in direction i	km
F_{set-up}	Fetch length of wind set-up	m
F_{wave}	Fetch length of waves	m
$f_{\underline{x}}$	Joint probability density function of the input variables x	-
f_x	Marginal probability density function of variable x	-
$f_{x,y}$	Joint probability density function of variables x and y	-
$f_{x\|y}$	Conditional probability density function of variable x with respect to variable y	-
g	Gravity acceleration	m/s^2
H	Storm surge level	cm
H_1	Mean high water level during typhoon season	m
H_2	Estimated storm surge when a typhoon hits the bay	m
H_3	Height of the free board	m
h_{crown}	Crown level of the flood defence above bottom of structure	m
H_d	Height of embankment	m
H_{m0}	Wave height (related to zero moment of spectrum)	m
H_s	Significant wave height	m
i	Position of data point in increasing order	-
J	Jacobian	
$L.W.L.$	Low water level (=C.D. level)	m
m_0	Zero moment of spectrum	m^2

[I] Some of the dimensions are not given in SI units; these dimensions have been adopted from the original expressions

Variable	Description	Unit
N	The number of data points	-
p	Atmospheric pressure at a distance from the typhoon centre	hPa
P	Central pressure of a typhoon	hPa
p_∞	Peripheral Pressure	hPa
p_c	Pressure in eye of hurricane	hPa
p_f	Probability of failure	-
R	Resistance of the structure	-
r	Distance from typhoon centre	km
r_m	Radius to the maximum cyclostrophic wind speed	km
$r_m(t)$	Radius to maximum wind after typhoon landing in time	km
r_{m0}	Radius to maximum wind at time of typhoon landing	km
r_t	Radius of the curvature of trajectory	m
S	Load on the structure	-
s_0	Wave steepness related to the wave spectrum	-
s_p	Wave steepness	-
t	Time after typhoon landing	h
$T_{m-1,0}$	Spectral wave period	s
T_p	Peak wave period	s
T_s	Significant wave period	s
V_{gr}	Gradient wind speed	m/s
V_s	Surface wind speed	m/s
W	Wind speed	m/s
x_i	Input variable i	-
Z	Reliability function	-
z	Vector describing the geometry of the structure	-
$Z_{overtop}$	Reliability function of overtopping	-
$z_{2\%}$	2% wave run –up level above still water line	m

Greek symbols

Variable	Description	Unit
α	Angle of slope of flood defence	º
α	Deflection of the surface wind direction from the isobar	º
β	Angle between wind direction and direction of the radial	º
γ	Direction of forward movement after typhoon landing	º
$\gamma(t)$	Direction of forward movement after typhoon landing in time	º
γ_f	Influence factor for roughness elements on slope	-
γ_β	Influence factor for angle of wave attack	-
γ_0	Direction of forward movement at time of typhoon landing	º
$\dfrac{\partial y}{\partial x}$	Derivative of variable y with respect to variable x	-
Δh_p	Pressure set-up	m
Δh_w	Wind set-up	m
Δp	Central pressure depth	hPa
Δh	Total water level increase	m
Δh_{tide}	Tidal water level	m
Δh_{wp}	Storm surge level	m
Δp	Central pressure depth	hPa
$\Delta p(t)$	Central pressure depth in time	hPa
Δp_0	Central pressure depth at time of landing	hPa
θ	Direction angle of radius vector from direction of typhoon	º
θ	Parameter of Generalized Pareto Distribution	-
θ	Difference between critical wind direction and wind direction at wind speed peak	º
μ	Fit parameter for wave height	-
μ	Parameter of Lognormal distribution	-
μ	Parameter of Normal distribution	-
v	Fit parameter for wave period	-
ξ	Ratio between distance and radius to maximum wind speed	-
ξ_0	Breaker parameter	-
ρ	Air density	kg/m^3
σ	Parameter of Lognormal distribution	-
σ	Parameter of Normal distribution	-

1   Introduction

This chapter is an introduction to the various subjects that are discussed in the report. The two main threats related to the flood defence of Japan are given. The immediate motive to start the research on the hydraulic boundary conditions for a bay in Japan is described. Major historical typhoons that have attacked Japan are briefly discussed and the current design philosophy of the flood defence system is analysed. Based on this information a problem analysis is done and the objectives of the research are stated. Finally, the approach to derive the statistical properties of hydraulic boundary conditions is given, together with the report structure and outline.

1.1   Threats to the Japanese flood defence system

There are two major threats to the Japanese flood defence system. On the one hand there is the threat of typhoons with a resulting storm surge; an abnormal sea-level rise caused by low pressure and severe winds that attend a typhoon. On the other hand there is a threat of tsunamis; a series of long waves generated by sudden displacement of a large volume of seawater at seafloor level due to a large earthquake. Because of the independence of both phenomena, they are usually investigated separately. The first threat plays a central role in this research. In an overall design of the dike system, the hydraulic loads due to the tsunami threat should also be taken into account.

1.2   Motive to start this research

The 18th typhoon in the Northwest Pacific Ocean in the year 1999 (hence no. 9918) struck the western part of Japan. In the early morning of September 24th, Typhoon Bart landed on Kyushu Island, south of Suo-nada Bay (Figure 1-1), with an atmospheric pressure at the typhoon centre of 940 hectopascal and a forward speed of 40 kilometres per hour. The typhoon path was right over Suo-nada Bay. It heavily damaged many coastal facilities and houses and was responsible for the death of 12 people. At Suo-nada Bay, the storm surge and additional wind-driven high waves made many seawalls collapse; different areas amongst which an airport were inundated. This enormous disaster could not only be ascribed to Typhoon Bart, because it was not the most intensive typhoon of the past decades. The simultaneous occurrence of storm surge, high tidal level and high waves caused this enormous disaster. On the north and west side of Suo-nada Bay the rise of the water level due to the storm surge was 2 to 3 meters and due to the astronomical tide 1 to 2 meters (above Tokyo Bay average water level). The total water level reached from 3 to 4.5 meters. The peak significant wave height was 3.5 to 4 meters. Not since the Ise Bay typhoon of 1959 (Figure 1-1) had such a major disaster occurred in Japan (Takahashi, 2005).

Figure 1-1: Japan with location of major bays and historical typhoon tracks (www.agora.ex.nii.ac.jp)

1.3   Historical typhoons attacking Japan

Every year a few typhoons pass through the Japanese main islands from south to north, thereby generating storm surges and waves (Figure 1-1). In 1959 a violent typhoon, called the Ise Bay Typhoon induced an extreme storm surge together with waves in Ise Bay, collapsing the coastal dikes and killing over 5000 people. In the history of Japanese meteorological observation the Ise Bay Typhoon was - measured in central pressure depth - only the third fiercest (after the Muroto Typhoon (1934) and the Makurazaki Typhoon (1945)), but the damage it caused was far beyond that of the other two typhoons (Tsuchiya et al., 1980). Still, over 3000 people were killed by the Muroto Typhoon (1934), travelling through Osaka Bay (Figure 1-1).

Since the Ise Bay typhoon few large storm surge disasters have struck Japan. This is due to the many flood defence facilities completed rapidly in the 1960's around major bays (e.g. Tokyo Bay, Ise Bay, Osaka Bay and Suo-nada Bay) and the small number of large typhoons that directly hit the Japanese islands. Countermeasures as typhoon warning systems and lock gates also contributed to prevent major disasters (Tsuchiya et al., 1986).

1.4   Current state of design of coastal defences related to typhoons

In the current design philosophy of flood defences in Japan, a tide level (i.e. mean high water level) is adopted together with the storm surge level that would have been caused by a 'design' typhoon, the scale of which is the same as the most severe typhoon ever recorded. The design height of the embankments is determined with the expression in equation (Nakagawa et al., 1995):

$$H_d = H_1 + H_2 + H_3 \tag{1-1}$$

H_d	Height of embankments	[m]
H_1	Mean high water level during the typhoon season	[m]
H_2	Estimated storm surge when a typhoon (of a scale similar to the one caused by the Ise Bay typhoon) hits the bay during the time of high water	[m]
H_3	Height of the free board	[m]

The storm surge level caused by a 'design' typhoon is computed with a numerical model. The Japanese standards (according to Takahashi et al., 2005) however lack detailed criteria on how to determine the minimum atmospheric pressure, radius, progression speed and route of the model typhoon for the design total water level. These typhoon parameters have traditionally been based on those of the Ise Bay Typhoon and other typhoons having actually attacked the area.

At the Port and Airport Research Institute[1] a deterministic typhoon hindcasting model has been developed, which is able to compute water levels and wave heights caused by a 'design' typhoon. The joint occurrence of tide and storm surge in combination with waves is not taken into account in this approach. Different deterministic typhoon tracks over Suo-nada Bay (Figure 1-2), together with a wide range of typhoon parameters such as central pressure, radius of the typhoon and proceeding speed, are used to determine the maximum storm surge level and maximum wave height. The sum of the design storm surge level and design tidal level on the one hand and the maximum tidal level (sum of storm surge and tide level) ever recorded at a tide station on the other are adopted as design water levels. In the first case however the return period is not exactly clear. In the second case there is no detailed criterion concerning how to determine the parameters of the model typhoon. The design wave conditions are generally determined based on statistical analysis of extreme events where the return period of the design condition is usually 50-100 years (Hashimoto et al., 2004).

---

[1] Further stated as PARI
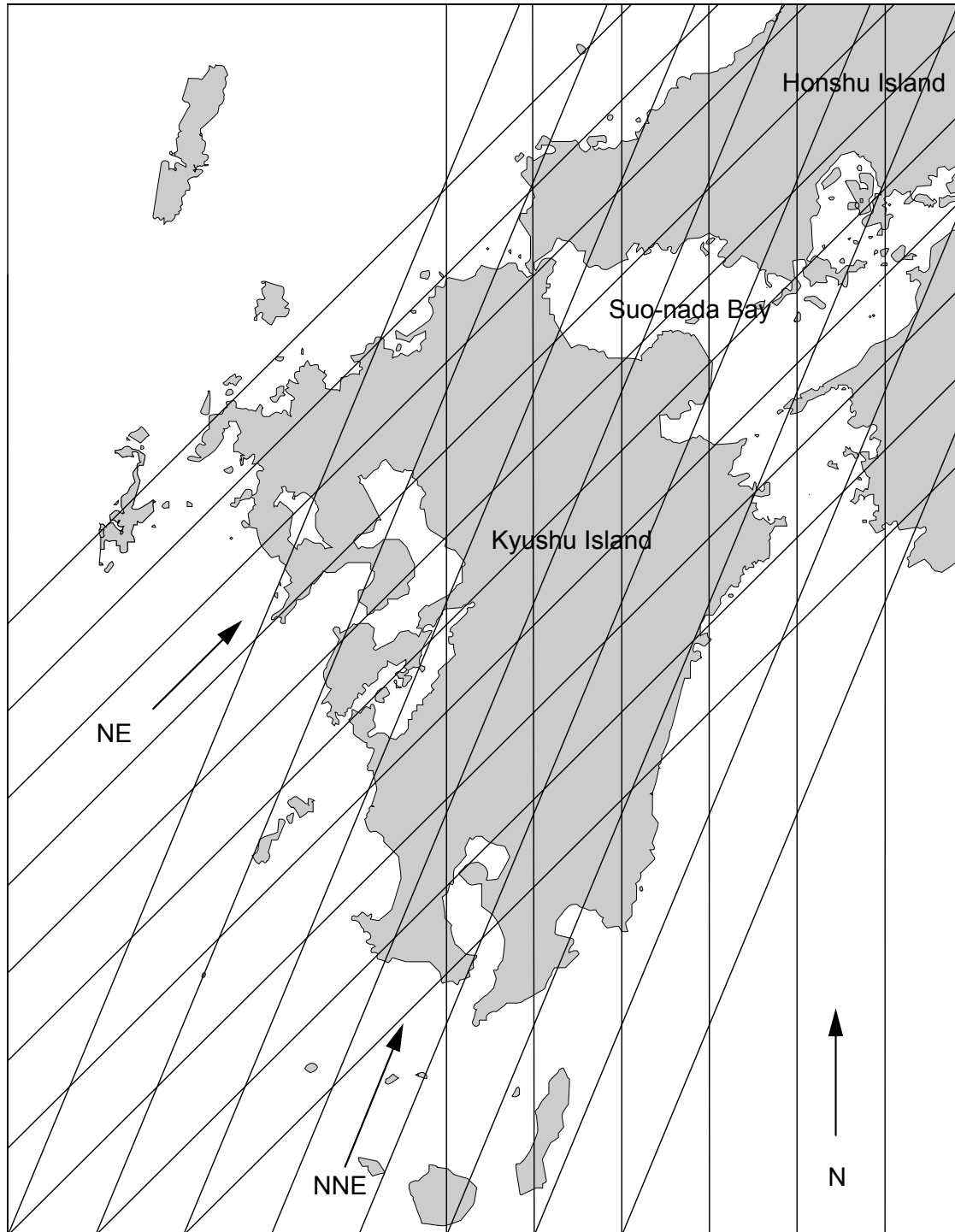
Figure 1-2: Tracks of typhoons used in current modelling of typhoon induced storm surges and waves (after Takahashi, 2004a)

Probabilistic evaluations of the tide level have been conducted (Torii et al., 2001, Yamaguchi et al., 1998), but the concurrent probability of high tides, storm surges and high waves cannot be evaluated precisely. This is because wave characteristics depend on the tide level. Further, waves and water levels have not been observed long enough for extreme statistical analysis (Kato et al., 2002).
Kato et al. (2002) derived a method for the evaluation of exceedance probabilities of water levels and waves. However, the hydraulic variables have been derived for other bays (e.g. Osaka Bay, Ise Bay, Tokyo Bay and Tosa Bay) and not for Suo-nada Bay.

Takahashi et al. (2004) state that with a prediction system using the probabilistic nature of typhoons, it will be possible to estimate the future expected damage due to storm surges and waves for designated areas. With an inventory of the value of the land behind the defence system and the value of loss of life, it is possible to set a performance level or an acceptable risk level. The framework of performance design (Takahashi et al., 2005), similar to reliability-based design applied in coastal engineering by various authors (i.e. Bakker and Vrijling, 1980, Burcharth et al., 1995, Voortman et al, 1998, 2002a and Vrijling et al. 1998), has to be used for the safety analysis of the flood defences.

1.5   Problem definition

Typhoons can be devastating and often result in loss of life and significant damage to infrastructure. The serious damage caused by Typhoon Bart (no. 9918) gives rise to review the level of protection against typhoon induced storm surges and waves and the possible flooding of areas behind the flood defence system (Kato et al., 2002).

Although probabilistic evaluation of the water level has been conducted, the concurrent probability of high water levels and high waves is not taken into account. In the current design method, the tidal level, storm surges and waves have been calculated deterministically. The lack of a probabilistic method to analyse the joint occurrence of the tidal level, storm surge and waves, results in a situation where a reliability-based analysis of the flood defence system is not possible.

For a probabilistic analysis only a small amount of data is available. The water levels in Suo-nada Bay have been observed for over 30 years. Waves have been observed for only 14 years. An extrapolation to very low probabilities of exceedance needed for reliability-based design has to be done with this limited amount of data.

1.6   Objective of the research

A reliability-based analysis of the flood defence system has to be done. Only a part of the analysis will be treated in this research since decisions on protection levels have not yet been made. The efforts will be concentrated on the estimation of tide level, storm surge level, wave heights and wave periods and their joint probabilities of occurrence. Therefore, the objective is to obtain the marginal and the joint probability density functions[2] of the hydraulic variables based on the joint occurrence of the tidal level, storm surge level and waves. The hydraulic conditions are caused by the typhoon system and are therefore interdependent. The description of the multi-variate statistics of the hydraulic boundary conditions has to include this dependence.

---

[2] Sometimes referred to as PDF or JPDF

1.7   Problem approach and structure

Some points of departure largely determine the path to obtain the marginal and joint probability density functions of hydraulic boundary conditions. The points of departure and the consequences on the research are summarised below and given in Figure 1-3:

Point of departure with respect to the method to derive the extreme values
The multi-variate statistics of the hydraulic boundary conditions will be calculated with a method that combines statistics and physical relations
Motive:
-   Few observations are available. A dependence structure for extreme conditions only based on these observations is weak. Therefore a combination of statistics and physics is preferable
-   The analytical models include physical relations that are used and found all over the world. This knowledge is then applied in this case
-   The statistical characteristics of variables related to the hydraulic variables can be used that have a better statistical basis than the hydraulic variables
-   Extrapolation of the hydraulic variables is done within physical boundaries. The physical models hold both under observed and under extreme conditions
Consequence:
Simple analytical models are to maintain insight in the physical relations between the input, intermediate and output variables (the hydraulic boundary conditions), especially under extreme conditions

Point of departure with respect to the various input distributions
A Monte Carlo analysis is used to derive the probability density functions of the storm surge levels, the wave height and the wave period
Motive:
-   The method is simple in use and a number of input variables can easily be included
Consequence:
For the Monte Carlo analysis a large number of computer simulations is needed, to obtain extreme storm surge levels and wave characteristics with low probabilities of exceedance. Simple analytical models are used because numerical models require more calculation time

This results in the following logical steps:
-   Research of the physical phenomena related to hydraulic loads that occur during the passing of a typhoon has to be done
-   Determine the models that describe these physical phenomena and how these models can be combined to determine the hydraulic loads on the flood defences
-   Because of the schematisations that accompany the simple analytical models and the range of values of model constants that are given, some models are calibrated. The observations of hydraulic variables are used for deterministic calibration and probabilistic validation
-   The calibrated model is used in the probabilistic analysis of the hydraulic boundary conditions
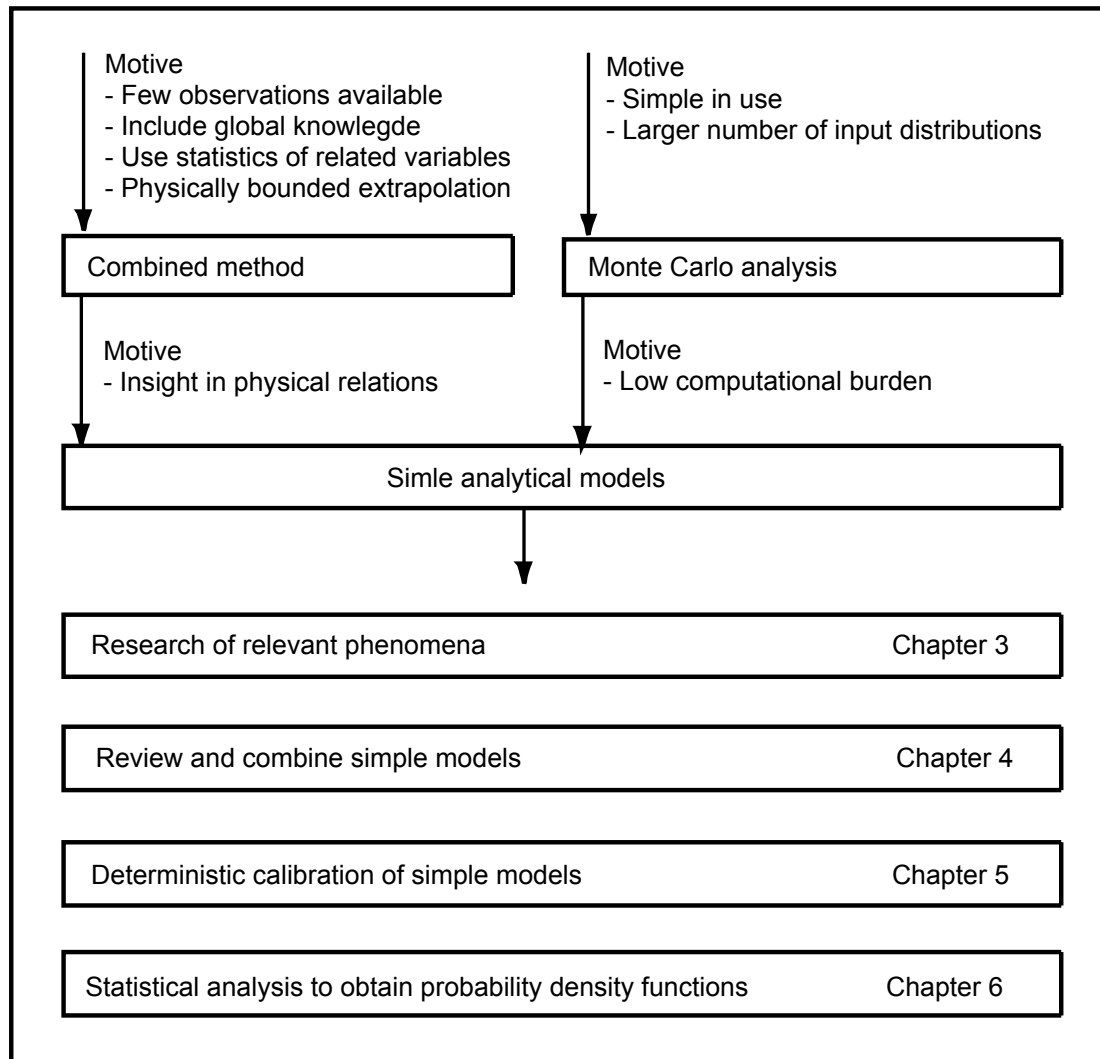
Figure 1-3: Problem approach and report structure

1.8   Outline of the research

The report contains the following different chapters (Figure 1-3):
Chapter 1 gives an introduction to the research. The problem is defined and the objective of this research is stated
Chapter 2 gives background information about the context of probabilistic design in flood defence design. The position of probabilistic design within reliability-based design is given
Chapter 3 gives background information about typhoon systems and describes which physical phenomena are relevant for the research
Chapter 4 describes the models used to calculate the physical phenomena and how these models are combined in a combined dependence model
Chapter 5 describes the deterministic calibration of the models used for the computation of storm surge, wave height and wave period
Chapter 6 states the marginal and joint probability distributions of the hydraulic boundary conditions. Further a statistical validation of the hydraulic variables is done
Chapter 7 states the conclusions and recommendations of the research

2 Context of probabilistic analysis within flood defence design

The context of probabilistic analysis of hydraulic boundary conditions related to flood defence design, is pointed out in this chapter. For the total analysis of a flood defence system, a risk-based design is often applied. The role of the probabilistic analysis within this risk-based design is pointed out. Further, the method that is used to derive the probability density functions in the research is presented.

2.1 Decision making on level of safety of flood defences

The appropriate level of protection provided by a flood defence system is in the ideal case obtained by balancing the cost of protection against the risk reduction in the protected area. Based on this idea, risk-based design methods have been developed over the past decades. A risk-based design method (performance design) has been proposed by Takahashi et al. (2004), to be used in the analysis of the Japanese flood defences.

To come to a workable framework of risk-based decision making, it should be recognised that several decisions have to be made to determine the appropriate level of protection of the area protected by the flood defence system. The decisions range from the geometry of a flood defence system to the acceptable flooding probability of the area, given economic and societal consequences of flooding. The safety level of flood defences should reflect the demands posed by nature and society. A method to analyse appropriate safety levels for possible flood areas is available in the form of the risk-based design method for flood defences. Risk-based design typically incorporates not only the flooding probability but also the consequences of flooding. The advantages of this approach are:

- The choice of the safety levels can be further rationalised if the consequences of flooding and the costs of protection are made explicit
- Risk-based approaches exist also in other fields where safety levels have to be defined, so that a risk-based approach to flooding safety provides the possibility of comparing the risk levels.

Risk-based design is defined as a design approach where the costs of protection are weighed against the risk reduction in the protected area. The failure probability for which the structure is designed is flexible and depends on the consequences of failure. This is in contrast with reliability-based design.
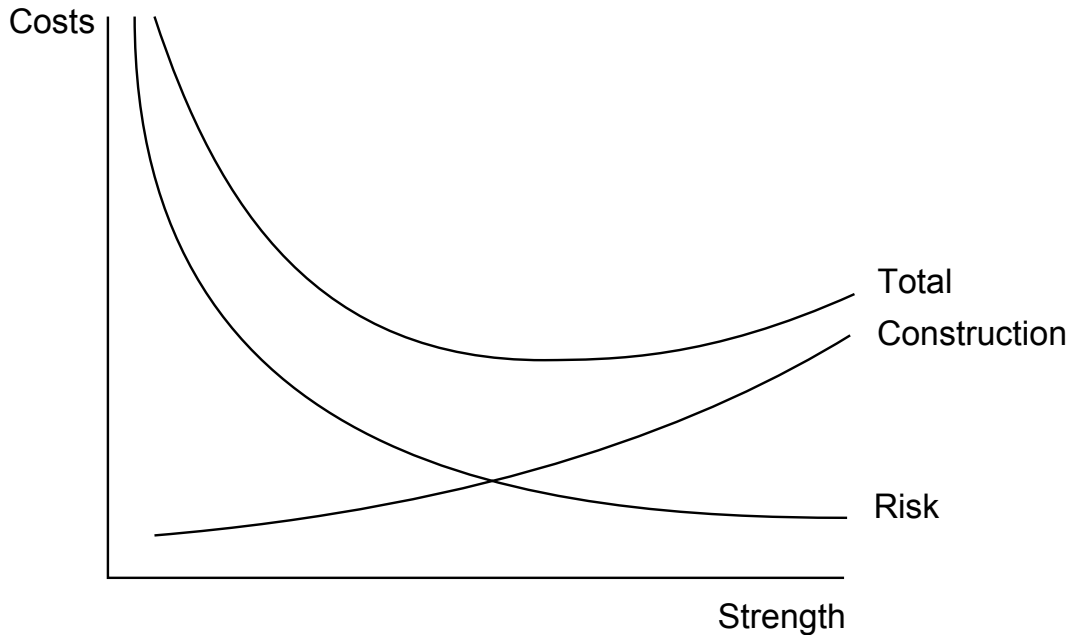
Figure 2-1: Construction cost versus risk reduction

Figure 2-1 shows the ideas behind an economic based design method: a very strong structure runs little risk of failure but is expensive, while a less strong structure is cheaper but the risk is high. Somewhere in between there is an optimum. The risk of failure is

$$Risk = probability \cdot consequence$$

From the viewpoint of rational decision making the costs should be minimised provided that the design satisfies all requirements. The combination of the investment with a reliability requirement leads to the cheapest design that just suffices the reliability requirements. This is also denoted the optimal design.

2.2   Reliability analysis and evaluation of flood defence systems

In view of the reliability of a flood defence structure, the primary function of a flood defence system is the protection against flooding (apart from special purpose structures). Failure is denoted as inundation of the area.

2.2.1   Serviceability and ultimate limit state
A distinction is made between the serviceability limit state and the ultimate limit state of a flood defence system. The ultimate limit state defines collapse or such deformation that the structure as a whole can no longer perform its main task. It is usually related to extreme load conditions. The probability of reaching an ultimate limit state should be much lower than reaching a serviceability limit state. The hydraulic climate in the ultimate limit state and in the serviceability state is needed.
The research focuses on the ultimate limit state load of the flood defence system. The ultimate limit state is related to extreme load conditions. Extreme loads on the flood defence system caused by typhoons are determined.

2.2.2   Fault tree
The failure of the system can be broken down in elements and in individual failure modes. The failure modes and their relation to failure of the structure and the

structures and their relation to overall failure of the system can be represented in fault trees. Quantitative analysis starts at the level of failure modes with the definition of limit state functions and the description of the joint probability distribution of random input variables. For an arbitrary system, the definition of the failure boundary can be found by following the deterministic analysis of the fault tree (Figure 2-2).
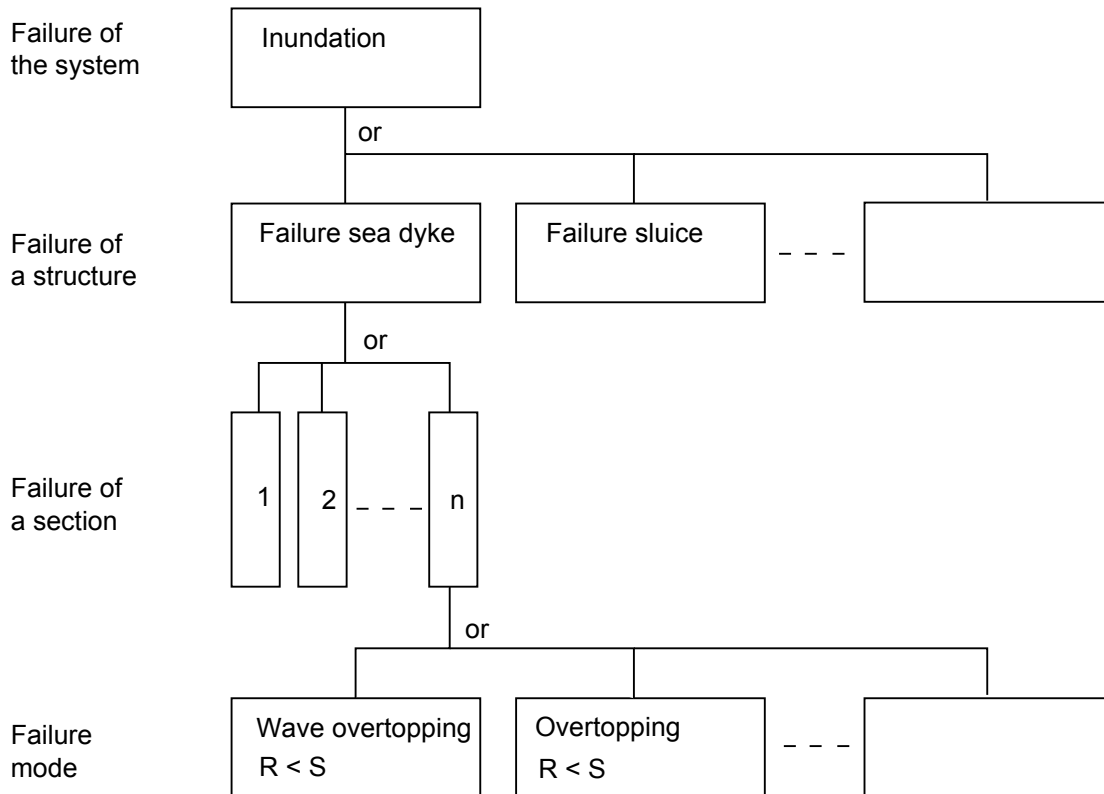
Figure 2-2: Simplified fault tree for the failure of a dike system

Every individual structure of the overall system has to be analysed with respect to its possible causes of failure. To enable a quantitative analysis of the reliability of the structure every failure mode has to be cast in a mathematical limit state function. The individual structure has to be analysed further with respect to its possible causes of failure (failure modes). Also on the level of individual structures a fault tree can be used to visualise the failure modes and their interactions.

2.2.3   Limit state functions

To enable quantitative analysis of the reliability of the structure every failure mode has to be cast in a mathematical form. This is often done with limit state functions:

$$Z = R - S \qquad\qquad (2\text{-}1)$$

       Z   Reliability function
       R   Resistance of the structure
       S   Load on the structure

Negative values of the reliability function indicate failure by the failure mode described by the limit state function. On the lowest level in a fault tree every failure mode has to be written in the form of this equation if a quantitative analysis is performed. Once the limit state functions are defined there are two different ways to judge the performance of the structure: deterministic and probabilistic.

In the deterministic analysis the margins are calculated for one or more discrete sets of values for the load and strength variables. The structure fails under the prescribed load and strength combination or not. No estimate of the likelihood of failure is given by this type of method. The probabilistic analysis takes the uncertainties in load, strength and physical models into account. The combination of probabilities of Z<0 determines the total probability of failure p_f. p_f is the volume of the part of the probability mountain where the reliability function is less than zero (Z<0). This volume is given by:

$$p_f = p(Z < 0) = \int\limits_{Z(x)<0} \int ... \int f_{\underline{x}}(x) dx_1 ... dx_n \tag{2-2}$$

p_f	Probability of failure
Z	Reliability function
x_i	Input variables
$f_{\underline{x}}$	Joint probability density function of the input variables

2.2.4 An example of a limit state function

The failure mode overflowing and wave overtopping occurs in the situation where the water level exceeds the crest level of the flood defence structure and the attack of waves. The failure mode overflowing and wave overtopping is an initiating failure mode. A definition of a limit state for this failure model is given by

$$Z_{overtop}(\text{dh}, \text{H}_s) = \text{h}_{crown} - \text{dh} - \text{z}_{2\%} \tag{2-3}$$

$Z_{overtop}$	Reliability function of overtopping	[-]
h_{crown}	Crown height of flood defence relative to bottom of structure	[m]
dh	Total water level increase	[m]
$z_{2\%}$	Wave run-up that is exceeded by 2%	[m]
H_s	Significant wave height	[m]

The definition of $z_{2\%}$ and a flood defence cross section is given in chapter 6. The results are plotted in Figure 2-3. The curve gives the combinations of the water levels and wave heights at which the structure is still capable of handling the loads (reliability function with Z=0). Right of this line the strength is exceeded (Z<0) resulting in failure.
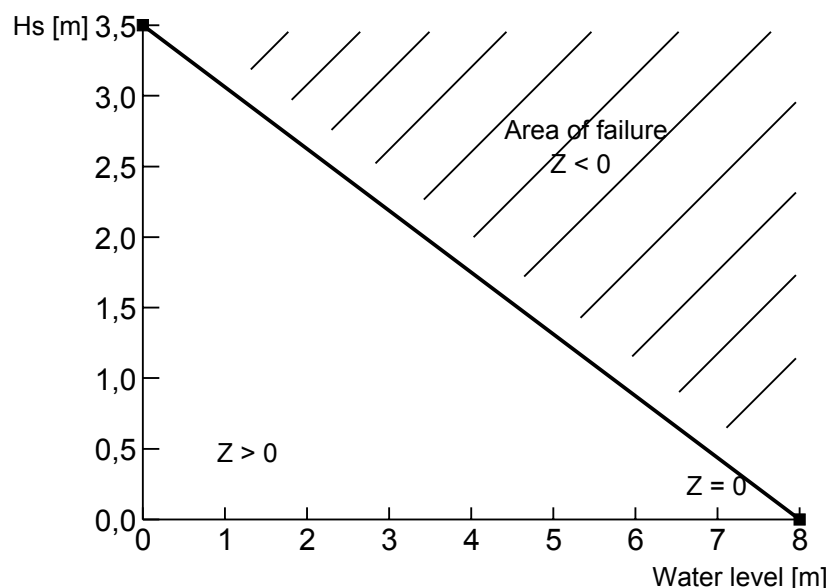
Figure 2-3: The failure area of the failure mode overtopping

2.3   Probabilistic calculation methods

The integration of a probability density integral can generally not be solved analytically. A number of methods have been developed to solve this. A distinction is made between level 2 methods and level 3 methods.

In the level 2 approach, the joint probability density function is transformed to a space normally distributed independent variables and the limit state function is replaced by its first order Taylor approximation in one point. The probability of failure of the system depends on the probabilities of failure of the individual failure modes and on the dependence between the failure modes. For arbitrary dependence between the components of the system, analytical solutions provide upper and lower bounds to the exact probability of failure.

In the level 3 approaches the integral is solved direct by a numerical method. This may be done with a Riemann integration or a Monte Carlo analysis. Riemann integration transforms the integrals of the analytical functions that describe the probability density of the failure area in more dimensional cells. The volume of these cells are then determined and summed. In the case of a lot of variables this method results in extensive calculations. In the level 3 Monte Carlo approach, for all input parameters a random number is drawn from their probability distribution. The Monte Carlo method can be used to obtain the number of counts of load combinations in the failure domain.

With the Monte Carlo analysis the distribution of the hydraulic loads is determined. The research will be done with this method since the Monte Carlo approach provides an easy tool to derive the probabilities occurrence in cases with various input variables.

2.4   Hydraulic boundary conditions

It is clear that a reliability-based analysis can only be done with the joint probability distribution of the stochastic variables that describe the load and resistance of the structure. This research focuses on the hydraulic loads on the flood defence structure. It concentrates on the description of the marginal and joint probability density functions of the hydraulic boundary conditions. Which PDF should be used in the reliability analysis depends on the failure mode that is investigated as explained in the previous section. Earlier case studies show that for coastal structures, the uncertainty of the hydraulic boundary conditions (water level and wave conditions) dominates the reliability of the structure (Vrijling et al 1998a, Voortman et al 1998, 1999).

The models, chosen to define the limit state functions for a flood defence structure, determine the choice of variables for the description of the hydraulic boundary conditions. For the limit state functions the following three aspects of the hydraulic conditions need to be quantified

-    Water level (i.e. tidal level and storm surge level)
-    Wave height
-    Wave period

Hydraulic conditions in front of flood defences generally show a strong dependence. The dependence can be explained by the fact that the same physical processes determine the hydraulic conditions. In coastal regions wind conditions dominate the hydraulic conditions. The local conditions depend on the properties of the driving process and on local conditions like orientation of the structure, bathymetry etc. The parameters of pressure set-up, wind set-up, wave height and wave periods are caused by the same driving force; the atmospheric pressure field of the typhoon and

the resulting wind field. Dependence between these parameters can therefore be expected.

2.5   Methods used for extrapolating hydraulic boundary conditions

The major issue related to the determination of the probability density space is the extrapolation of the hydraulic boundary conditions to an exceedance probability far beyond the period of observation. There are two different methods that can be used for extrapolating the observed data and their correlations into the regions of low probability of occurrence: the fully statistical methods and the statistical methods combined with physics.

In the case of the fully statistical method, the dependence structure between the hydraulic variables is derived solely from the data. In the design of flood defences the interest lies in the extreme hydraulic conditions that are scarce by definition. Observations therefore appear to provide a weak basis for the dependence structure under extreme conditions. Extrapolations may even exceed physical limits.

An alternative approach of combining the statistics with the physics is proposed by Vrijling and Bruinsma (1980) and developed further by Repko et al. (2001) and Webbers et al. (2003). In this approach, a parametric dependence model is developed that is based on physical concepts. In that way the shape of the dependence structure is fixed and only a limited number of parameters need to be estimated from the data. Physical models can be assumed to hold both under measured conditions and under extreme conditions.

Because hydraulic boundary conditions depend on the same driving force, a strong dependence between the two can be expected in extreme conditions. From the design point of view of a flood defence structure, especially the extreme conditions are important, which implies that the dependence between hydraulic conditions needs to be accounted for. Further, global knowledge of physical relations can be included in the method and the statistics of related variables can be used that are based on a broader statistical basis. The combined method is therefore used.

2.6   Input variables for the combined method

Vrijling and Bruinsma used the water level offshore as the input variable and described the wave conditions as a function of the water level. The dependence model was derived on the basis of parametric physical models. Vrijling and Bruinsma (1980) observed that both water level and wave conditions are wind driven and are therefore dependent. Nevertheless they based their description of the JPDF of hydraulic conditions on the water level instead of the wind field. The reason was that at the time a long series of water level observations was available but joint observations of wind speed, water level, wave height and wave period were scarce.

In the Japanese case, the physical origin of all typhoon-related phenomena can be found in the atmospheric pressure field of the typhoon and the resulting wind field. The analysis is therefore done with the characteristics derived from historical typhoon pressure-fields. The characteristics of these typhoons are observed longer than the water level and the waves and will therefore also have a better statistical basis. To be able to compute the probabilistic hydraulic boundary conditions, input distributions of variables are needed. Therefore, the available statistics of characteristics related to typhoons are an important restriction in the use of models and their input parameters.

2.7 Models that describe the phenomena

Research into the behaviour of water level and waves in extreme wind conditions has resulted in a number of (numerical) models, which are used to compute these hydraulic variables. However, the possible choice of models for this research is reduced drastically by the choice of using a Monte Carlo approach. In the process of reliability evaluation of a flood defence structure a large number of calculations is performed. Therefore, the models in the dependence model should have a low computational burden. This limits the choice to simple parametric models. This simplification cast some doubt on the validity of the results that are obtained. Parametric dependence models should be calibrated against field data. An estimate of the model error can be obtained to account for observed differences between model and field data.

3 Physical phenomena related to typhoons and the hydraulic loads

To be able to describe the hydraulic boundary conditions, an overview of the relevant physical phenomena that cause extreme water levels, wave heights and periods is needed. The basics of a typhoon system are given, together with the typhoon related hydraulic phenomena. At the end of the chapter an overview is given of the phenomena included in the further analysis.

3.1 Geometry and bathymetry of Japan and Suo-nada Bay

Japan faces the Pacific Ocean in the south and the Japan Sea in the north (Figure 3-1). Water depths around the Japanese islands reach to several thousands of meters. The Japanese coastline includes many bays that are shallow and partially protected from the Pacific Ocean by natural barriers.
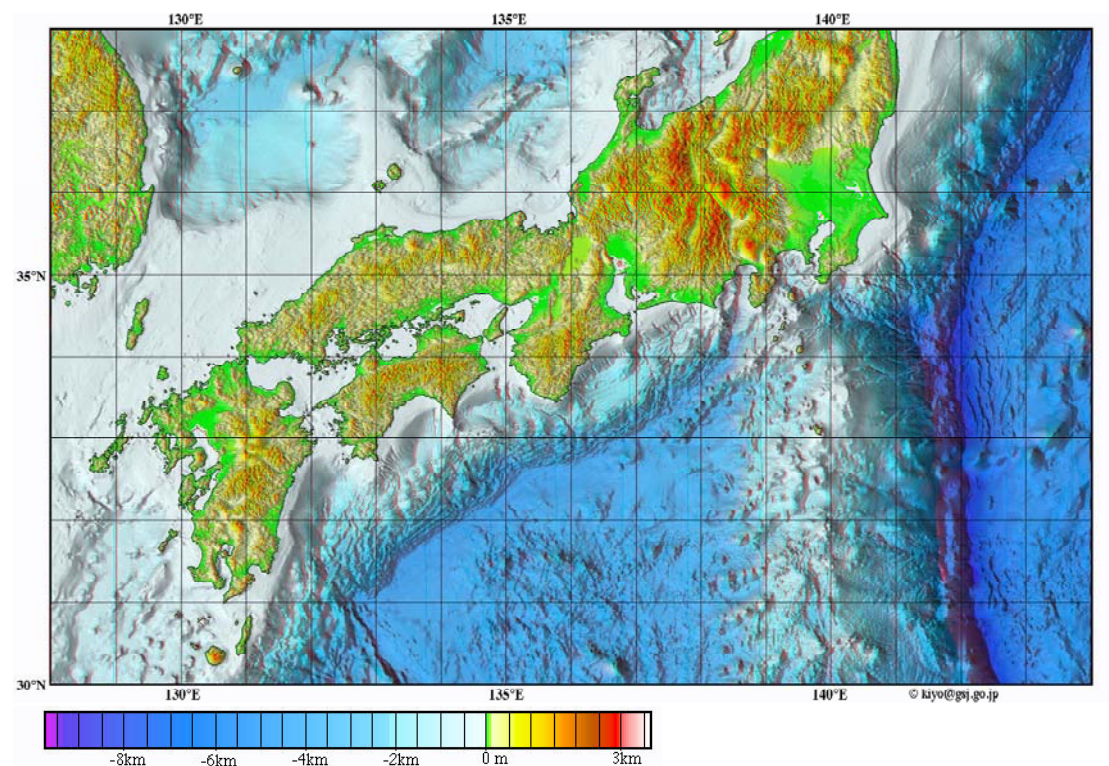
Figure 3-1: View of the water depths around the Japanese main islands (www.gsj.go.jp)

Suo-nada Bay is S-shaped and about 90 kilometres long from east to west and 50 kilometres long from north to south, and surrounded by the islands of Kyushu and Honshu (Figure 3-2). The water depth (based on low water level) exceeds 40 meters in the east region and is 10 meters or less within 10 kilometres of the coastal line in the west. The location of the Port of Kanda is also given in the figure. The water levels and waves are observed at this point.
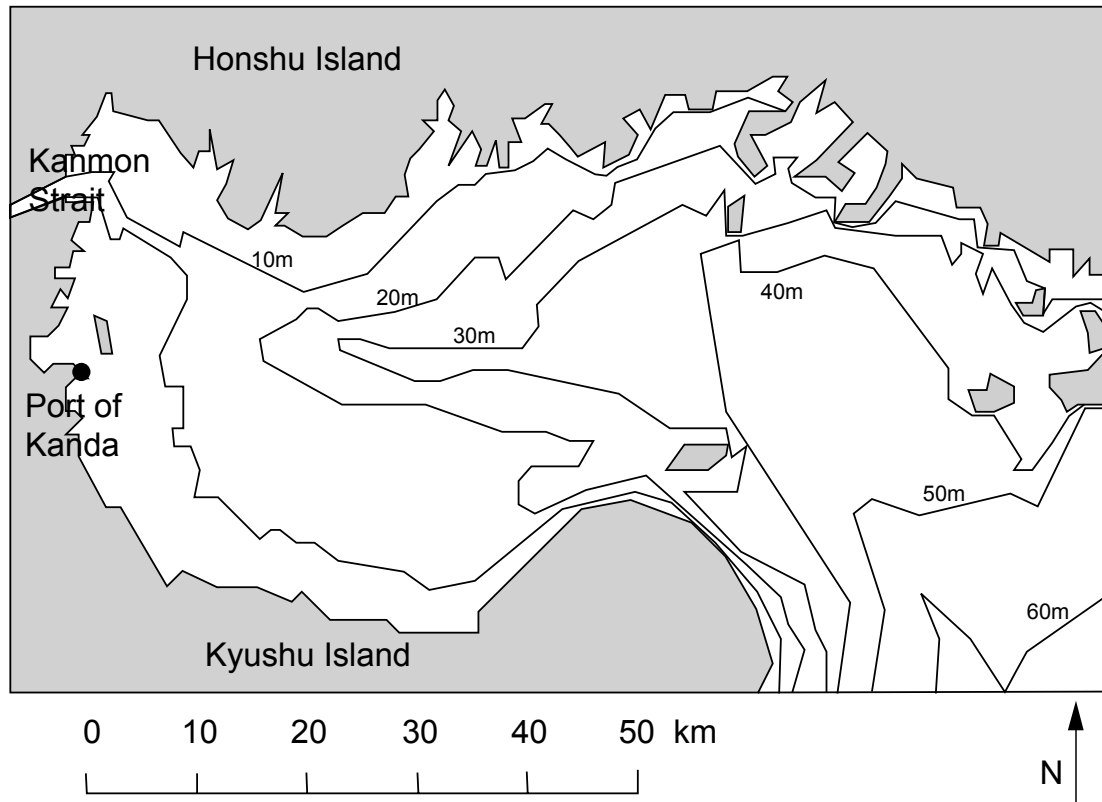
Figure 3-2: Suo-nada Bay geometry and bathymetry relative to low water level (after Kawai, 2004)

3.2   Background information on typhoons in general

3.2.1   Typhoons, Hurricanes and Cyclones
There are different basins around the world that encounter the typhoon phenomenon. Every basin uses own names for what is actually the same natural phenomenon. The names are given Figure 3-3. In the research the phenomenon will be denoted with typhoon. Some exceptions are made in cases where the name is explicitly described.
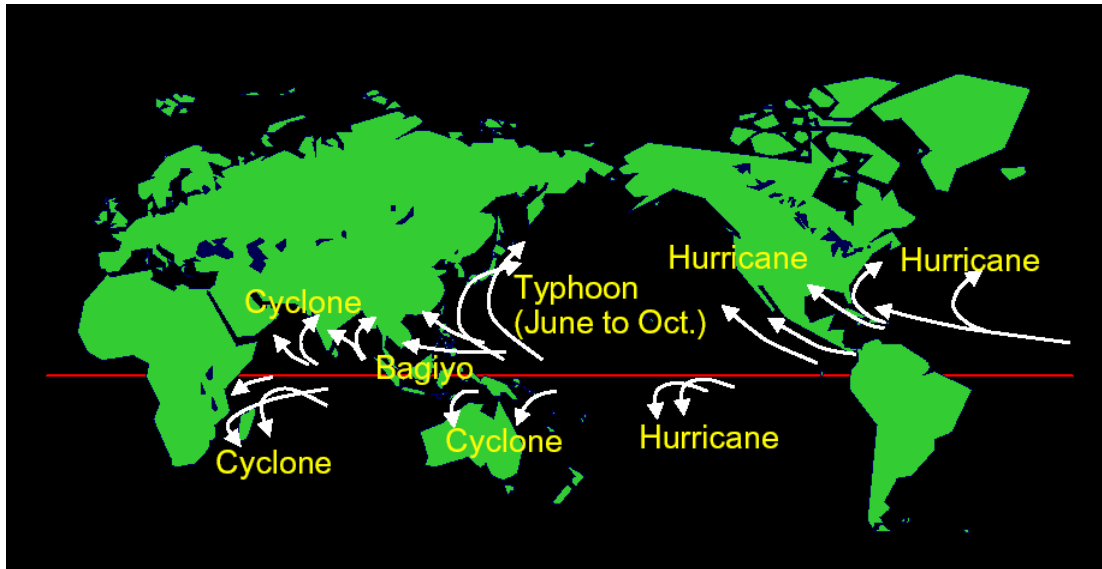
Figure 3-3: Origins and tracks of tropical typhoons together with the different names around the world (Kawai, 2004a)

3.2.2 Individual typhoon names
Two types of conventions are used to give names to typhoons: a number-based convention and a list-based convention. Number-based conventions are based on the sequential number from the beginning of a typhoon season. This kind of simplified two-digit (e.g. no. 14) convention is very popular in Japan and often used in the media. A four-digit (e.g. no. 0414) identification code is a more preferred convention in technical and professional areas. The first two digits denote the year of occurrence. In special cases, the Japan Meteorological Agency gives a name to the typhoon when it resulted in severe disaster or when significant meteorological phenomena were observed. In this case, the typhoon is usually named after that place or that accident. List-based conventions are based on a list of typhoon names defined in advance by the committee of meteorological organizations worldwide. A new name is automatically chosen from the list upon the genesis of a typhoon. Since five years a list of Asian typhoon names has been applied for the North West Pacific region instead of western names (agora.nii.ex.ac.jp).

3.2.3 Typhoon generation and typhoon movement
Typhoons are low-pressure weather systems that develop over warm ocean waters, mostly located between latitudes of 30ºS and 30ºN. The systems rotate counter clockwise in the northern hemisphere and clockwise in the southern. Tropical cyclone formation requires six concurrent conditions:

- Warm ocean waters of at least 26.5º Celsius to a depth of 50 meters minimal
- An atmosphere that cools rapidly vertically transforming stored heat energy from the water into thunderstorm activity that fuels the tropical system
- Moist layers at mid troposphere elevations (5 kilometres altitude)
- Significant Coriolis forces to rotate the cyclone
- Presence of a near surface organised rotating system with spin and low-level inflow
- Minimal vertical wind shear at varying altitudes that can slice apart the cloud mass

Since warm ocean water is the generative element, only the midsection of the planet can conceive typhoons. The pole-seeking centrifugal Coriolis force is needed to spin the thunderstorms into a closed circulation. Tropical cyclones cannot form within 500

kilometres of the Equator (Shultz et al., 2005). An overview of the anatomy of a northern hemisphere hurricane is given in Figure 3-4.
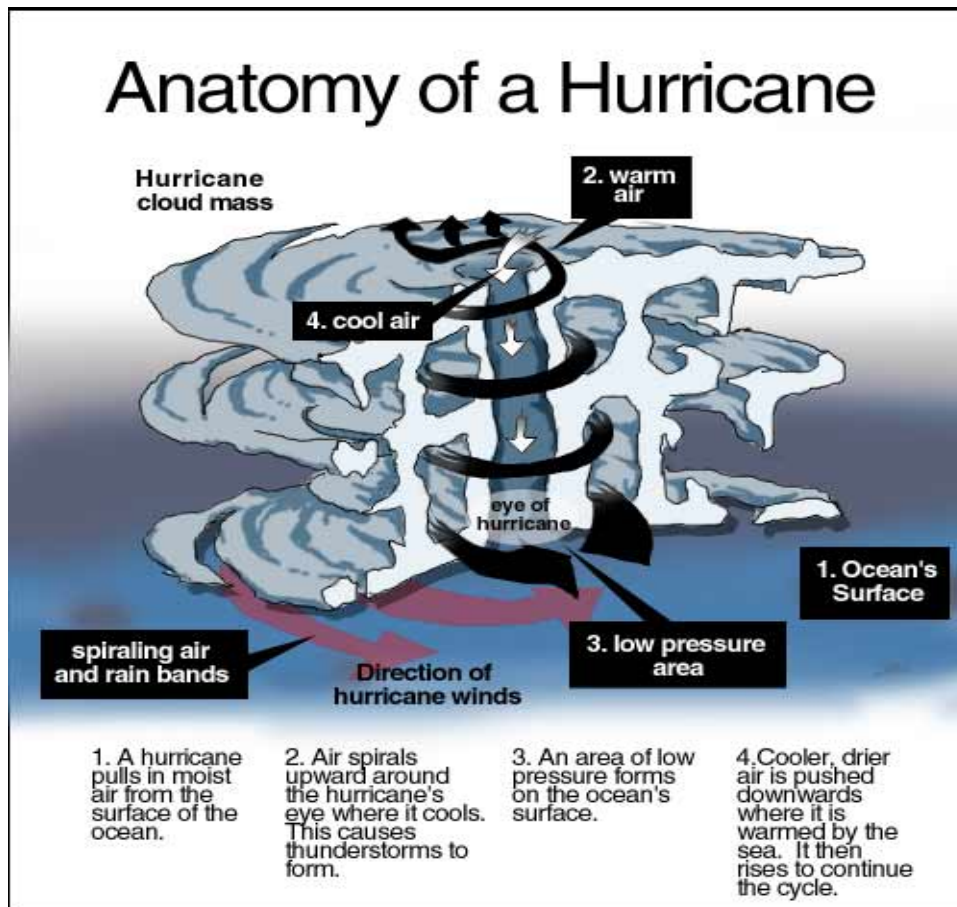
Figure 3-4: Anatomy of a hurricane (www.bocc.citrus.fl.us)

3.2.4 Typhoon paths for Japan

The typical typhoon season in Japan is between June and October. Typhoons originate in tropical regions and as they move north (in the northern hemisphere), caused by the Earth's rotation, they gradually weaken. This weakening is caused by the decrease in the sea surface temperature as the typhoon moves north, eventually resulting in the vapour supply falling short of the energy loss caused by friction. When a typhoon hits land, the vapour supply is completely cut off.

Typhoons are pushed by high-altitude winds. Therefore, typhoons move west (while gradually veering north) in low latitudes, since east winds are generally prevalent. When typhoons come to mid-latitude regions where strong west winds are blowing in high altitudes, typhoons move towards the northeast (Figure 3-3). In August, high-altitude west winds are still weak, so typhoon movement can be unstable. As a result, typhoons can meander and cause unexpected damage. After September, high-altitude west winds become stronger. This causes typhoons to move in an arc from southern seas towards Japan. Past typhoons that caused large damage, such as the Muroto Typhoon (1934) and the Ise Bay Typhoon (1959), followed this specific course (www.city.sendai.jp). After recurvature into westerly direction and the association with a colder environment, tropical cyclones lose their tropical characteristics. The size of the circulation usually expands, the speed of the maximum wind decreases, the translational (forward) speed of motion increases and the distribution of winds, rainfall and temperature becomes increasingly asymmetric (www.cnmoc.navy.mil/ japan).

3.2.5 Different scales to classify hurricanes and typhoons

Several scales are used to categorise hurricanes and typhoons, based on a combination of the hurricane characteristics of pressure, wind speed, storm surge and structural damage. The Saffir-Simpson scale is used for the Atlantic and Northeast Pacific basin and contains the destructive potential of hurricanes (Table 3-1). In Japan a scale of the Japan Meteorological Agency is used to classify typhoons (Table 3-2). The Beaufort scale (for wind speed) ends with category 12, with maximum sustained wind speeds above 118 km/h (appendix A). That is equal the lowest category on the Saffir-Simpson scale.

Table 3-1: Saffir-Simpson scale to classify hurricanes

Cat.	Maximum Sustained Wind (1-min mean)		Effects
	[kt]	[km/h]	
One	64-82	118-152	No real damage to building structures. Damage primarily to unanchored mobile homes, shrubbery, and trees. Also, some coastal road flooding and minor pier damage
Two	83-95	153-176	Some roofing material, door, and window damage to buildings. Considerable damage to vegetation, mobile homes, and piers. Coastal and low-lying escape routes flood 2-4 hours before arrival of centre. Small craft in unprotected anchorages break moorings.
Three	96-113	177-208	Some structural damage to small residences and utility buildings with a minor amount of curtain wall failures. Mobile homes are destroyed. Flooding near the coast destroys smaller structures with larger structures damaged by floating debris. Terrain continuously lower than 5 feet ASL may be flooded inland 8 miles or more.
Four	114-135	209-248	More extensive curtain wall failures with some complete roof structure failure on small residences. Major erosion of beach. Major damage to lower floors of structures near the shore. Terrain lower than 10 feet ASL may be flooded requiring massive evacuation of residential areas inland as far as 6 miles.
Five	135	>248	Complete roof failure on many residences and industrial buildings. Some complete building failures with small utility buildings blown over or away. Major damage to lower floors of all structures located less than 15 feet ASL and within 500 yards of the shoreline. Massive evacuation of residential areas on low ground within 5 to 10 miles of the shoreline may be required.

Table 3-2: Typhoon scale according to the Japan Meteorological Agency (www.agora.ex.nii.ac.jp)

JMA Category	Maximum Sustained Wind (10-min mean)		International Category	Class
	[kt]	[km/h]		
Tropical Depression	- 33	- 62	Tropical Depression (TD)	2
Typhoon	34 - 47	63 - 88	Tropical Storm (TS)	3
	48 - 63	89 - 118	Severe Tropical Storm (STS)	4
Strong Typhoon	64 - 84	119 - 156	Typhoon (TY) or Hurricane	5
Very Strong Typhoon	85 - 104	157 - 192		
Extreme Typhoon	105 -	193 -		

The scales illustrative the effects and wind speeds that can be caused by a typhoon. In this research the scales are not explicitly used. The characteristics that determine the scale and intensity of the typhoon are used instead.

3.3 Typhoon characteristics influencing hydraulic loads

3.3.1 Number of typhoon landings per year in Japan

Several typhoons hit the Japanese islands per year. An average of twenty-seven typhoons develops every year in the Northwest Pacific basin, from which approximately three hit Japan. In an extreme year this number can increase to ten typhoons (Figure 3-5).
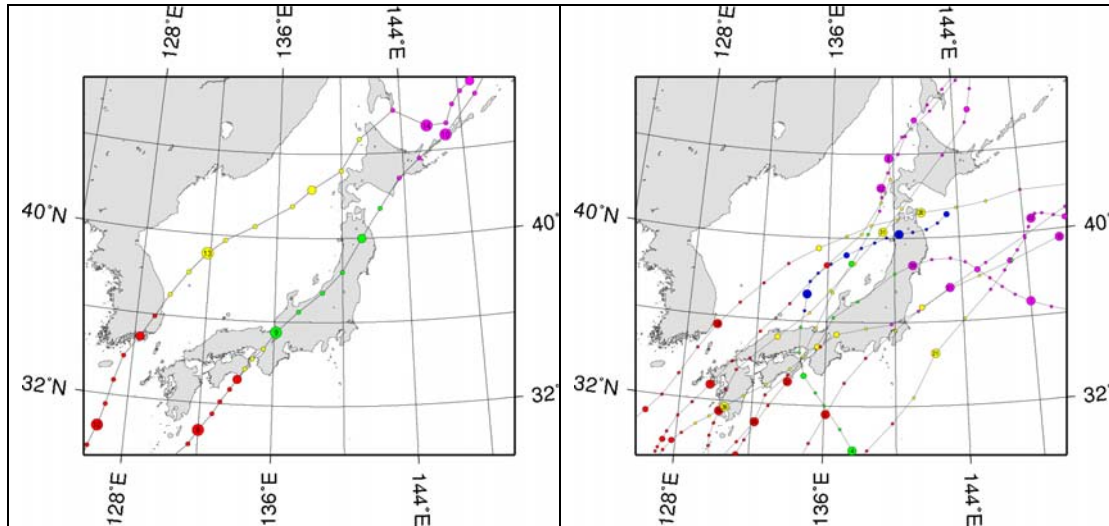
Figure 3-5: Number of typhoon landings on the Japanese main islands
For a normal year two typhoons (in 2003, left) and for an extreme year ten (in 2004, right) (agora.ex.nii.ac.jp)

3.3.2   Typhoon tracks over a bay

The typhoon track is of major influence on the possible occurrence of flooding. The highest wind speeds are located to the right (east) of the typhoon centre (northern hemisphere) and the direction of the wind relative to a bay depends on the typhoon track (Figure 3-6). Most Japanese bays have a north-south orientated bay axis. If a typhoon centre passes to the west of such a bay, a large amount of water piles up at the north end of the bay. In that case, the maximum winds right of the typhoon centre affect the bay precisely.

The typical typhoon track at Suo-nada Bay (east-west orientated bay axis) is going north through the bay. The wind that generates the storm surge piling up against the end of the bay is the easterly wind in the front quadrant of the typhoon field. The highest wind velocities to the right of the track also generate wind set-up, but the fetch length is more limited in that case (Figure 3-6).
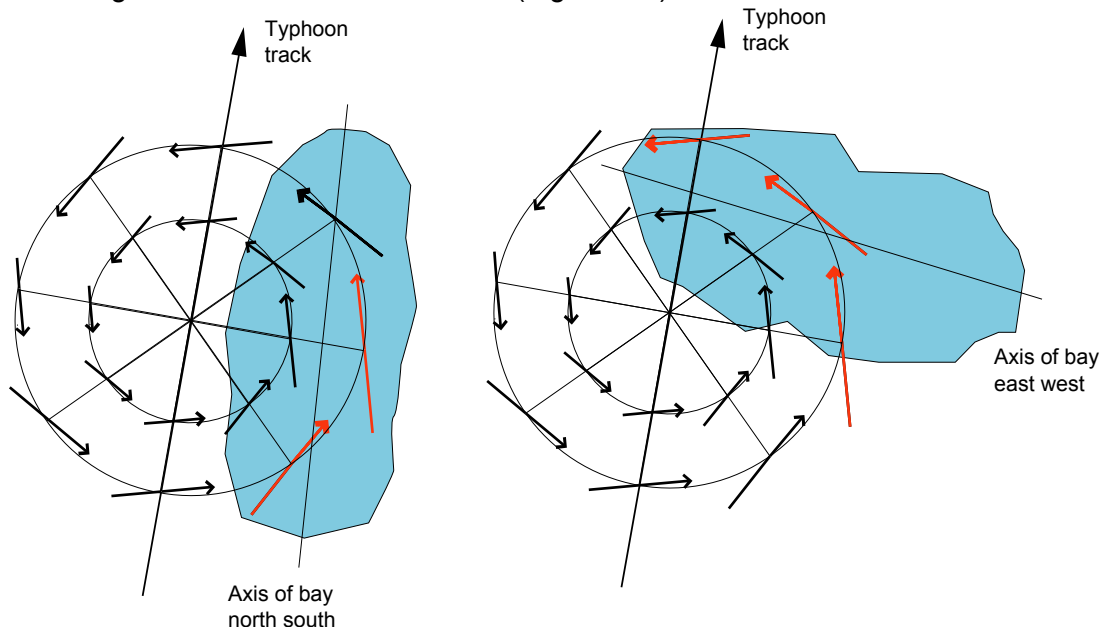
Figure 3-6: Different orientations of bay-axes relative to a typhoon track, with high wind speeds causing wind set-up and waves (after Kawai, 2004a)

3.3.3 Parameters that are used to describe a typhoon field

Typhoon wind fields can be well represented by a small number of parameters. The minimal atmospheric pressure of the typhoon centre indicates the intensity of the storm. Another parameter is used for the forward speed. The radius to maximum wind speed of the typhoon describes the size of the typhoon field (see Figure 3-7).
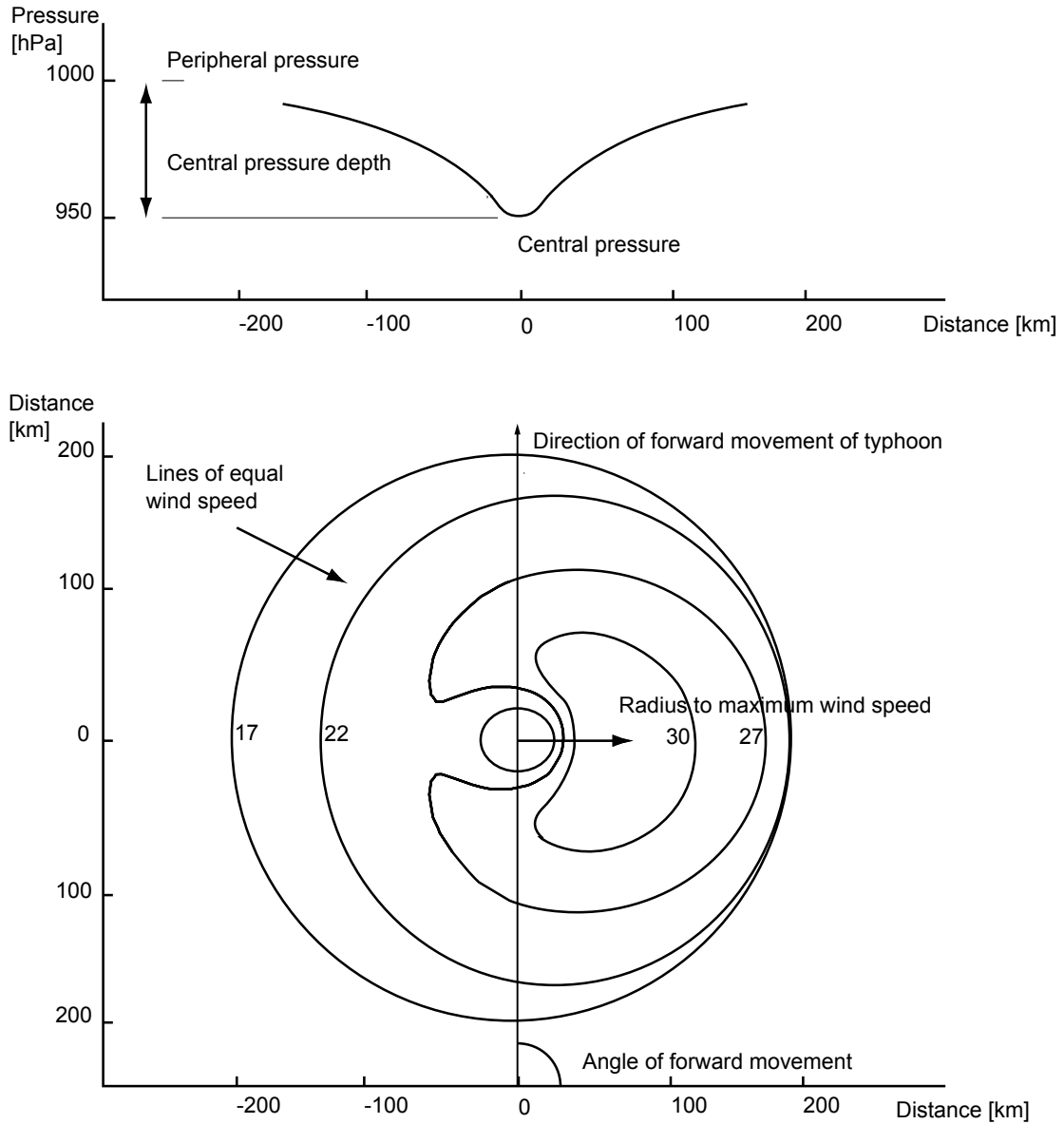
Figure 3-7: Parameters that describe a typhoon field for a typhoon with average parameters:
Pressure distribution (central pressure depth: 50hPa), magnitude of wind field (radius to maximum wind speed: 84 km) and angle of forward movement relative to a certain fixed direction (example: 90 degrees); wind speeds in m/s

3.4   Typhoon related storm surges

A storm surge may be visualised as a raised dome of water, moving with the typhoon, centred to the right of its path (northern hemisphere). The higher winds to the right of the typhoon centre originate from the summation of the round wind speed profile and the forward movement of the typhoon. The height of the storm surge is related to local pressure (i.e. a barometric effect) and to wind stress on the water caused by local winds. Contributing factors to the pressure and wind field are storm speed, direction of approach, bottom topography, and coincidence with high tide level (www.cnmoc.navy.mil/korea). Three different phenomena generate a storm surge:

- The suction effect of the decrease in atmospheric pressure or pressure set-up
- The wind drift effect or wind set-up
- Static wave effects caused by wave breaking or wave set-up

3.4.1   Pressure set-up
The increase in water level under the low pressure 'eye' of a typhoon is also known as the Inverse Barometer Rise effect or pressure set-up. The increase of the water level is concentric under the centre of the typhoon. A rule of thumb is that with every hectopascal decrease of atmospheric pressure, the water level rises with one centimetre.

3.4.2   Wind set-up
The increase in the mean water level due to the piling up of water on the shore is a result of friction between the typhoon wind and the water surface. The friction of the wind speed over the water surface results in inclination of the water level in situations with limited water depths. The wind set-up is not only dependent on the wind speed, but also on the fetch length and the water depth.

3.4.3   Wave set-up
The wave set-up can reach about ten percent of the offshore wave height. In the case of Suo-nada Bay, the waves break when entering the bay from the Pacific Ocean. This results in wave set-up over the entire bay. Since this effect is not observed separately in Suo-nada Bay, it is not directly taken into account in the research. The effect could have an influence on the water level.

3.4.4   Shoaling of storm surges
Because of shoaling, the speed and length of a wave decrease with a constant wave period. This affects the storm surge height. Whether the influence is visible for storm surges can be seen from hindcasted typhoons by the numerical model of the PARI. In appendix B the tracks of two typhoons (no. 0318 and no. 9810) and the computed resulting storm surges are given. The suction effect of the typhoon (pressure set-up), the wind drift effect (wind set-up) and the total increased water level (summation of the pressure set-up and the wind set-up) are given. The effect of shoaling on storm surge heights in Suo-nada Bay is negligible according to the simulation. This is probably due to the perpendicular direction of bay axis of Suo-nada Bay relative to the typhoon tracks. On average the direction of the typhoon is perpendicular to the bay axis. It is decided to neglect the shoaling effect related to storm surges.

3.5   Other physical phenomena related to the water level

3.5.1   Tidal water level
The tidal water level at Japan is a combination of different effects influencing the water level, such as the astronomical tide, the ocean current and the density of the (salt) water. There is a slight seasonal change in mean sea level. The mean sea level is maximal in autumn. If the typhoon storm surge and high tide occur simultaneously, the water level will be maximal. The impact of typhoons over the last decades depends on this joint occurrence of a typhoon with a high tidal water level. The tide system in the Suo-nada area is a semi-diurnal one with a range (high water level - low water level) of 3.5 to 4 meters.

3.5.2   Seiches
Seiches are standing waves or oscillations of the free surface of a body of water in a (semi closed) basin. These oscillations are of a relatively long period. The oscillations result primarily from changes in atmospheric pressure and the resultant wind conditions and occur over the entire basin. The frequency of oscillation is a function of the forcing mechanism, together with the geometry and bathymetry of the system. For Suo-nada Bay this effect has not been detected and is therefore not addressed in the research.

3.5.3   Relative sea level rise
An increase of $3°$ Celsius in temperature and 65 centimetres in sea level by the end of the 21st century is predicted for Japan (KSRGW, 1991). Because of the location of Japan on the boundaries of four continental plates, the ground level is going up or down gradually caused by crustal movement. Some Japanese researchers say that the relative sea level has been going up on the Pacific coast and going down on the Japan Sea coast. Since there is no univocal verdict on the Japanese sea level rise, it is not taken into account in this research.

3.5.4   Rain oscillations
Typhoons consist of massive clusters of cumulonimbus clouds with cyclonic rotation that cause large amounts of rain. Rain caused by typhoons includes the rain that falls from the typhoon itself, but also rain that falls from other weather fronts that are activated by the typhoon. Rain oscillation has not been detected during typhoons for Suo-nada Bay and is therefore not addressed in the research.

3.5.5   Tidal inlet hydrodynamics
If the entrance of a bay acts as a barrier to the incoming tide, a delay in the advance of the tide and a difference of head between the water outside and inside the inlet can be caused. Since the tide is observed inside the basin, the possible occurrence is already taken into account in the tide level. An evaluation of the inlet currents and tidal elevations is ignored.

3.6   Various types of wind-generated waves

Usually a distinction is made between two types of wind-generated waves: swell and locally generated waves. Swell is generated on the Pacific Ocean and penetrates into the Japanese bays. Locally generated waves are the result of the typhoon winds within the vicinity of the bay.

3.6.1   Locally generated waves by typhoons
Locally generated waves within the bay consist of the waves generated by typhoons. The storm waves by typhoons dominate extreme statistics in the Japanese region

that faces the Pacific Ocean (Goda, 2000). The typhoon-generated waves are much larger than those by other meteorological disturbances. Results of Young (1988) indicate that both the velocity of forward movement and the maximum wind velocity within a typhoon play an important role in determining the magnitude and the spatial distribution of the waves generated. The physics of the generation process of waves within typhoons is complicated by the rapidly turning winds and also by the lack of reliable field data. Locally generated wind sea can be seen in high frequency peaks with a broad directional distribution.

3.6.2   Swell generated by typhoons
Many of the wave spectra also have a lower frequency swell peak. Tracing this swell back reveals that it was generated in the intense wind region to the right of the typhoon centre (northern hemisphere). The wind velocity is maximal in this region and the wind direction is approximately parallel to the storm track. The waves that will dominate are those that remain in the high wind regions for a maximum time. So waves generated in this region move forward with the typhoon and maximise the time for which they experience strong winds. As the forward movement of the hurricane increases, the hurricane outruns the waves it generates and the region where the dominant waves are generated moves into the right rear quadrant.

3.6.3   Swell penetrating Suo-nada Bay
Suo-nada Bay is orientated in a way that the inner part is perpendicular to the direction of the bay entrance to the Pacific Ocean and therefore partly protected. The west minor entrance, the Kanmon Strait (Figure 3-2), is sufficiently narrow and curved to prevent waves from penetrating from the Japan Sea (Kawai, personal communication). In most cases, if the typhoon track changes from northwest to northeast direction, stagnation of the forward movement of a typhoon occurs at this turning point. If a typhoon stagnates at low latitude for a very long time and the wind duration increases to an extreme, waves can develop their energies rapidly (Komaguchi et al., 1990). The offshore waves generated by the typhoon system still have to travel to the bay. The increasing forward movement of the typhoon and the curved path into the bay, result in a small probability of joint occurrence of this type of swell and locally generated typhoon waves. Swell that was generated in the Roaring Forties hardly reaches Japan. The continent Australia and several islands (Malaysia, Indonesia, Papua New Guinea and New Zealand) are natural breakwaters for Japan (Kawai, personal communication). In general, swell occurs during a typhoon event and should be added to locally generated wind waves.

3.6.4   Waves observed at Suo-nada Bay
The simultaneous observation of the significant wave height and the peak wave period during historical typhoons (no 9117, 9119, 9210, 9313) are plotted in Figure 3-9. The wave steepness above a significant wave height of 0.5m is independent of the significant wave height and normally distributed as can be seen from Figure 3-8. The following equation can be stated for the wave steepness:

$$s_p(H_s, T_p) = \frac{H_s \cdot 2\pi}{g \cdot T_p^2} \tag{3-1}$$

s_p	Wave steepness	[-]
H_s	Significant wave height	[m]
T_p	Peak wave period	[s]
g	Gravity acceleration	[m/s^2]

This distribution is used to construct the lines in Figure 3-9. From this figure it can be seen that swell has occurred during typhoon events (region outside 95% interval with wave heights under 0.5m). Further, young swell (in a lake) will have a wave steepness of around 5%, independent of the wave height. In cases of swell the wave steepness will be around 1%. The average wave steepness in Suo-nada Bay of 3.16% therefore includes some swell. Since wave spectra are not available, the exact properties of swell cannot be stated. If the wave steepness relation is used for the computation of the wave period the value of the wave steepness (and therefore swell) is taken into account.
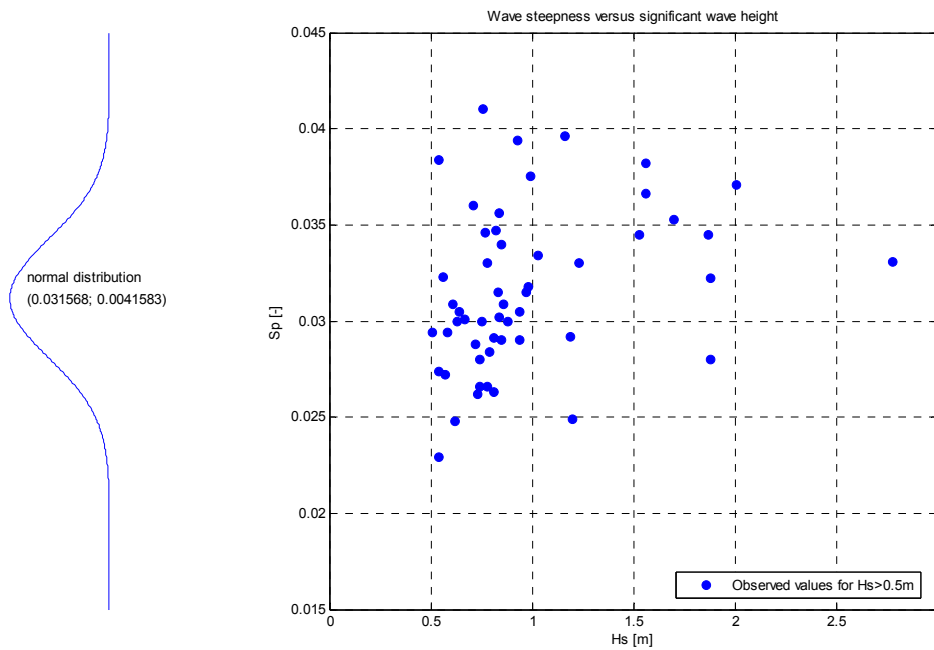
Figure 3-8: Independent wave steepness and wave height for wave heights above 0.5m with normal distribution of the wave steepness (typhoons 9117, 9119, 9210, 9313)
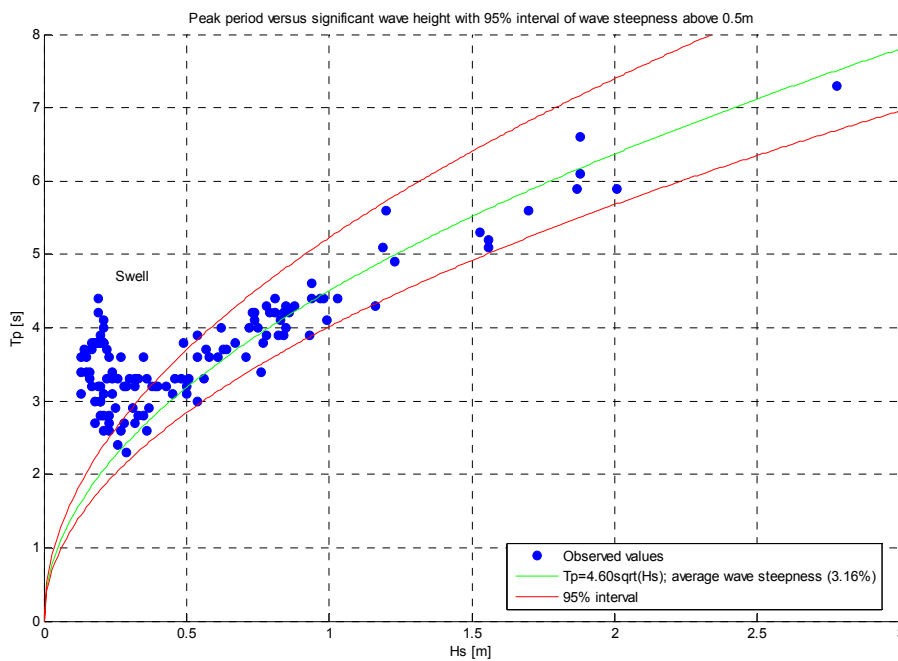
Figure 3-9: Peak periods plotted against significant wave heights during typhoons (no 9117, 9119, 9210, 9313)

3.7   Scheme of phenomena taken into account in the research

In the previous paragraphs different phenomena are described and their influence on the hydraulic boundary conditions. For simplicity reasons and because of the limited availability of data, not all effects that contribute to the hydraulic variables are taken into account. An overview of the phenomena used in the analysis is given in a diagram together with the phenomena that are left out as described in the previous paragraphs (Figure 3-10).
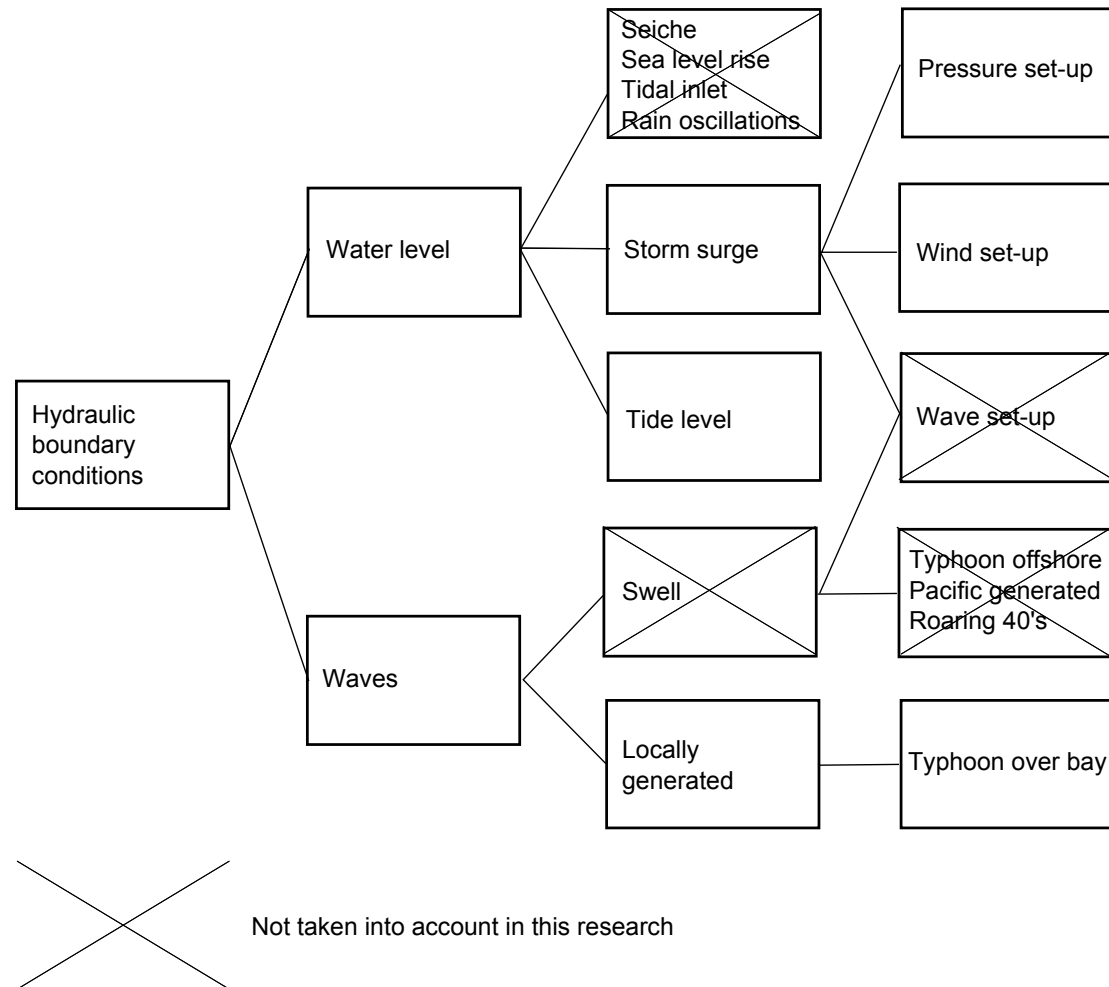
Figure 3-10: Diagram of the hydraulic phenomena that are taken into account in the research

4 Models for physical phenomena related to typhoons and the hydraulic loads

In this chapter, different models related to the typhoon induced hydraulic loads will be reviewed. The applicability of the models to the Japanese situation is discussed and a choice is made as to which models are used in the further analysis of the hydraulic boundary conditions. A calculation schedule is presented with the relations between the models to obtain the hydraulic boundary conditions. Further, the schematisations and simplifications that are done in order to apply the models are pointed out.

4.1 Various models used for the description of the physical phenomena

An analysis of simple analytical models that describe the physical phenomena is done. Numerical models are not applied, because of the computational burden if used in a Monte Carlo simulation, in comparison with simple analytical models. Further, the mutual relations of the different variables are more evident if they are expressed in analytical formulae. In Appendix C the different models pointed out in this paragraph are described more in detail. The formulae of the models are given in paragraph 4.4 and onward.

4.1.1 Manuals of the USACE[3]

There are different manuals that provide information about hydraulic loads generated by typhoons. The Shore Protection Manual and the Coastal Engineering Manual, mainly based on hurricanes that have passed through the Gulf of Mexico, are analysed.

- *Shore Protection Manual (1977 and 1984)*

The Shore Protection Manual gives the model of Myers (1954) for the description of the spatial distribution of atmospheric pressure and the resulting wind field for slowly moving hurricanes. The pressure distribution can be derived from the central and peripheral pressure, together with the radius to maximum wind speed. Further, models are given to calculate the wave height and period with the help of the same variables used as input for the atmospheric pressure model of Myers (1954).

- *Coastal Engineering Manual (2002-2003)*

The Coastal Engineering Manual gives the model of Holland (1980) for the description of the spatial distribution of atmospheric pressure for slowly moving hurricanes. From this spatially distributed atmospheric pressure field, the spatial distribution of the wind speed can be derived.

---

[3] United States Army Corps of Engineers

4.1.2   Parametric Hurricane models

Two parametric models for the prediction of hurricane wave characteristics have been analysed: the model of Cooper and the model of Young. Both models are applicable to deep-water conditions.

- *Cooper's model (1988)*

With Cooper's model a spatial distribution of the wind speed can be computed based on different input variables (e.g. direction of movement of the typhoon, pressure difference between the typhoon centre and the outer edge of the hurricane, forward movement of the hurricane and the radius to maximum wind speed). The wave height is assumed to be 25% of the local wind speed. The wave period is computed with the wind speed and the angle of forward movement of the typhoon. The average wave direction can be computed with the radius to maximum wind speed and the direction of forward movement of the hurricane.

- *Young's model (1988)*

Young created a hurricane wave prediction model based on results from simulations with a numerical spectral model. Given some typhoon parameters (e.g. forward movement of the hurricane, maximum wind velocity and radius to maximum wind speed), the wave characteristics can be determined. The significant wave height and period can only be derived if spatial distribution diagrams, based on simulations, are used.

4.1.3   Models used in Japan

There have been a number of studies in Japan related to typhoons. Only a few are described here. First, the model used by the PARI is discussed. Further, different models from the Japanese Journal of Natural Disaster Science[4] are given and a model applied by Kato et al. (2002) is described.

- *Models used by the PARI (Kawai et al., 2004)*

The PARI uses the model of Myers (1954) to describe the spatial distribution of the atmospheric pressure. Further, numerical models based on the finite difference method and non-linear long wave-approximation-theory are used to calculate storm surges. A third generation numerical wave prediction model WAM (WAMDI, 1988) is used.

- *Models described in the JNDS (1979-now)*

In the JNDS the model of Schloemer (1954) is used to describe the spatial distribution of the atmospheric pressure. This model depends on the same typhoon parameters as the model of Myers (1954). With the help of this spatial distribution of the atmospheric pressure field, the spatial wind speed distribution can be computed. With the Blaton formula, the forward movement of the typhoon is added to the circular typhoon wind field. A simple model is given to compute the pressure set-up, using the pressure difference between the typhoon eye and the peripheral pressure. The wind set-up is computed as a part of this pressure set-up.

- *A model used by Kato et al. (2002)*

Kato et al. (2002) use the model of Myers (1954) to describe the spatial distribution of the atmospheric pressure and the spatial distribution of wind speed. A model of the Japan Meteorological Agency (1999) determines the total storm surge as a function of the angle to the critical wind, the wind speed and the central pressure of the typhoon as input variables. The significant wave height and period are computed with the Sverdrupp, Munk (1947) and Bretschneider[5] (1952 and 1958) model. The wind speed, the fetch length and the water depth are input variables for the SMB model.

---

[4] Further stated as JNDS
[5] Further stated as SMB model

4.1.4 Models applied in studies for the Gulf of Mexico

Two works are described here concerning Jamaica (Gulf of Mexico). Banton et al. (2002) give a method to calculate hurricane waves and Smith Warner International Ltd. (1999) describes some models for hurricane storm surge calculations.

- *Banton et al. (2002)*

Banton et al. (2002) derived an empirical formula to determine the central pressure of a hurricane depending on the maximum wind speed. From the central pressure of a hurricane, the radius to maximum wind speed is computed empirically. The wave characteristics are computed with the parametric hurricane model of Cooper (1988).

- *Smith Warner International Ltd. (1999)*

At Smith Warner International Ltd. (1999) a formula from the SPM'84 is applied for the calculation of the pressure set-up (Inverse Barometer Rise) caused by the low atmospheric pressure of the typhoon field. The pressure set-up is calculated with the peripheral pressure, the central pressure and the radius to maximum wind speed. For the wind set-up, generated by the wind field of a typhoon, a formula (SPM'77) is applied using the quadratic wind speed, the fetch length and the water depth as input variables.

4.1.5 Models applied to the North Sea

Three approaches are summarised which have been used to analyse the (not typhoon related) hydraulic boundary conditions for the Dutch coast (i.e. the methods of Vrijling and Bruinsma (1980), Webbers (2000) and Voortman (2002a)).

- *Vrijling and Bruinsma (1980)*

The Weenink (1958) model is used for the calculation of the wind set-up during a storm, with the quadratic wind speed as input variable. The astronomical tide level is added to the wind set-up, to derive the total water level during a storm. The wave height is computed with the SMB model.

- *Webbers (2000)*

Webbers (2000) extends the method of Vrijling and Bruinsma (1980). A wave steepness model is used to calculate the wave period using the wave height and the wave steepness.

- *Voortman (2002a)*

Voortman (2002a) extends the method of Vrijling and Bruinsma (1980) to an omni-directional model (for wind set-up, wave height and period). The characteristic wind direction and the direction dependent geometry determine in this case the hydraulic variables.

4.2 Qualitative evaluation of the described models

4.2.1 Applicability of the models

The models, described in the previous part, can be evaluated on their applicability to Suo-nada Bay. This is done qualitatively and not based on calculated values. The following criteria are important for extracting the models that will be used in this research:

- Input and output parameters of the physical models must fit into a total combined model to calculate the hydraulic loads
- Validity to the situation of Suo-nada Bay

- Models described in the manuals of the USACE

For the spatial distribution of pressure the model of Myers and Holland are given in the manuals of the USACE. The Schloemer formula is found in other literature. The models of Myers and Schloemer are actually the same. Both give concentric circular isobars for the pressure profile and the pressure depth decays exponentially from the

centre of the typhoon. Holland extends the Schloemer formula by adding an extra constant. In an investigation of the pressure of typhoon Bart (Fujii et al., 2002), the Holland formula resulted in the original Schloemer formula. The forward movement of the typhoon is not (yet) included in the formulae. Since in the Japanese situation, the Holland formula transforms into the other, only the Myers/Schloemer model remains.

- Parametric hurricane models

The possibility to use the parametric hurricane models for wave predictions is limited because they are specially developed for deep-water conditions.

- Models used in Japan

The PARI uses numerical models to derive the storm surges and wave characteristics caused by typhoons. Numerical models are not used in this research. Kato et al. (2002) on the other hand performed an analysis using an analytical model proposed by the JMA (JMA, 1999) for several Japanese Bays. This simple analytical model combines a pressure set-up model and a quadratic wind set-up model to compute the storm surge. The SMB model is used for wave predictions. Unfortunately, the parameters of the model have not been defined for Suo-nada Bay. Estimating all parameters is not possible with the available information and therefore this model is not applied.

- Models applied in studies for the Gulf of Mexico

The model of Banton et al. (2002) gives formulae calibrated to the Jamaican situation. It applies the parametric deep-water hurricane model of Cooper (1988) and is therefore not of interest to Suo-nada Bay. Smith Warner International Ltd (1999) gives some useful models for estimating the wind set-up and pressure set-up. These models both originate from the SPM. The pressure set-up model is described with the same kind of expression as the atmospheric pressure formula of Schloemer.

- Models applied to the North Sea

The models that are applied to the North Sea use the quadratic wind speed model for the calculation of the wind set-up. For wave height and period predictions the SMB model is used. Also the wave steepness model is used to compute the wave period.

4.2.2   Available statistics for input variables

From the method described in chapter 2, it was clear that in order to obtain the probabilistic distribution of hydraulic boundary conditions, the probabilistic input distributions of typhoon characteristics are needed. The determination of the minimum atmospheric pressure, radius, progression speed and track of typhoons is essential to be able to model typhoons. Also the number of landings in a year is important.

A research into available statistics of typhoon characteristics has been done. For the Japanese main islands the statistical properties of typhoon characteristics at the time of landing and their change after landing have been investigated. These works have been done for the Standard Project Typhoon (Mitsuta, 1965) and provide general typhoon specifications, geographically and meteorologically consistent, for typhoon protection works. The analysis of pressure patterns of typhoons hitting the Japanese islands of Kyushu, Shikoku, Honshu and Hokkaido was done. Only severe typhoons from 1951 onward were used with a central pressure below 980 hectopascal at the time of landing. Mitsuta et al. (1979) used the Schloemer formula to describe the spatial distribution of the atmospheric pressure field, because the cyclostrophic wind speed profile balancing to the pressure profile was more realistic than other profiles. The typhoon parameters of central pressure depth, radius to maximum wind speed, forward movement and angle of forward movement were determined at the time of landing of the typhoons on the boundary of sea and land. Also the average changes of these characteristics during the hours after landing are given. For individual typhoons, the characteristics are stated by Fujii (1998) (Appendix D). These characteristics are obtained in the same way as the statistical properties. The

individual characteristics can be used to calibrate the model for individual typhoons and this calibrated model can be used for the statistical analysis.

4.2.3   Choice of models used in the combined method

The Myers/Schloemer model remains for the description of the atmospheric pressure distributions, according to the discussed analyses of typhoons in Japan. The models of Myers and Schloemer are actually the same. The model will be referred to as Schloemer model in the further research.

For the surface lifting or pressure set-up there are different formulae. Nakagawa et al. (1995) give a formula related to the difference between the peripheral pressure and the pressure. The Japan Meteorological Agency gives a formula for storm surges (see Kato et al., 2002) that sums the wind set-up and the pressure set-up. In that formula the pressure set-up is the same for the entire typhoon field because it only depends on the central pressure of the typhoon. The formula for pressure set-up by Smith Warner International Ltd. (1999)) is similar to the pressure formula given by Schloemer (i.e. related to the distance from the centre). This one is chosen because it is related to the total pressure field. From the earlier mentioned pressure field parameters the surface lifting can be calculated.

According to Nakagawa et al. (1995), the wind set-up is equal to the pressure set-up. Other authors use the quadratic relation between wind speed and wind set-up (i.e. SPM'77, Kato et al. (2002), Smith Warner International Ltd. (1999), Vrijling and Bruinsma (1980)). Besides that, the wind set-up is dependent on the fetch length and the water depth. This seems physically correct, since the force resulting from the wind on the water surface should be in equilibrium with the inclination of the water level. The quadratic relation of wind set-up and wind speed will be used.

To calculate the significant wave height many authors (e.g. SPM'77, Kato et al., 2002, Vrijling and Bruinsma, 1980) use the empirical SMB-model. There is a model for the significant wave height and a model for the significant wave period. These models use the wind speed, water depth and fetch length to derive the significant wave height and period. Because of its simplicity, this model is also used in this research. The peak wave period can also be computed on the basis of the wave steepness relationship (see Webbers, 2000) that relates the peak period with the significant wave height by means of the wave steepness.

4.3   A combined model to derive the joint typhoon related hydraulic variables

The hydraulic variables can be derived from different input variables and dependence models combined in a model. The input variables are given for historical typhoons, which enables the deterministic calibration of the model. Also the statistical properties of the input variables are given. Therefore the same dependence model can be used for the analysis of the probability distributions of the hydraulic loads. The scheme with the mutual relations between the input variables and the hydraulic boundary conditions is given in Figure 4-1.
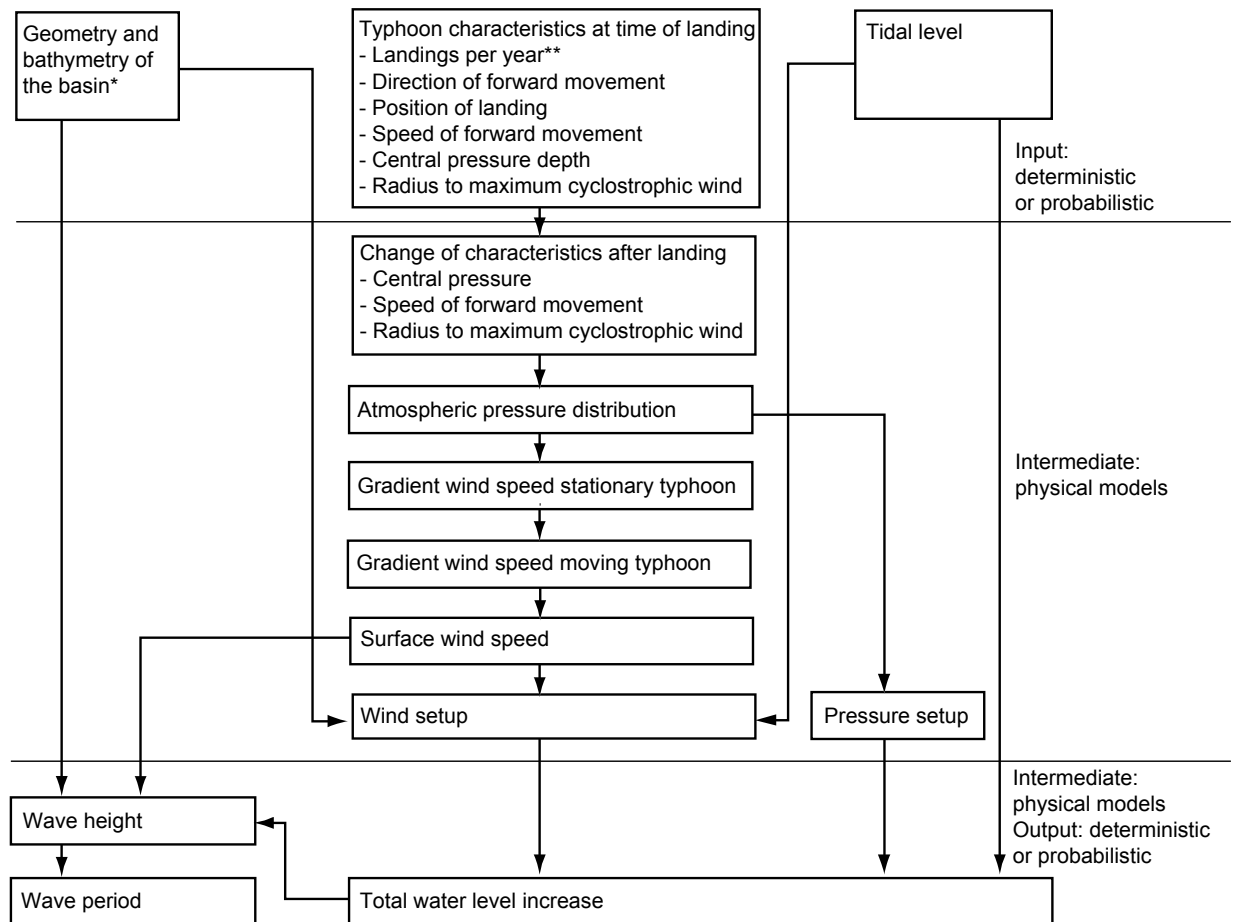
Figure 4-1: A combined model that determines the hydraulic boundary conditions with different input variables
* In both cases only deterministically determined
** This input variables is only used in the statistical analysis

The concurrent occurrence of water levels and wave heights follows directly from the combined model[6]. The tidal level influences the wind set-up. The wind set-up, pressure set-up and tidal level influence the wave height and the wave period.

_____

[6] Referred to as 'combined model' in the further report; not to be confused with the 'combined method'

4.4 Change of typhoon characteristics after landing

After the landing of the typhoon, the typhoon characteristics change. In the analyses from Mitsuta and Fujii (1979, 1986), the characteristics are determined at the moment of typhoon eye landing. The change rates are determined starting from that moment. The position of the change of typhoon characteristics relative to the total model is given in Figure 4-2.
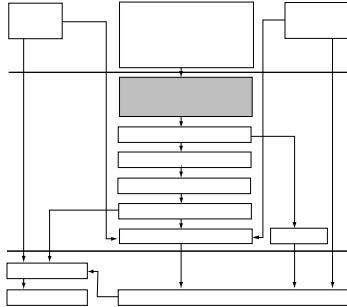
Figure 4-2: Position of change of typhoon characteristics relative to the total model

The central pressure depth decreases after landing. This phenomenon is referred to as the filling rate. Intense typhoons have larger filling rates than weak ones. The filling rate of the pressure depth with time after landfall can be given with a formula of Matano (1956).

$$\Delta p(t) = \Delta p_0 \exp(-a_p t) \tag{4-1}$$

$\Delta p(t)$	Central pressure depth in time	[hPa]
Δp_0	Central pressure depth at time of landing	[hPa]
a_p	Change rate of pressure depth	[1/h]
t	Time after typhoon landing	[h]

The typhoon parameters of forward movement and radius to maximum cyclostrophic wind are assumed to change with linear trends. The following equations are used:

$$r_m(t) = r_{m0} + a_r t \tag{4-2}$$

$$C_{fm}(t) = C_{fm0} + a_c t \tag{4-3}$$

$$\gamma(t) = \gamma_0 + a_d t \tag{4-4}$$

r_{m0}	Radius to maximum wind at time of typhoon landing	[km]
$r_m(t)$	Radius to maximum wind after typhoon landing in time	[km]
a_r	Change rate of radius to maximum wind	[km/h]
C_{fm0}	Forward movement of typhoon at time of landing	[km/h]
$C_{fm}(t)$	Forward movement of typhoon after typhoon landing in time	[km]
a_c	Change rate of forward movement	[km/h^2]
γ_0	Direction of forward movement at time of typhoon landing	[deg]
$\gamma(t)$	Direction of forward movement after typhoon landing in time	[deg]
a_d	Change rate of direction of forward movement	[deg/h]
t	Time after typhoon landing	[h]

An example of the change in typhoon characteristics after typhoon landing is given in Figure 4-3.

Change in typhoon characteristics of typhoon 8513 after landing
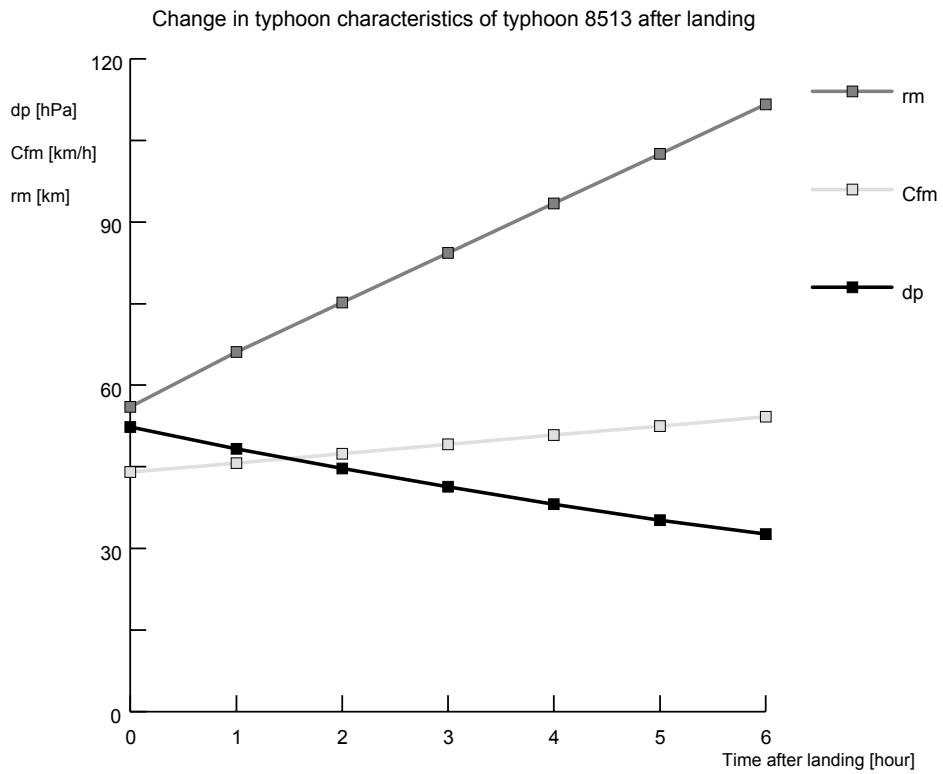
Figure 4-3: Example of change in typhoon characteristics after landing of typhoon no. 8513
(Characteristics used: Δp_0 = 52,3hPa; a_p = 0.079/h; r_{mo} = 52km; a_r = 5.0km/h; C_{fm0} = 42km/h; a_c = 2.7km/h^2)

4.5   The model that describes the atmospheric pressure distribution

With some of the input typhoon characteristics and the change in these characteristics the typhoon pressure field can be described (Figure 4-4)
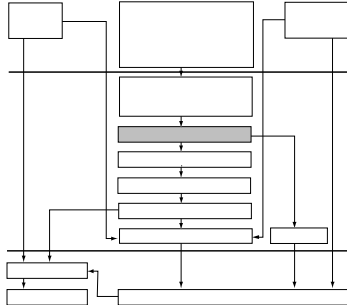
Figure 4-4: Position of pressure distribution relative to the total model

The Schloemer formula for the spatial distribution of the atmospheric pressure is given in equation:

$$p = p_c + \Delta p e^{-(r_m / r)} \qquad\qquad (4\text{-}5)$$

p	Atmospheric pressure at a distance from the typhoon centre	[hPa][7]
p_c	Central sea level pressure	[hPa]
Δp	Central pressure depth	[hPa]
r_m	Radius to the maximum cyclostrophic wind speed	[km]
r	Distance from typhoon centre	[km]

Figure 4-5 gives the estimated pressure profile of typhoon Bart (no. 9918). Input parameters stated by Fujii et al. (2002) are used.
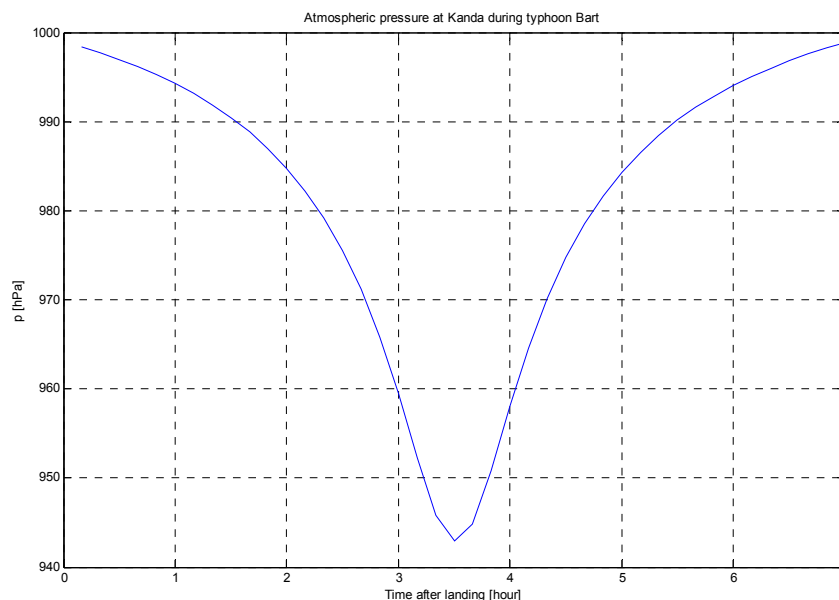
Figure 4-5: Pressure profile of Typhoon Bart (no.9918) from the moment of landing at Kanda, Suo-nada Bay (Characteristics used: Δp = 73hPa; r_m = 42km; C_{fm} = 56km/h; no change rates included)

---

[7] Meteorologists worldwide have measured atmospheric pressure in millibars for a long time. After the introduction of SI units, many preferred to preserve the customary pressure figures. Therefore, meteorologists use hectopascals today for air pressure, which are equivalent to millibars.

4.6   The model that describes the wind field

From the pressure distribution, the wind field can be derived. First the gradient wind speed is described, then the gradient wind speed for moving typhoons and finally the surface wind speed. The wind field phenomena related to the pressure field, relative to the total model of Figure 4-1 is given in Figure 4-6.
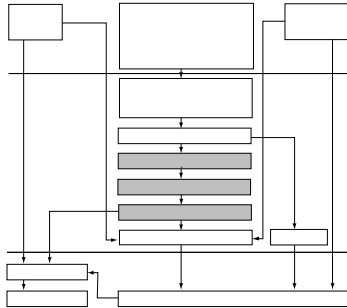
Figure 4-6: Relation between wind speed models relative to the total model

4.6.1   Atmospheric pressure field - gradient wind distribution

The equation of motion provides a formula to derive the gradient wind speed (or friction free wind) from the Schloemer (1954) formula for atmospheric pressure (see Mitsuta et al., 1986):

$$\frac{V_{gr}^2}{r_t} + fV_{gr} = \frac{1}{\rho}\frac{\partial p}{\partial r} \qquad (4\text{-}6)$$

V_{gr}	Gradient wind speed	[m/s]
r_t	Radius of the curvature of trajectory	[m]
f	Coriolis parameter $8.34 \ 10^{-5}$ /s	[1/s]
ρ	Air density 1.1 kg/m^3 (960hPa, 300K)	[kg/m^3]
p	Atmospheric pressure	[hPa]
r	Radius from typhoon centre	[m]

4.6.2   Gradient wind distribution - gradient wind for moving typhoons

The isobars of a typhoon are modelled to be circular. However if a typhoon moves forward with a constant speed, the radius of the trajectory of the air parcel differs from the radius of an isobar. The relation is described with the formula of Blaton (Figure 4-7):

$$\frac{1}{r_t} = \frac{1}{r}\left(1 + \frac{C_{fm}}{V_{gr}}\sin\theta\right) \qquad (4\text{-}7)$$

r	Radius of an isobar	[m]
r_t	Radius of the curvature of trajectory	[m]
C_{fm}	Forward movement of typhoon	[m/s]
V_{gr}	Gradient wind speed	[m/s]
θ	Direction angle of radius vector from direction of typhoon movement	[º]

Stationary typhoon   Forward movement   Resulting wind speed
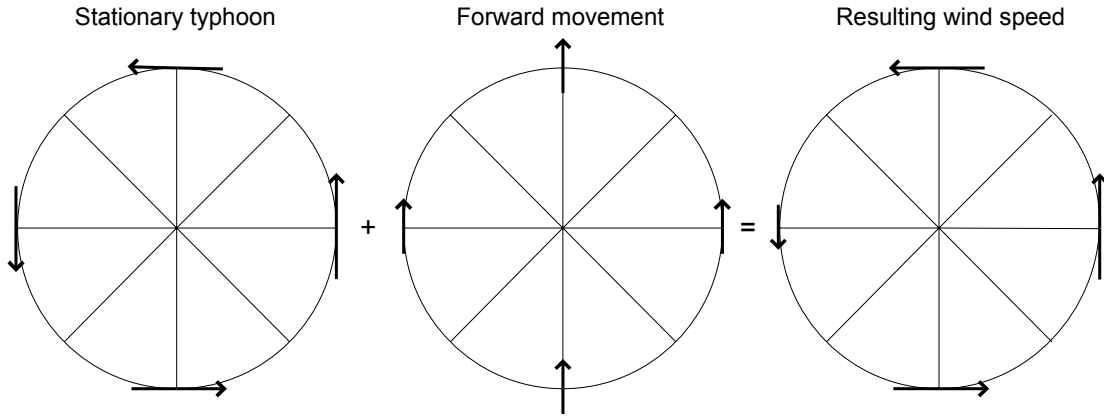
Figure 4-7: Effect of Blaton formula on wind speeds for moving typhoons

If the Blaton formula is substituted in the formula for gradient wind speed, the following relation can be derived for the gradient wind speed:

$$V_{gr} = \frac{1}{2}\left\{-(C_{fm}\sin\theta + rf) + \sqrt{(C_{fm}\sin\theta + rf)^2 + \frac{4\Delta p r_m}{\rho_a r}\exp\left(\frac{-r_m}{r}\right)}\right\} \qquad (4\text{-}8)$$

V_{gr}	Gradient wind speed	[m/s]
C_{fm}	Forward movement of typhoon	[m/s]
θ	Direction angle of radius vector from direction of typhoon movement	[º]
r_t	Radius of the curvature of trajectory	[m]
f	Coriolis parameter 8.34 10^{-5} /s	[1/s]
ρ	Air density 1.1 kg/m^3 (960hPa, 300K)	[kg/m^3]
Δp	Central pressure depth	[hPa]
r	Radius from typhoon centre	[m]

The spatial distribution of the gradient wind with average typhoon characteristics is given in Figure 4-8.
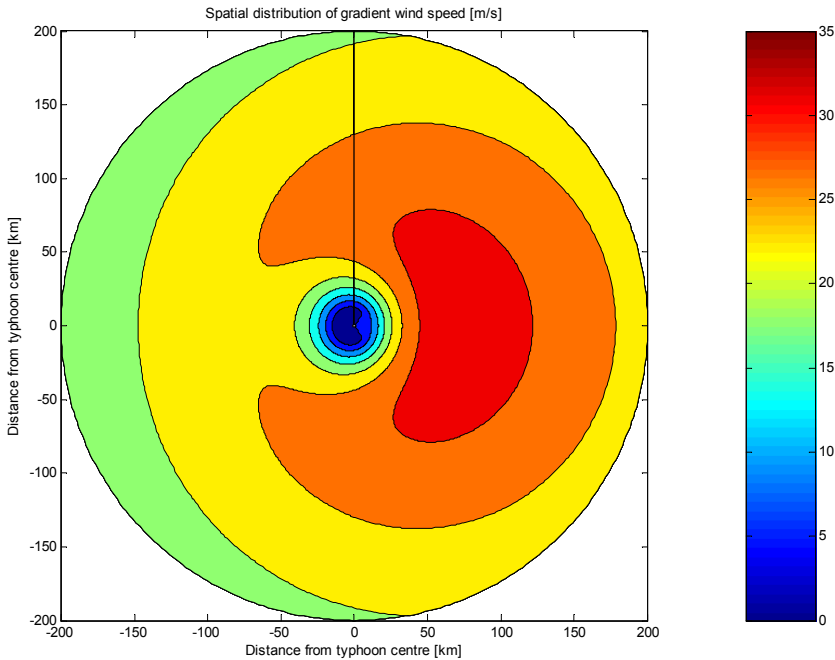
Figure 4-8: Gradient wind speed distribution (with average Δp=47hPa; r$_m$=84km; C$_{fm}$=33.7km/h; northward movement)

4.6.3 Gradient wind - surface wind

The surface wind speed is decelerated and deflected from the gradient wind speed by surface friction. Classical consideration (Brunt, 1939) shows that the surface wind speed can be calculated with the following formula:

$$V_s = V_{gr}(\cos\alpha - \sin\alpha) \tag{4-9}$$

V_s	Surface wind speed	[m/s]
V_{gr}	Gradient wind speed	[m/s]
α	Deflection of the surface wind direction from the isobar	[º]

The ratio Vs/Vg is 0.5 over flat land and therefore α would be 25º. Over water this ratio is 0.7, with a deflection angle of 15º. In literature a ratio of 2/3 is often used. This corresponds to an angle of deflection of the surface wind direction from the isobar of 17º. This value will be used if this formula is applied.

In a more extended form, Mitsuta and Fujii (1987) give a formula for the surface wind relative to the gradient wind that was derived from data obtained from two typhoons (no.7705 and no.7709). This relation is used in several Japanese analyses (e.g. Kawai et al., 2004):

$$\frac{V_s}{V_{gr}} = G(\infty) + \left\{G(\xi_p) - G(\infty)\right\}\left(\frac{\xi}{\xi_p}\right)^{m-1} \exp\left[\left(1-\frac{1}{m}\right)\left\{1-\left(\frac{\xi}{\xi_p}\right)\right\}^m\right] \tag{4-10}$$

$G(\xi_p)$	Coefficient (2/3)	[-]
$G(\infty)$	Coefficient (1.2)	[-]
ξ	Ratio between distance and radius to maximum wind speed	[-]
ξ_p	Coefficient (0.5)	[-]
m	Coefficient (2.5)	[-]
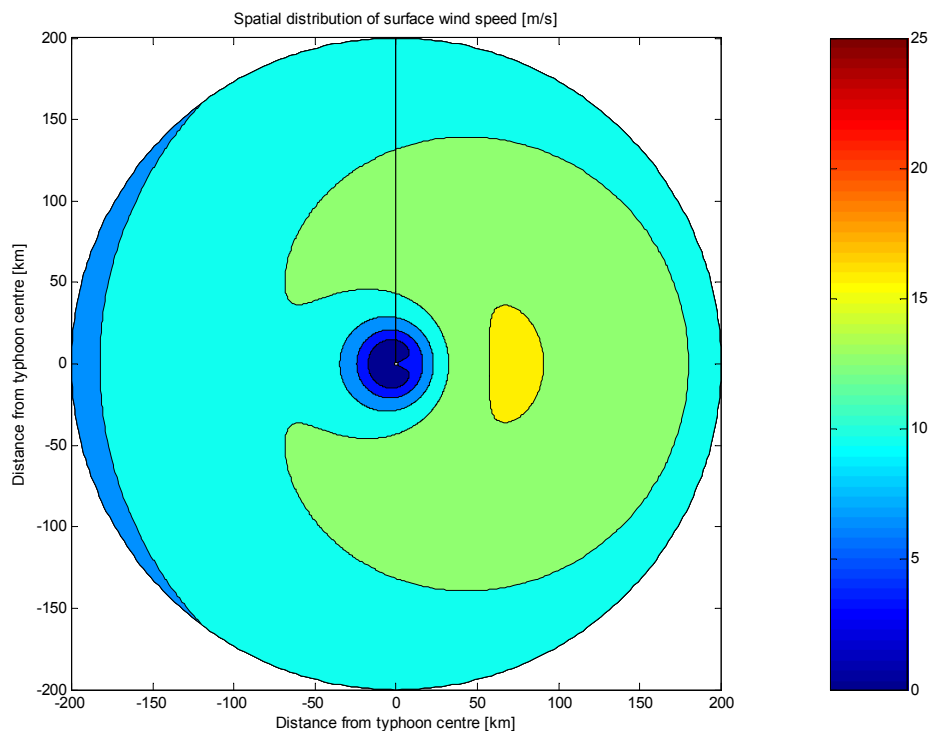
Figure 4-9: Surface wind speed distribution (with average Δp=47hPa; r_m=84km; C_{fm}=33.7km/h; V_s/V_{gr} = 0.67; northward movement)

4.7   The models that describes the storm surge

As mentioned earlier, in this model, the wind set-up and pressure set-up are responsible for storm surges (relative to the combined model see Figure 4-10).
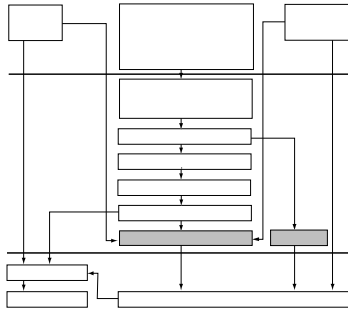
Figure 4-10: Position of storm surge phenomena relative to the total model

4.7.1   Pressure set-up
The formula given by Schloemer is used for the description of the pressure set-up. is chosen because it is related to the total pressure field. From the earlier mentioned pressure field parameters the surface lifting can be calculated with:

$$\Delta h_p = c_1 \cdot (p_\infty - p_c)(1 - e^{-r_m/r})$$ (4-11)

Δh_p	Pressure set-up	[m]
c_1	Constant ~0.01-0.04	[m/hPa]
p_∞	Peripheral Pressure	[hPa]
p_c	Pressure in eye of hurricane	[hPa]
r_m	Radius to maximum wind speed	[m]
r	Radius to a particular location	[m]

In Figure 4-11 the pressure field and the resulting pressure set-up is given for typhoon Bart.
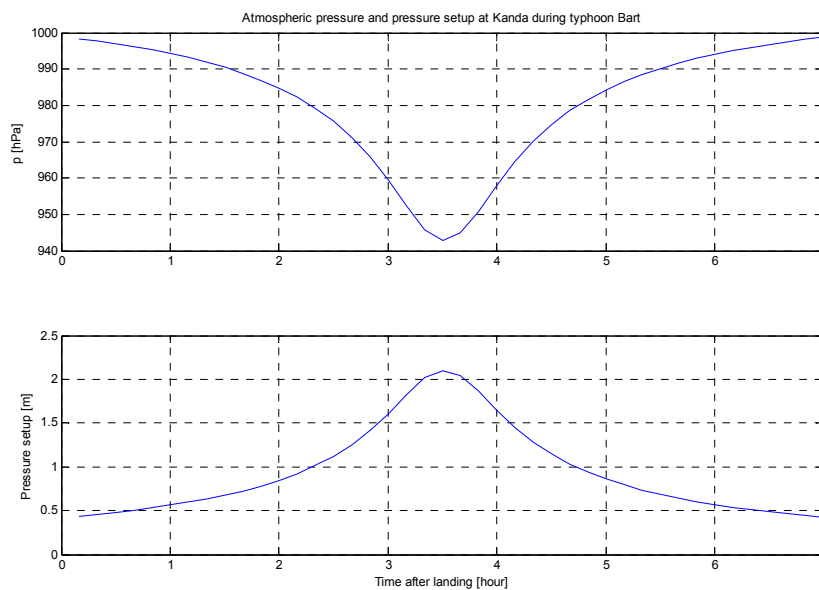
Figure 4-11: Computed pressure and resulting pressure set-up for typhoon Bart relative to the time of landing (Characteristics used: Δp = 73hPa; r_m = 42km; C_{fm0} = 56km/h; no change rates included and c_1=0.03m/hPa)

4.7.2 Wind set-up formula

The quadratic relation of wind set-up and wind speed is used. The formula is given below:

$$\Delta h_w = F_{set-up} \cdot c_2 \cdot \frac{V_s^2}{gd} \tag{4-12}$$

Δh_w	Wind set-up	[m]
c_2	Empirical constant ~2 10^{-6} to 4 10^{-6}	[-]
V_s	Surface wind speed	[m/s]
F_{set-up}	Fetch length of wind set-up	[m]
d	Water depth	[m]
g	Gravity acceleration	[m/s^2]

In an enclosed basin any increase of the water level on the down wind side needs to be compensated by a decrease of the water level on the upwind side. In case of a marginal sea connected to a large ocean, the large supply of water from the ocean ensures that mass is conserved without a decrease of the upwind water level. Because Suo-nada Bay is connected to the open sea, the wind set-up can be added to the present water depth. In Figure 4-12 this situation is sketched together with the parameters as given in the formula for wind set-up.
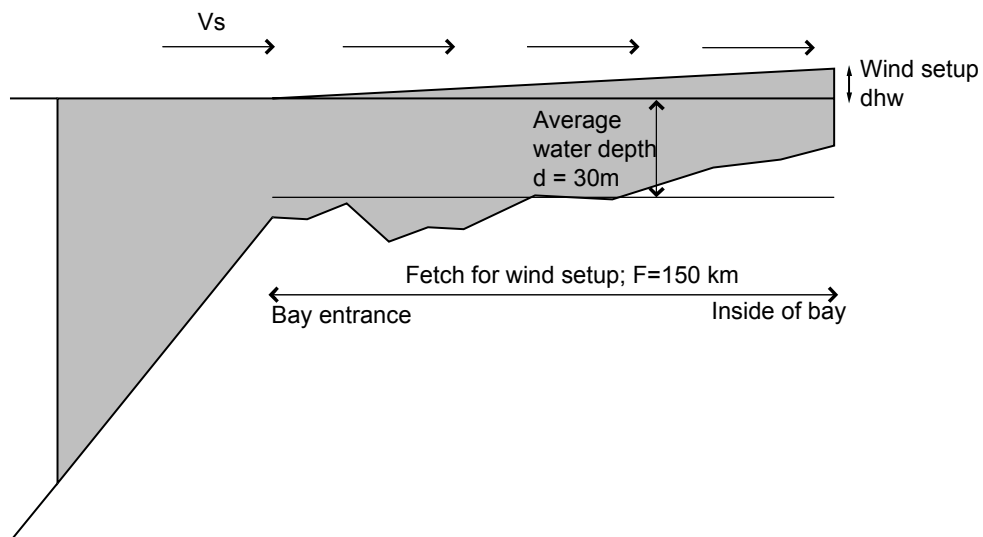
Figure 4-12: Wave set-up in an open basin connected to the sea

4.8 The models that describe the wave height and period

To calculate the significant wave height and the significant wave period. the SMB-model is also used. The peak wave period can also be computed on the basis of the wave steepness relationship (see Webbers, 2000) that relates the peak period with the significant wave height by means of the wave steepness. The position of the models with relative to the overall model is given in Figure 4-13.
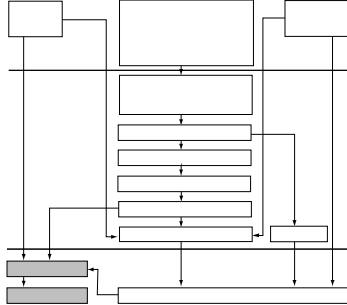
Figure 4-13: Position of wave height and period relative to the total model

4.8.1 The wave height model

The significant wave height, based on the SBM-model, is given in the following equation:

$$H_s(u,d,F) = \frac{V_s^2}{g} H_\infty \tanh(k_3 \left(\frac{dg}{V_s^2}\right)^{m_3}) \tanh \left(\frac{k_1 \left(\frac{F_{wave}g}{V_s^2}\right)^{m_1}}{\tanh\left(k_3 \left(\frac{dg}{V_s^2}\right)^{m_3}\right)} \right) \quad (4\text{-}13)$$

H_s	Significant wave height	[m]
V_s	Surface wind speed	[m/s]
g	Gravity acceleration	[m/s^2]
d	Water depth	[m]
F_{wave}	Fetch length of waves	[m]
H_∞	Coefficient 0.283	[-]
k_1	Coefficient 0.0125	[-]
k_3	Coefficient 0.53	[-]
m_1	Coefficient 0.42	[-]
m_3	Coefficient 0.75	[-]

- Wave height limitation

The Miche (1944) criterion limits the growth of the waves in the bay. In a shallow bay this criterion results in waves that have to be smaller than approximately half the water depth (Vrijling et al., 2002):

$$\begin{align} H_s &= H_s \quad \text{for } H_s \leq 0.5d \\ H_s &= 0.5d \quad \text{for } H_s > 0.5d \end{align} \quad (4\text{-}14)$$

H_s	Significant wave height	[m]
d	Water depth	[m]

The water depth differs depending on the different directions from which the waves approach the observation point. The water depth is built up from the bottom depth to

chart datum level (low water level) with additionally the storm surge and the tidal level relative to low water level. The influence of the limitation on the wave height is discussed in appendix E.

4.8.2 Wave period models

The same sort of formula as used for the significant wave height is derived for the significant wave period. The SMB-formula for the wave period is:

$$T_s(u,d,F) = \frac{V_s}{g} T_\infty \tanh(k_4 \left(\frac{dg}{V_s^2}\right)^{m_4}) \tanh\left(\frac{k_2 \left(\frac{F_{wave} g}{V_s^2}\right)^{m_2}}{\tanh\left(k_4 \left(\frac{dg}{V_s^2}\right)^{m_4} \right)} \right) \tag{4-15}$$

T_s	Significant wave period	[s]
F_{wave}	Fetch length	[m]
d	Water depth	[m]
V_s	Surface wind speed	[m/s]
g	Gravity acceleration	[m/s^2]
T_∞	Coefficient 7.54	[-]
k_2	Coefficient 0.077	[-]
k_4	Coefficient 0.833	[-]
m_2	Coefficient 0.25	[-]
m_4	Coefficient 0.375	[-]

The wave steepness model can also be applied to calculate the wave period. Between the parameters H_s and T_p there is a unique dependency. From analysis of all over the world (Repko et al., 2001) it seems that the wave height and steepness are statistically independent.

$$T_p(H_s, s_p) = \sqrt{\frac{H_s \cdot 2\pi}{g \cdot s_p}} \tag{4-16}$$

T_p	Peak wave period	[s]
H_s	Significant wave height	[m]
s_p	Wave steepness	[-]
g	Gravity acceleration	[m/s^2]

- Wave period limitation

Recent studies in shallow water (Jensen, 1993) indicate that fetch limited wave growth in shallow water, follow growth laws that are close to deepwater wave growth for the same wind speeds up to a point where an asymptotic depth dependent wave height is attained. The only constraint is that no wave period can grow past a limiting value (Vincent, 1985): The influence of the wave limitation on the wave period is discussed in appendix E. The relation is given below:

$$T_p \leq 9.78 \left(\frac{d}{g}\right)^{\frac{1}{2}} \tag{4-17}$$

T_p	Peak wave period	[s]
d	Water depth	[m]
g	Gravity acceleration	[m/s^2]

The observation of the wave period is stated as the significant wave period (T_s). The SMB wave period model also determines the significant wave. The wave steepness model is related to the peak wave period. To compare these values, the significant wave period is translated into the peak period. For narrow spectra, as in swell from distant storms the significant wave period is roughly equal to the spectral peak period. Spectra of wind driven waves ('sea') have a high frequency tail in which case the significant wave period (T_s) is roughly equal to 0.9 times the peak wave period (T_p) (Battjes, 2001). It is assumed that the significant wave period and the peak wave period have this mutual relation. From now on only the peak wave period is used and significant wave period is translated into this value.

4.8.3   Wave direction

The wave direction is often modelled to be correlated to the wind direction. Only the parametric hurricane models by Cooper (1988) and Young (1988) give an explicit description of the wave direction. The direction is approximately the same as the direction of the typhoon wind field. The direction of the waves depends on the location of the typhoon centre compared to the point for which the waves are computed.

In the case of the SMB model the wind direction determines the fetch and also the direction from which the waves can be expected. Since the direction of the wind and the fetch changes constantly, the direction of the waves can only be estimated roughly and a critical wave direction is therefore not given.

4.9   Schematisations and simplifications done in modelling

To be able to apply the models to the Suo-nada Bay situation, some schematisations and simplifications have been done. The schematisations and simplifications directly show the limitations of these models. The main assumptions concern the choice of a point of interest in Suo-nada Bay, the schematisation of the curved wind field, the response of the water to the wind field and the use of the SMB wave height model.

4.9.1   Assumptions in relation to the bay

The point of interest is chosen to be Kanda Port, inside Suo-nada Bay (Figure 4-14). This point is chosen because the observation of waves is done at that point. Also, in the vicinity of this site, the water levels have been observed since the late 1960's. The wave gauge was installed about 9 m below the low water level. The influence of depth-induced wave breaking on the wave height is negligible (according to Kawai et al., 2004).
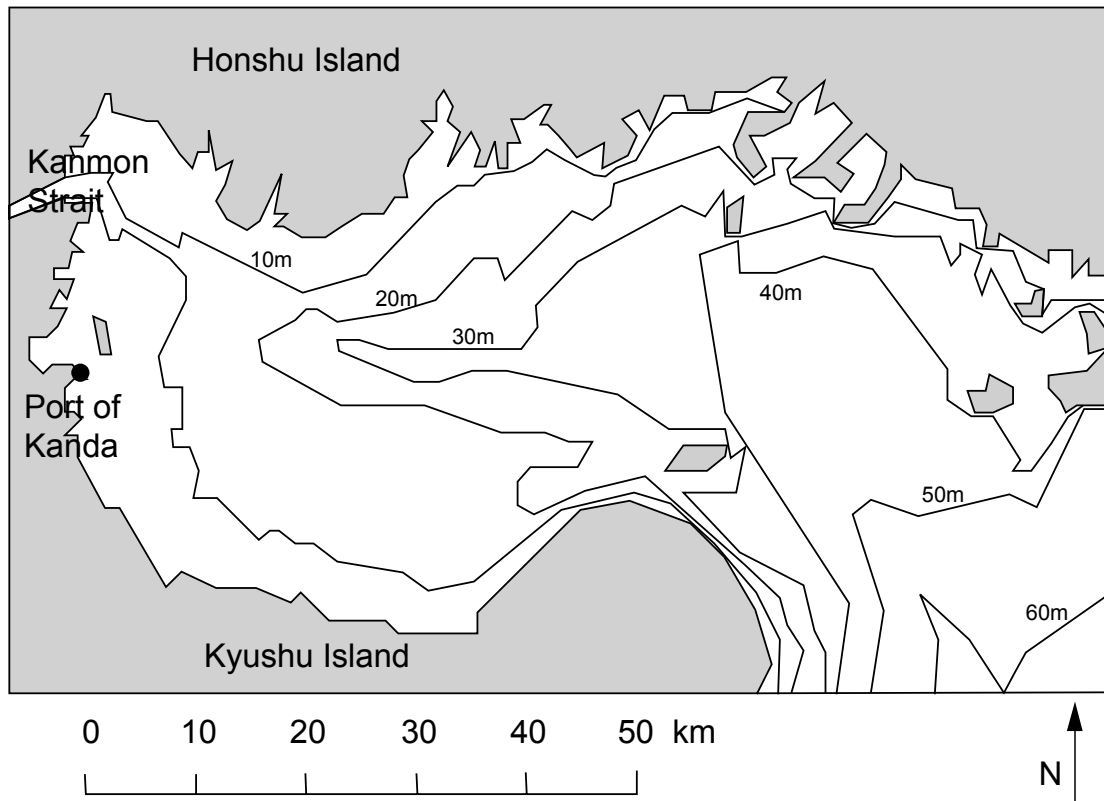
Figure 4-14: Bathymetry and geometry of Suo-nada Bay with the point of wave observation (Port of Kanda)

4.9.2   Assumptions in relation to wind field

Near mountainous coasts, the wind above the sea is often channelled and forced to flow parallel to the mountains. Still there will remain a strong curvature in the wind field if it passes over the bay. The wind field is not constant but rapidly moving over the bay, so the restriction of a constant and uniform wind field over the bay is not fulfilled.

Suo-nada Bay can roughly be compared to a rectangle of 50km by 100km. In Figure 4-15 the distance is given on the horizontal and vertical axes and a comparison can be made between the dimensions of an average wind field and the dimensions of the bay. The maximum wind speed used for the calculation should occur approximately over the length of the bay. With the average radius to maximum wind speed given in the figure, the bay is relatively small in comparison to the wind field. The wind speed at Kanda is used to for the computation of the hydraulic variables related to the wind. It is assumed that on the scale of the typhoon system, the wind speed at the Port of Kanda is a valid estimation of the wind speed over the entire bay.
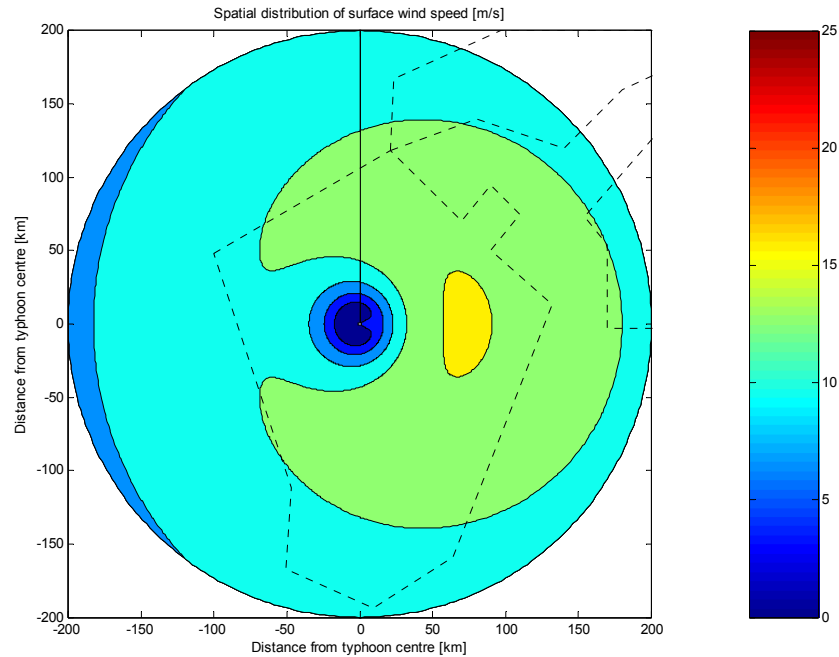
Figure 4-15: Example of the surface wind speed distribution relative to the dimensions of Suo-nada Bay
(with average typhoon parameters Δp=47hPa; r_m=84km; C_{fm}=33.7km/h; northward movement)

The direction of the wind field changes during the typhoon event. If the typhoon centre is very near to the bay the direction of the wind field changes very rapidly. An illustration of a typhoon track and the wind speeds over Suo-nada Bay is given in Figure 4-16.
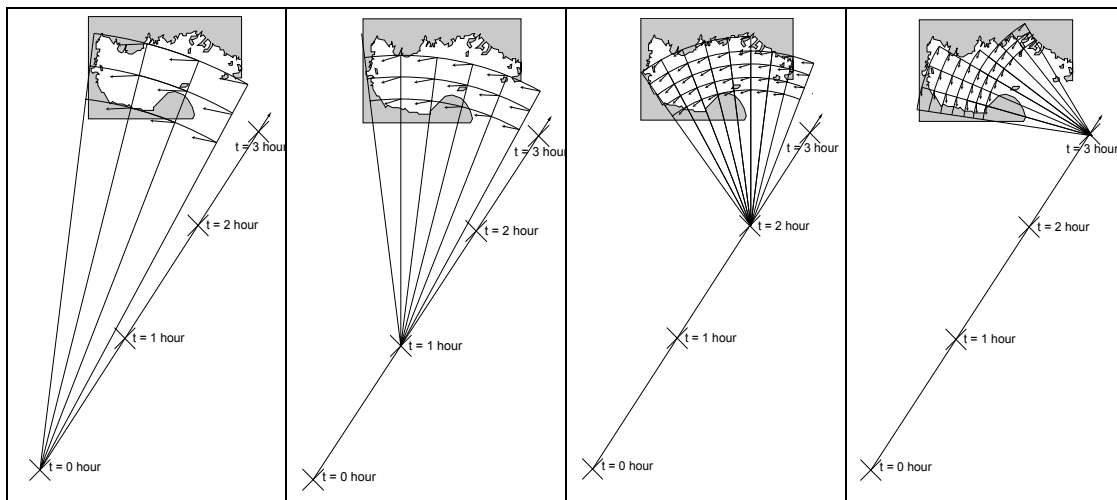
Figure 4-16: Hourly change in wind speeds over bay during passing of a typhoon

4.9.3 Assumptions of wind set-up and waves in relation to the wind field

The friction of the wind over the water surface results in wind set-up and waves. The water level is assumed to react instantaneously to the driving force. A sudden drop in wind speed will therefore result in a sudden drop of water level or decrease in wave height. The inertia of travelling waves and change in inclination of the water level is not taken into account, so the computed values will decrease faster than the observed ones. This also holds for the pressure field and the resulting pressure set-up.

4.9.4 Assumptions in relation to the SMB wave model

The fetch length is usually computed with a wind from a critical wind direction. That implies a straight wind field over that fetch. If the typhoon centre is far away, the error of this schematisation is negligible. If the typhoon centre is near the bay, the estimation is harder to justify (Figure 4-16). However for the first order model this is assumed and the wind direction in the observation point is used to determine the fetch.

- Duration limited or fetch limited waves

The waves in Suo-nada bay can be either fetch limited or duration limited (see appendix F). The influence of the increased wind field of a typhoon over the bay is long enough for waves travelling from one side to the other. The duration of the severe winds over the bay is shorter, but these winds influence the already generated waves. The fetch limited wave model is used in this research.

- Determination of effective fetch for the SMB model

The width of a fetch in basins normally places a very definite restriction on the length of the effective fetch. The less the width length ratio, the shorter the effective fetch. The SPM'77 gives a procedure to determine the effective fetch. The effective fetch distance can be constructed out of a number of radials from the wave station at fixed intervals (e.g. 7.5º). The total angle is limited to 45º on either side of the wind direction. The radials should be extended until they first intersect the shoreline (Figure 4-17). The component of length is multiplied by the cosine square of the angle between the radial and the wind direction. The resulting values for each radial are summed and divided by the sum of the cosines square of all angles. The average depth in the direction of the fetch is computed in a similar way. Figure 4-18 gives the fetches in the direction of Kanda. Table 4-1 gives the deterministically computed values for Suo-nada bay.

$$F_{eff} = \frac{\sum F_i \cdot \cos^2 \beta}{\sum \cos^2 \beta} \qquad (4\text{-}18)$$

$$d_{eff} = \frac{\sum d_i \cdot \cos^2 \beta}{\sum \cos^2 \beta} \qquad (4\text{-}19)$$

F_{eff}	Effective fetch length	[km]
F_i	Fetch in direction i	[km]
d_{eff}	Effective depth	[m]
d_i	Average depth in direction i	[km]
β	Angle between wind direction and direction of the radial	[°]
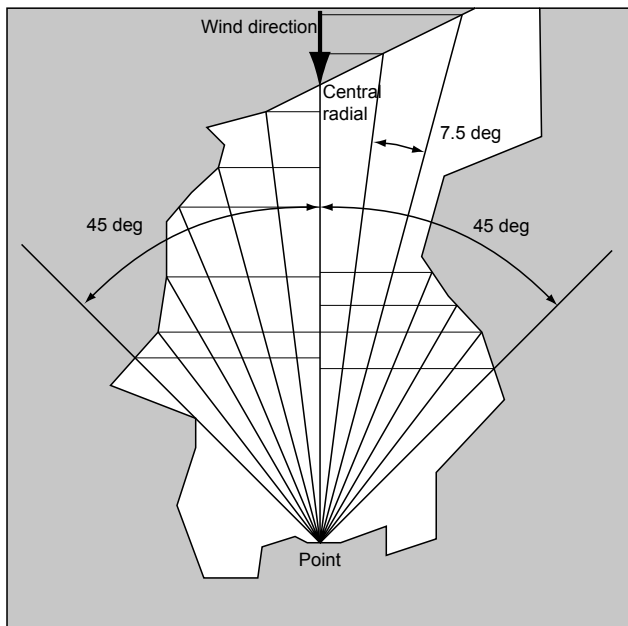
Figure 4-17: Effective fetch calculation according to the SPM'77

The method is based on the following assumptions:
- Wind moving over a water surface transfers energy to the water surface in the direction of the wind and in all directions within 45º on either side of the wind direction
- The wind transfers a unit amount of energy to the water along the central radial in the direction of the wind and along any other radial an amount modified by the cosine square of the angle between the radial and the wind direction.
- Waves are completely absorbed at shorelines
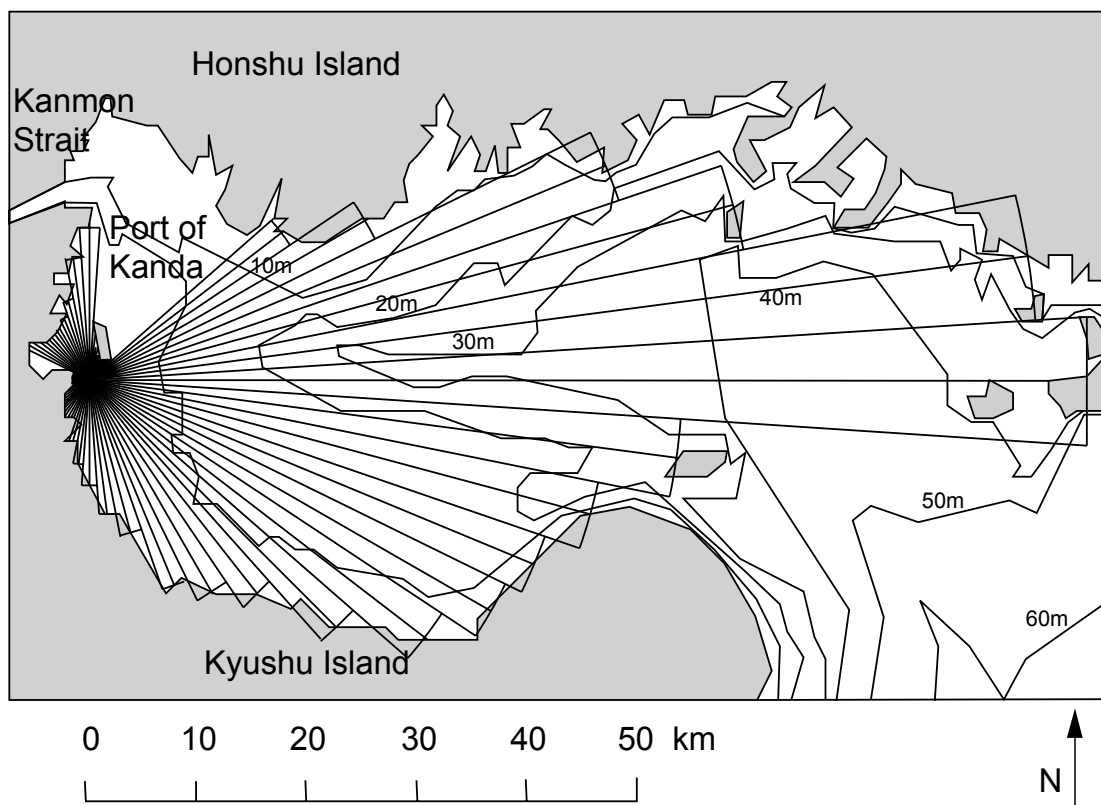
Figure 4-18: Fetches used for calculating the effective fetch and the effective depth

Table 4-1: Effective fetch and depth for all wind directions

Direction	E	ENE	NE	NNE	N	NNW	NW	WNW	W
F_{eff} [km]	49.80	43.50	33.22	21.17	15.01	10.48	6.16	3.66	4.23
D_{eff} [m]	14.9	13.7	10.4	6.6	5.4	4.1	3.0	2.5	2.5

Direction	E	ESE	SE	SSE	S	SSW	SW	WSW	W
F_{eff} [km]	49.80	46.55	34.04	22.68	14.77	9.74	6.31	5.01	4.23
D_{eff} [m]	14.9	13.6	8.9	5.0	3.4	2.5	2.5	2.5	2.5

For every direction the waves encounter a different water depth. The model to checks the breaking criterion for every direction. Only in a small distance from the observation point the water depth increases, related to the shipping channel near the Port of Kanda.

4.9.5   Assumptions in relation to wind set-up

The wind set-up is caused by the friction between the wind and the water surface. Equilibrium is reached with the force resulting from the inclination of the water level. This inclination can travel around any obstacle as long as the equilibrium holds. The dimensions of the fetch however are not directly clear. The boundary of the fetch for the wind set-up has to be chosen carefully. From numerical simulations done by the PARI, it followed that the inclination caused by wind set-up starts at the entrance of Suo-nada bay (Kawai, personal communication). The wind field is assumed to be uniform over the fetch with a magnitude that is estimated with the wind speed in Kanda. The component of the wind in the direction of the bay axis is used for the computation (Figure 4-19).
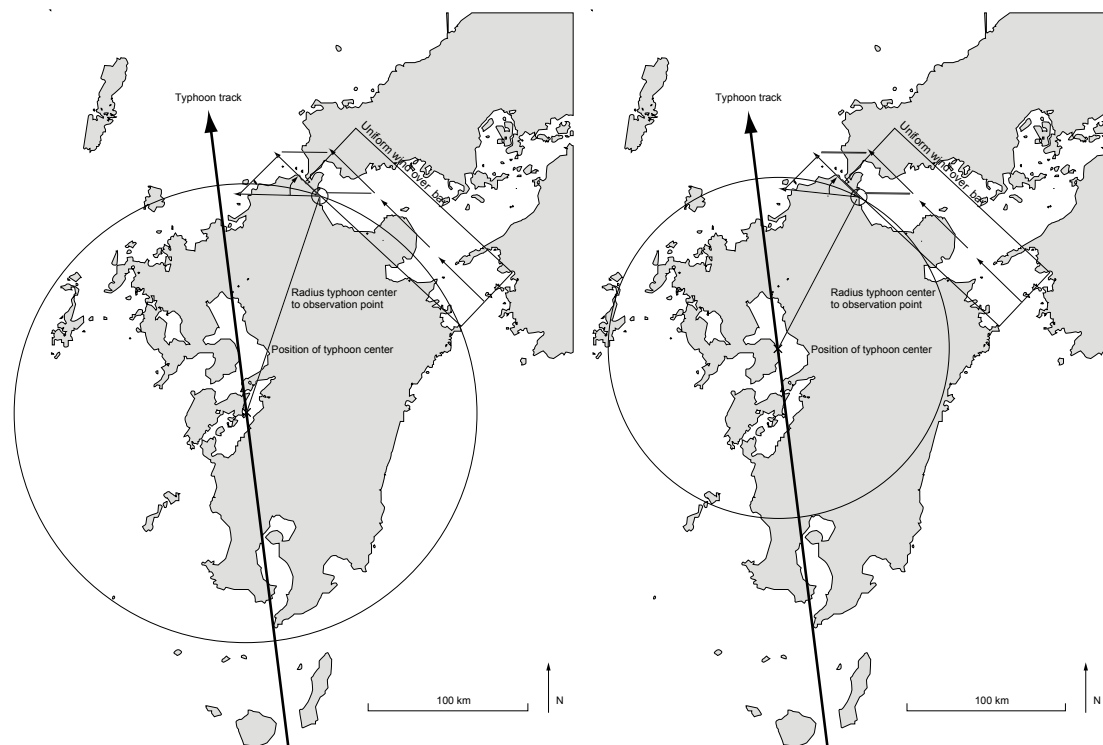
Figure 4-19: Schematisation to compute the wind set-up at Kanda, with wind speeds transformed to wind speed in the direction of the bay axis

5 Deterministic calibration of the combined model based on historical typhoons

Some of the models that have been proposed in the previous chapter are calibrated and validated with the available observations. The computed storm surge level (wind set-up and pressure set-up) together with the wave height and period are only deterministically calibrated. A deterministic validation step has been left out due to the small number of observations. Only typhoons of which the characteristics are known can be used for hindcasting and thus for calibration of the models.

5.1 Data available for deterministic calibration

5.1.1 Characteristics of historical typhoons

The analysis of Fujii (1998) contains the characteristics that describe the different historical typhoons that have hit Suo-nada Bay and Kyushu Island. These specific typhoon characteristics are given for typhoons between 1955 and 1994 (see Appendix D). The Pacific coast can be divided into areas A, B and C for analysing typhoons according to Mitsuta and Fujii (1979 and 1986) and Fujii (1998) (Figure 5-1). This distinction is made because typhoons that struck the western part of Japan were significantly different from those that struck the eastern part. Suo-nada Bay is assumed to be located in area A. Only the typhoons that landed in that area are used in the analysis (Table 5-1). Typhoons landing on the boundaries of area B could have a path in the direction of Suo-nada Bay. The probability that such a typhoon affects Suo-nada Bay is small and will not be considered.

Table 5-1: Typhoons that have landed in area A with typhoon characteristics (from Fujii, 1998)

Year	Typh. name	Typh. number	Δp [hPa]	r_m [km]	C_{fm} [km/h]	γ [°]	a_p [km/h]	a_r [km/h]	a_c [km/h^2]	a_d [°/h]
1955	Louise	5522	63.8	97.5	29	-17	0.049	4.3	2.9	6.8
1957	Bess	5710	48.2	84.5	35	44	0.064	5.0	-3.9	-5.6
1963	Bess	6309	31.4	105.0	29	25	0.070	9.7	-3.9	-11.6
1964	Kathy	6414	40.0	77.5	13	-4	0.021	1.5	-0.3	3.5
1964	Wilda	6420	83.2	50.5	33	29	0.097	6.7	0.6	1.7
1965	Jean	6515	50.6	50.5	37	29	0.117	10.2	3.6	-3.4
1969	Cora	6909	43.1	54.0	40	64	0.042	3.4	-1.8	-2.1
1970	Wilda	7009	47.7	56.0	26	47	0.072	5.9	2.4	-0.9
1971	Olive	7119	38.1	71.0	27	36	0.068	3.5	1.4	-9.2
1971	Trix	7123	33.1	123.5	24	18	0.009	-0.8	-2.3	1.9
1972	Tess	7209	21.2	99.5	15	-63	0.031	-3.4	5.7	7.1
1976	Fran	7617	42.4	81.0	19	27	0.074	12.7	3.4	2.4
1980	Orchid	8013	26.9	273.0	76	6	0.010	-29.4	-6.4	1.2
1981	Ogden	8110	32.3	36.5	22	-42	0.092	3.2	2.0	-1.7
1982	Ellis	8213	40.9	82.0	18	24	0.050	6.8	3.4	-3.8
1985	Pat	8513	52.3	52.0	42	-6	0.079	5.0	2.7	0.7

Year	Typh. name	Typh. number	Δp [hPa]	r_m [km]	C_{fm} [km/h]	γ [°]	a_p [km/h]	a_r [km/h]	a_c [km/h²]	a_d [°/h]
1991	Kinna	9117	42.2	72.0	40	30	0.108	9.7	2.5	-1.7
1991	Mireille	9119	69.0	83.5	67	61	0.068	14.6	11.0	-4.5
1992	Janis	9210	50.9	83.0	38	38	0.073	9.8	-0.6	-1.8
1993	Yancy	9313	77.1	56.0	44	28	0.100	9.1	1.7	-8.5
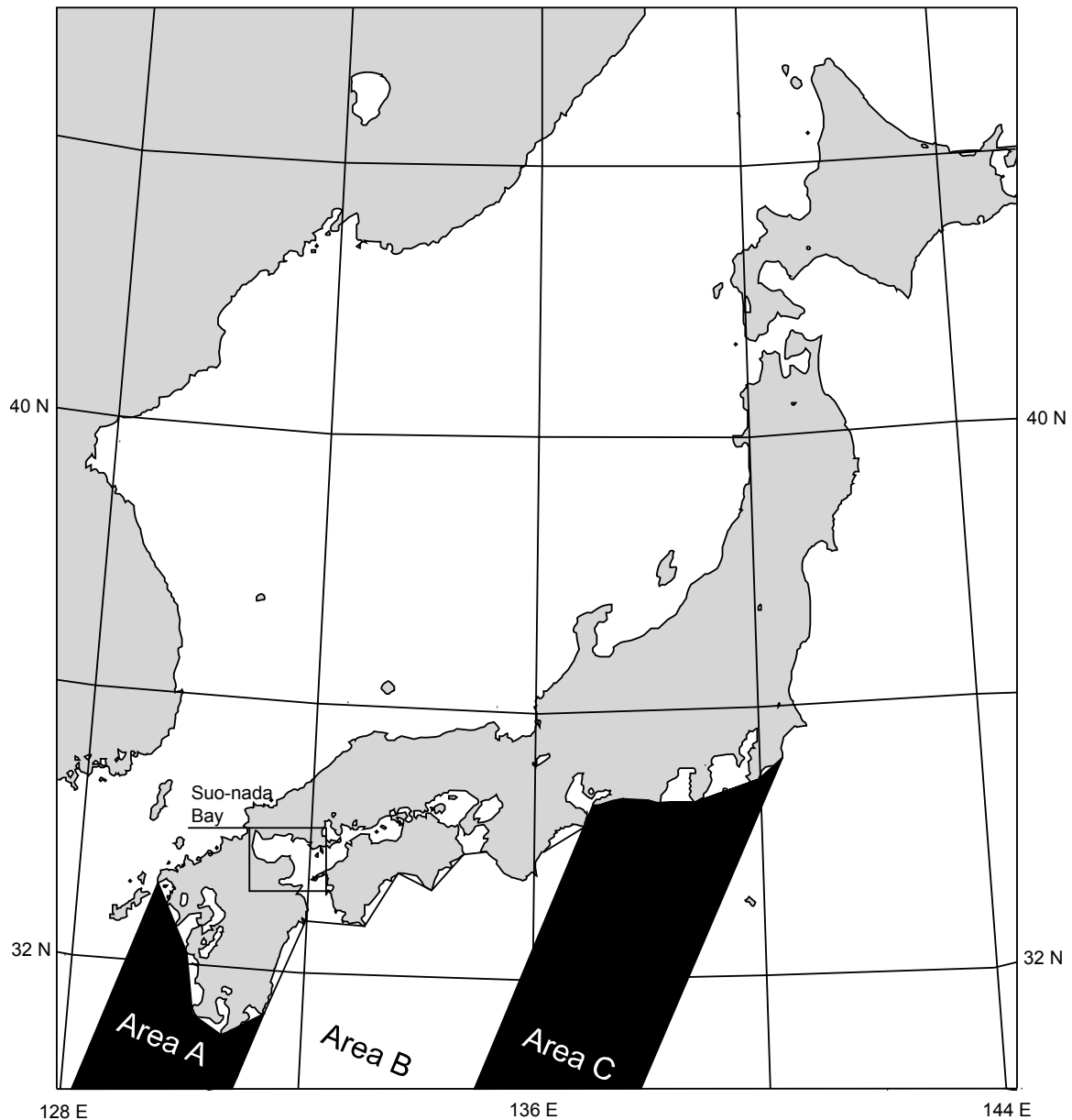
Figure 5-1: Different areas of typhoon landing as used in the analysis of typhoons by Mitsuta et al. (1979, 1986) and Fujii (1998) (background: agora.ex.nii.ac.jp)

5.1.2 Observations of water level and waves in Suo-nada Bay

The observations done by the PARI are divided in observations of the storm surge level and the observations of the wave height and period.

- Storm surge level

The observation of water levels started in 1968. All typhoon induced storm surges, starting from 1968 in the Suo-nada Bay area, can be deterministically calibrated with the observations. Since the data of only four typhoons is available, these observations are used for calibration purposes. The storm surge is the difference

between the observed water level and the astronomical tide at that moment. The observation point is located at Aohama, nearby Kanda.

- Wave height and period

The observation of wave height and period in the Port of Kanda (Suo-nada Bay) started in the year 1991. The overlap of the typhoons of which characteristics are known (of Fujii, 1998) and the observations of the wave properties is only four years (i.e. also four typhoons). The observed values will all be used for the deterministic calibration of the wave height and wave period model.

The observations of water level and wave height from 1994 onward cannot be used for deterministic calibration, since the characteristics of the individual historical typhoons have not been determined yet (Fujii, personal communication). The observations after 1994 can be used for the statistical validation of the modelled hydraulic boundary conditions. This is subject of the next chapter. In Figure 5-2 the data that could be available for calibration and validation is pointed out in a graphical way.
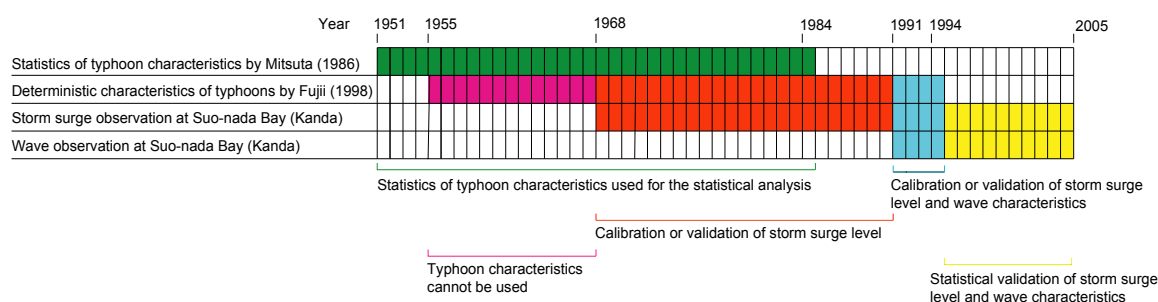
Figure 5-2: Overview of data that could be used for calibration and validation of the hydraulic boundary conditions

5.1.3 Typhoons used for calibration and validation

As mentioned before, a deterministic validation step has been left out since not all observations are available. For the wave height all possible observations are available, only these are used for calibration purposes due to the small number. The deterministic validation would be possible for the storm surge level, but not all observations were available at the time. In Table 5-2 the individual typhoon names and numbers are given with an indication whether they are used for deterministic calibration.

Table 5-2: Overview of typhoons that are actually used for deterministic calibration

Year	Typhoon Name	Typhoon Number	Characteristics by Fujii	Calibration of storm surge level	Calibration of wave characteristics
1955	Louise	5522	V	*	*
1957	Bess	5710	V	*	*
1963	Bess	6309	V	*	*
1964	Kathy	6414	V	*	*
1964	Wilda	6420	V	*	*
1965	Jean	6515	V	*	*
1969	Cora	6909	V	n.a.	*
1970	Wilda	7009	V	V	*
1971	Olive	7119	V	n.a.	*
1971	TriV	7123	V	n.a.	*
1972	Tess	7209	V	n.a.	*
1976	Fran	7617	V	V	*
1980	Orchid	8013	V	n.a.	*
1981	Ogden	8110	V	n.a.	*
1982	Ellis	8213	V	n.a.	*
1985	Pat	8513	V	n.a.	*
1991	Kinna	9117	V	V	V
1991	Mireille	9119	V	V	V
1992	Janis	9210	V	n.a.	V
1993	Yancy	9313	V	n.a.	V

* = No observations; V = available; n.a. = not available

5.2   Derivation of additional typhoon characteristics

To be able to compare historical typhoons with the observations of storm surges and wave characteristics, the exact time and position of typhoon landing are needed.

5.2.1   Translation of time of landing from charts to observations
The historical typhoon tracks are not given by Fujii (1998), but are obtained from charts found on a website (agora.ex.nii.ac.jp) with historical track of typhoons in Japan. The time scale used for the typhoon track of the agora charts is given in Universal Time Coordinate[8]. The observations are given in Japanese Standard Time[9], which differs 9 hours from the UTC. In Table 5-3 the time of landing on the boundary of area A is given for the individual historical typhoons.

5.2.2   Determination of position of landing of typhoons
The exact position of the typhoon (centre) landing is needed, because the characteristics of historical typhoons (derived from Fujii, 1998) and the statistics of typhoons (derived from Mitsuta and Fujii, 1986) are given at the time of landing on the boundary of area A. To get an idea about the tracks of the typhoons used by Mitsuta and Fujii (1986) and Fujii (1998), an overview is given of all typhoon tracks with the analysed (severe) typhoons plotted in red (Figure 5-3 and Figure 5-4).
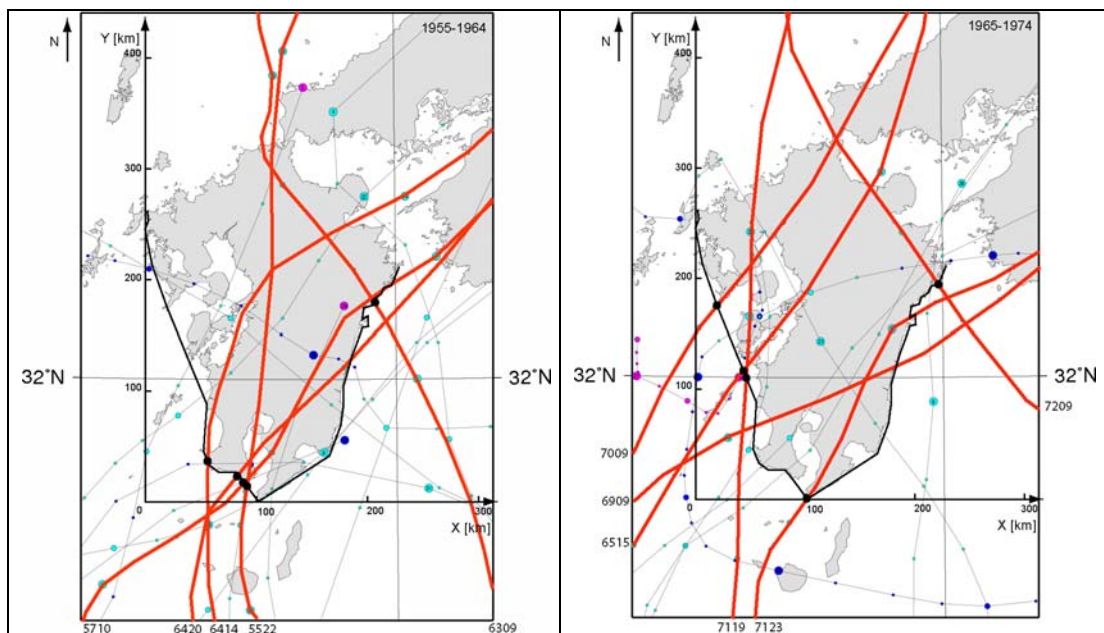
Figure 5-3: All typhoons that landed in the Kyushu area with the severe typhoons (in red) that landed on the boundary as defined by Mitsuta and Fujii (1979 and 1986) and Fujii (1998).
Left the typhoons in the period 1955-1964; right the typhoons in the period 1965-1974.

---

[8] Further stated as UTC
[9] Further stated as JST
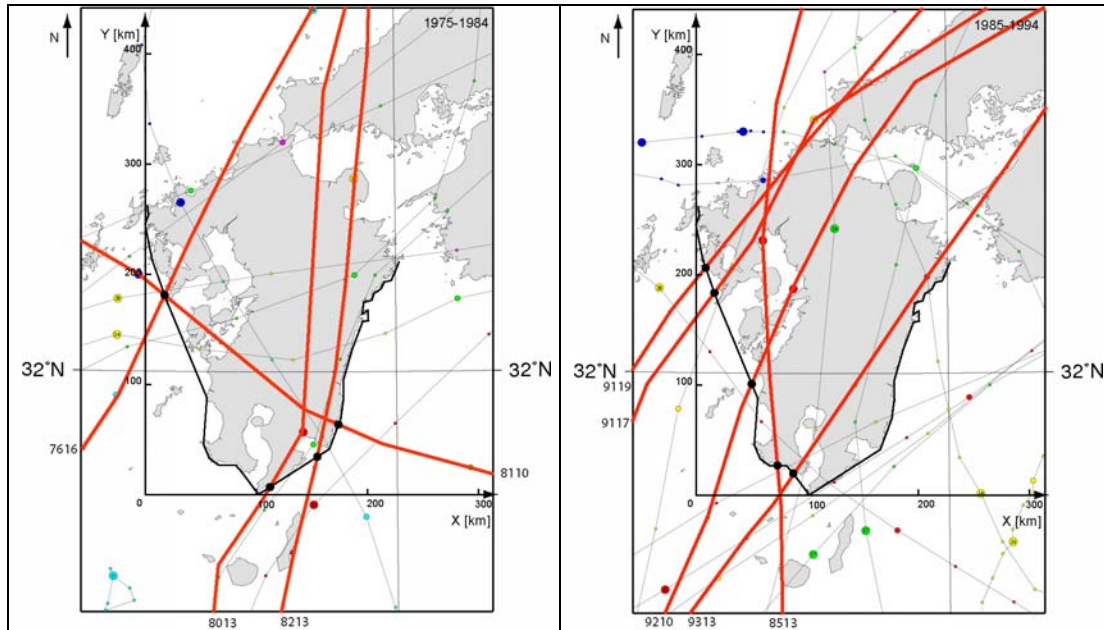
Figure 5-4: All typhoons that landed in the Kyushu area with the severe typhoons (in red) that landed on the boundaries as defined by Mitsuta and Fujii (1979 and 1986) and Fujii (1998).
Left the typhoons in the period 1975-1984; right the typhoons in the period 1985-1994

In Table 5-3 the positions of landing are given for the historical typhoons relative to axes with orientations in northern and eastern direction. Typhoons that occurred in the period 1955-1964 are not stated in the table because there are no observations done in that period.

Table 5-3:Time and position of landing

Period	Year	Typh. Name	Typh. No.	Date (relative to UTC)	Time of landing of typhoon eye [hh.mm] (UTC)	Position of landing in x-direction [km]	Position of landing in y-direction [km]
1965-1974	1969	Cora	6909	22-08-1969	00.48	51	64
	1970	Wilda	7009	14-08-1970	13.00	16	172
	1971	Olive	7119	05-07-1971	18.54	43	107
	1971	Trix	7123	30-08-1971	14.54	105	8
	1972	Tess	7209	23-07-1972	10.18	217	197
1975-1984	1976	Fran	7617	13-09-1976	16.00	16	180
	1980	Orchid	8013	11-09-1980	21.48	111	8
	1981	Ogden	8110	31-07-1981	16.48	158	63
	1982	Ellis	8213	27-08-1982	15.24	152	33
1985-1994	1985	Pat	8513	31-08-1985	19.00	70	27
	1991	Kinna	9117	14-09-1991	19.48	14	184
	1991	Mireille	9119	27-09-1991	06.48	8	209
	1992	Janis	9210	08-09-1992	21.36	47	102
	1993	Yancy	9313	03-09-1993	06.48	84	18

5.3   Analysis of historical typhoon tracks

With the characteristics and the time and position of landing of the relevant historical typhoons, the computed tracks of the hindcasted typhoons can be plotted (Figure 5-5).
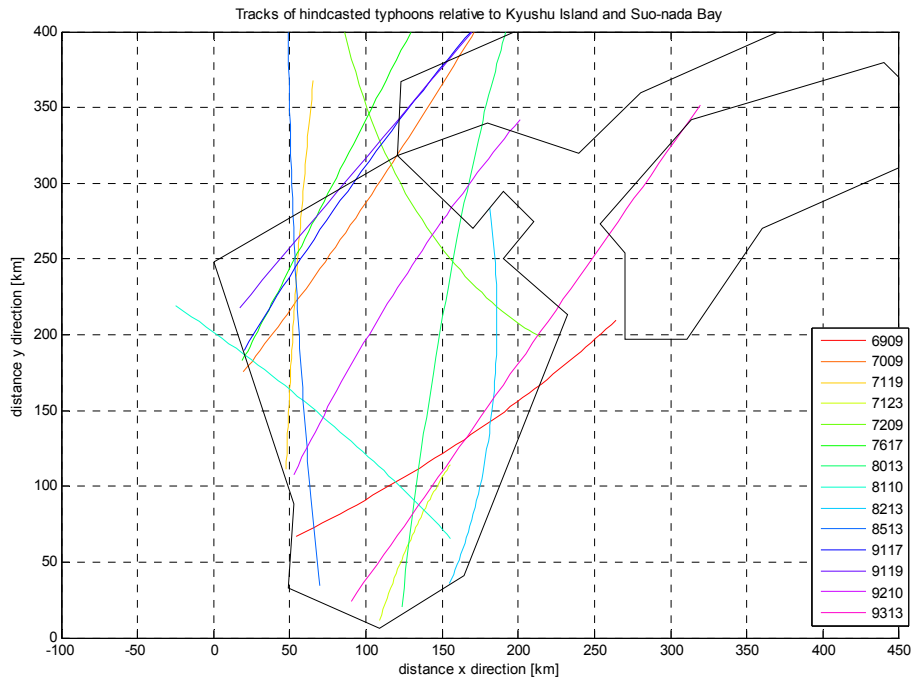
Figure 5-5: Tracks of hindcasted typhoons from the time of landing onward relative to the chosen axes

In the figure (Figure 5-5), the hindcasted typhoon tracks over Kyushu Island and Suo-nada Bay can be seen. Some of the computed tracks were significantly different from the actual tracks of the historical typhoons. Therefore, the direction of forward movement and the change of direction of forward movement of a number of typhoons that were obtained from the analysis of Fujii (1998), are adjusted. In Table 5-4 the values that have been adjusted are given together with the original values. The change of these values might affect the values used for the statistical analysis. This change is not accounted for in the further research.

Table 5-4: Adjusted direction of forward movement and change of direction of forward movement

Year	Typh. Name	Typh. Number	γ [^{0}] to north (Fujii)	γ [^{0}] to east	γ [^{0}] adjusted to east	a_d [^{0}/h] to north (Fujii)	a_d [^{0}/h] to east	a_d [^{0}/h] adjusted to east
1969	Cora	6909	64	26	-	-2.1	2.1	-
1970	Wilda	7009	47	43	52	-0.9	0.9	-0.5
1971	Olive	7119	36	54	88	-9.2	9.2	-0.5
1971	Trix	7123	18	72	-	1.9	-1.9	-
1972	Tess	7209	-63	153	-	7.1	-7.1	-
1976	Fran	7617	27	63	-	2.4	-2.4	0.0
1980	Orchid	8013	6	84	-	1.2	-1.2	-
1981	Ogden	8110	-42	132	-	-1.7	1.7	-
1982	Ellis	8213	24	66	-	-3.8	3.8	-
1985	Pat	8513	-6	96	-	0.7	-0.7	-
1991	Kinna	9117	30	60	-	-1.7	1.7	-1.1
1991	Mireille	9119	61	29	60	-4.5	4.5	0.0
1992	Janis	9210	38	52	-	-1.8	1.8	-1.1
1993	Yancy	9313	28	62	63	-8.5	8.5	0.0

5.4   Comparison of calculated and observed wind speed

For the surface wind speed a comparison is made between the observed surface wind speed and the computed surface wind speed. Only for one typhoon (no. 9918) of which the typhoon characteristics are not given in the analysis of Fujii (1998), wind observations are available. Other literature however gives indicative values for the typhoon characteristics (Fujii, 2002) and these are adopted here. It is chosen to visually compare the values computed by the classical method (Brunt, 1939) and the extended formula derived by Mitsuta and Fujii (1987).
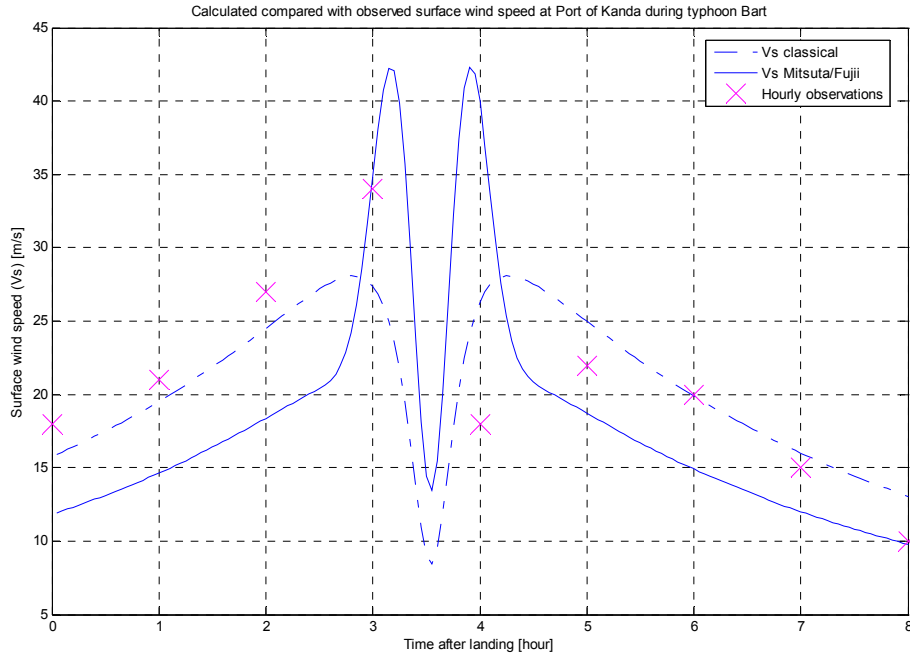
Figure 5-6: Calculated values of surface wind speed and observations of surface wind speed during typhoon Bart (Characteristics used: Δp = 73hPa; r_m = 42km; C_{fm0} = 56km/h; no change rates included and c_1=0.03m/hPa)

The two formulae used for the computation of the surface wind speed are given below (see for the complete formulae chapter 4).

$$V_s = V_{gr}(\cos\alpha - \sin\alpha) \qquad \text{Classical}$$

$$V_s = V_{gr}\left(G(\infty) + \left\{ G(\xi_p) - G(\infty) \right\} \left(\frac{\xi}{\xi_p} \right)^{m-1} \exp\left[\left(1 - \frac{1}{m} \right) \left\{ 1 - \left(\frac{\xi}{\xi_p} \right) \right\}^m \right] \right) \quad \text{M./Fujii}$$

Variables as defined before

The computed values match the values of the surface wind speed as can be seen in Figure 5-6. The main difference between the two computed wind speeds is that the peaks of the Mitsuta and Fujii wind speed are higher and the values beside the peak are lower than the wind speed computed with the classical method. The observed maximum wind speed is in between both computed maxima. The other observed values are more in the range of the simple classical wind speed model. Since not only the maximum wind speed is decisive for the hydraulic variables, but also the fetch length and water depth, the overall best fitted computed values will give the best results in modelling the typhoons. Further, the classical wind speed is lower and the duration of high winds above a certain threshold level is longer for the classical

method. The choice is therefore made to model the wind speed with the simple classical wind speed model.

5.5   Deterministic calibration of the storm surge model

Since a range of values for the constants in the formulae for pressure- and wind set-up is given, these constants should be determined for the specific case of Suo-nada Bay. The observations at the Port of Kanda only contain the total storm surge level on top of the tide level. Therefore, both pressure set-up model and wave set-up model have to be calibrated with the same observations. The maximal water level is of interest for the probabilistic analysis, but the two constants cannot only be calibrated based on one value. Therefore all observations (not only the maximum) of the storm surge during a typhoon event are calibrated to determine these model constants.

5.5.1   Fitting with least square error technique
The constants c_1 and c_2 in the formulae of pressure set-up and wind set-up respectively are deterministically determined by calculation of the square error between the computed wind- and pressure set-up combined and the observed total storm surge for every observation.

$$\Delta h_p = c_1 \cdot (p_\infty - p_c)(1 - e^{-r_m/r})$$

$$\Delta h_w = F_{set-up} \cdot c_2 \cdot \frac{V_s^2}{gd}$$

$$\Delta h_{wp} = \Delta h_w + \Delta h_p$$

Variables as defined before

The two constants c_1 and c_2 with the overall least square sum for all hindcasted storm surges compared to observations are chosen. The time for which the square error can be computed is limited to the time for which the storm surge is the direct cause of a typhoon. Otherwise, the typhoon system has no more influence on the water level and the model is calibrated with observations that may have been caused by other phenomena. The first observation of the storm surge during a historical typhoon, which is compared to the computed one, is determined by the time of landing of the typhoon, since that is the moment for which the initial typhoon characteristics are known. The observations (appendix G) within 8 hours from landing time are used in the analysis. The least square errors for the different parameters c_1 and c_2 for pressure- and wind set-up are given in Figure 5-7. The calibrated values are used for the calculation of the storm surge in Figure 5-8, which are stated together with the observed values.
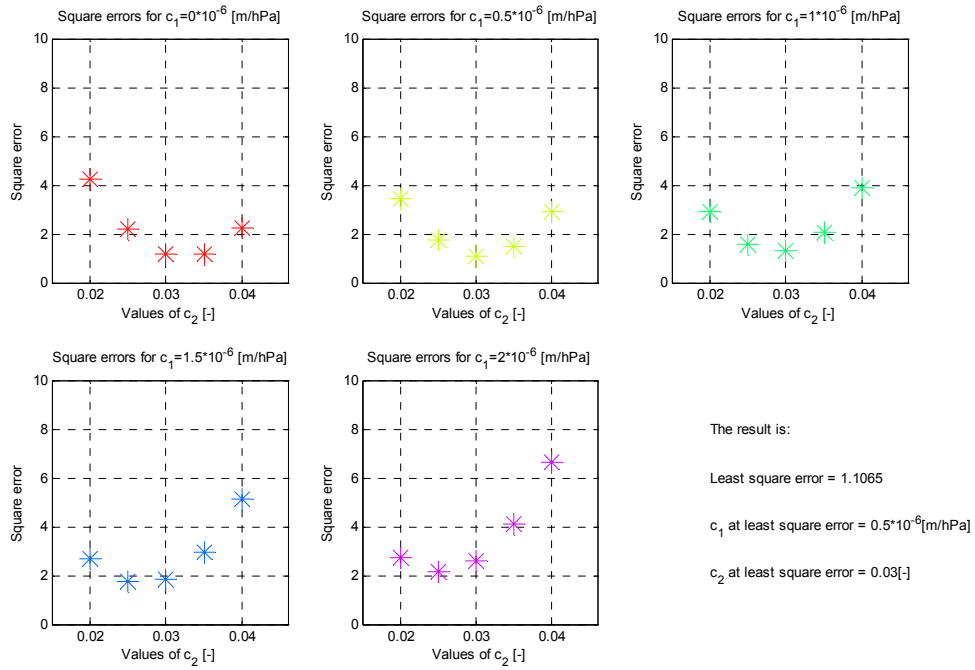
Figure 5-7: Square errors of observed and computed storm surge for varying constants c1 and c2
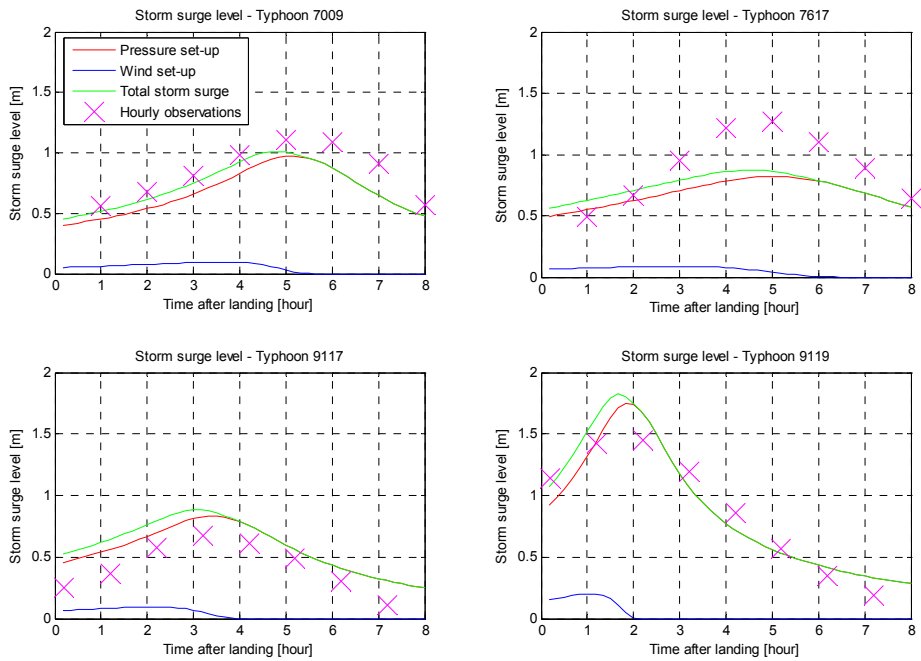
Figure 5-8: Storm surge calculated with least square constants c1 and c2 in comparison with observations

5.5.2   Discussion of deterministic calibration of the storm surge model

The values stated above can be checked with values used in other analyses. This is subject of this sub paragraph. Kawai et al. (2004) state that the wind set-up is larger than the pressure set-up for a typhoon induced storm surge (Kawai, 2004b; about three times larger). On the other hand the JMA (JMA, 1999) found constants for other bays (Table 5-5; also used in the analysis of Kato et al., 2002) that can be compared to the constants found for the wind set-up and pressure set-up with the least square error as computed in this research. The formula for the storm surge level according to the JMA is the following:

$$H = a(1010 - P) + bW^2 \cos\theta \tag{5-1}$$

H	Storm surge level	[cm]
a	Constant to determine pressure set-up	[cm/hPa]
P	Central pressure of a typhoon	[hPa]
b	Constant to determine wind set-up	[cm/m^2/s^2]
W	Wind speed	[m/s]
θ	Difference between critical wind direction and wind direction at wind speed peak	[°]

Table 5-5: JMA values in storm surge analysis (Kawai, personal communication)

Place	a	b	Direction	Place	a	b	Direction
Wakayama	2.608	0.003	SSW	Uno	4.109	-0.167	ESE
Osaka	2.167	0.181	S6.3degE	Kure	3.730	0.026	E
Kobe	3.370	0.087	S24degE	Matsuyama	4.303	-0.082	SSE
Sumoto	2.281	0.026	SSE	Takamatsu	3.184	0.000	SE

Constant a can be compared to the constant used for the computation of the pressure set-up (c_1) and constant b to the constant used for the computation of the wind set-up (c_2). To compare the value of b with the value of c_2 the values have to be in the same dimensions (the variables fetch, depth and gravity acceleration are the cause of this difference). The average of b is translated to the dimensions of constant c_2:

$$c_1 = 0.03 \text{ vs } a = 0.03 \qquad\qquad \text{[m/hPa]}$$

$$c_2 = 0.5 \cdot 10^{-6} \text{ vs } b = 0.2 \cdot 10^{-6} \qquad\qquad \text{[-]}$$

Constant c_2 is a factor 2.5 smaller than the estimate based on the observations. The order of magnitude is however approximately the same. The average of constant a coincides with the fitted value of c_1.

The average deviation (above and under) of the estimation of the maximum storm surge level is about 25% (0.3m). The standard deviation and average error can be computed but the number of observations (i.e. 4 maxima during typhoons) is too small to obtain a useful value.

5.6 Deterministic calibration of SMB wave height and wave period model

The SMB model contains empirical parameters. The values of these parameters have a broad empirical support. However, because the bottom depth, the fetch length and the curved wind field have all been schematised, it has been chosen to calibrate the SMB model for the Suo-nada Bay case. The parameters µ and v are used as fit parameters for the wave height and the wave period respectively:

$$H_s = \mu \cdot \frac{V_s^2}{g} H_\infty \tanh(k_3 \left(\frac{dg}{V_s^2}\right)^{m_3}) \tanh \left(\frac{k_1 \left(\frac{F_{wave}g}{V_s^2}\right)^{m_1}}{\tanh\left(k_3 \left(\frac{dg}{V_s^2}\right)^{m_3}\right)} \right) \tag{5-2}$$

$$T_p = v \cdot \frac{1}{0.9} \frac{V_s}{g} T_\infty \tanh(k_4 \left(\frac{dg}{V_s^2}\right)^{m_4}) \tanh \left(\frac{k_2 \left(\frac{F_{wave}g}{V_s^2}\right)^{m_2}}{\tanh\left(k_4 \left(\frac{dg}{V_s^2}\right)^{m_4}\right)} \right) \tag{5-3}$$

μ	Fit parameter for the SMB wave height model	[-]
v	Fit parameter for the SMB wave period model	[-]

Further the same as stated in equations 4-13 and 4-15

The values µ and v are obtained by calibrating the models to the available observations. The same least square technique is applied in this case as in the storm surge calibration. In this case however only the maximum observed values are compared with the maximal computed value for the wave height.

5.6.1 Fitting with least square error technique
The observed values for the wave height and the wave period during several typhoons are given in appendix G. The least square errors are given in Figure 5-9 for the range of parameters µ and v, used as fit parameters in the SMB formula. The computed values of the wave height and period (with the calibrated SMB model) are given in Figure 5-10 and Figure 5-11 respectively. The observed values are also plotted in the figures.
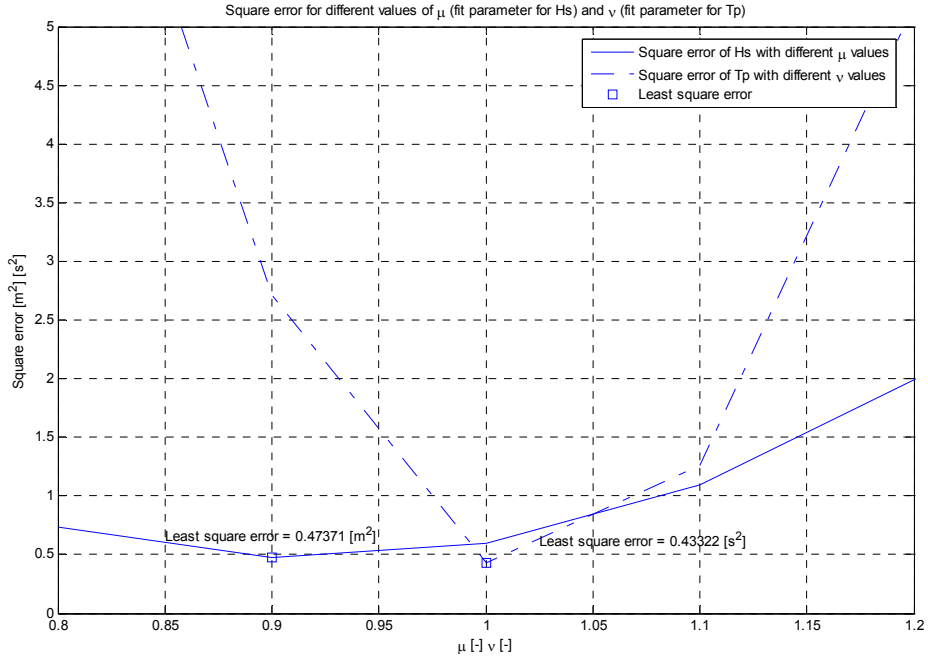
Figure 5-9: Square errors of different fit parameters for wave height and period
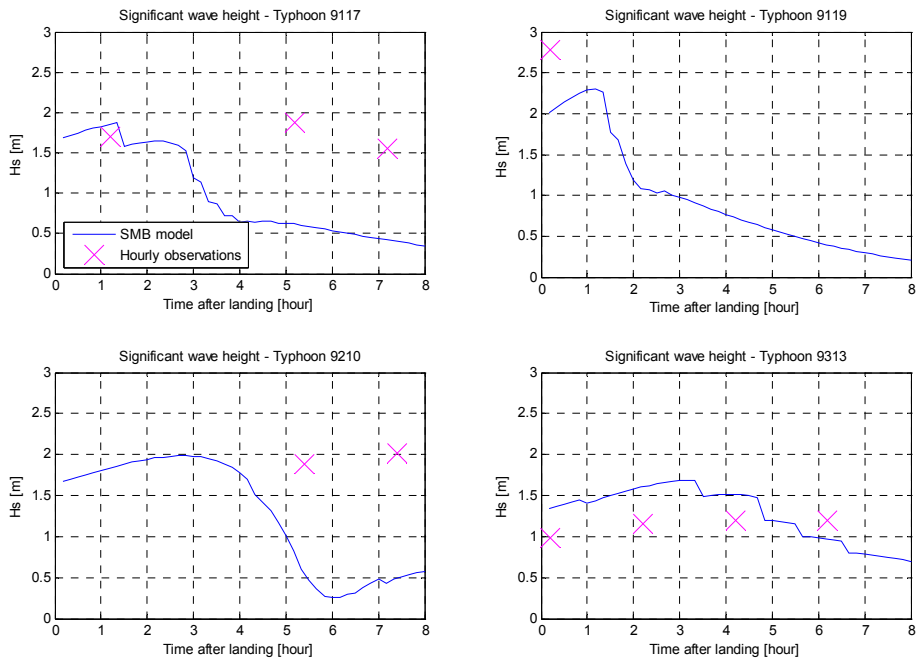
Figure 5-10: Observed wave height and calculated (SMB) wave height with calibrated coefficient μ (=0.9)
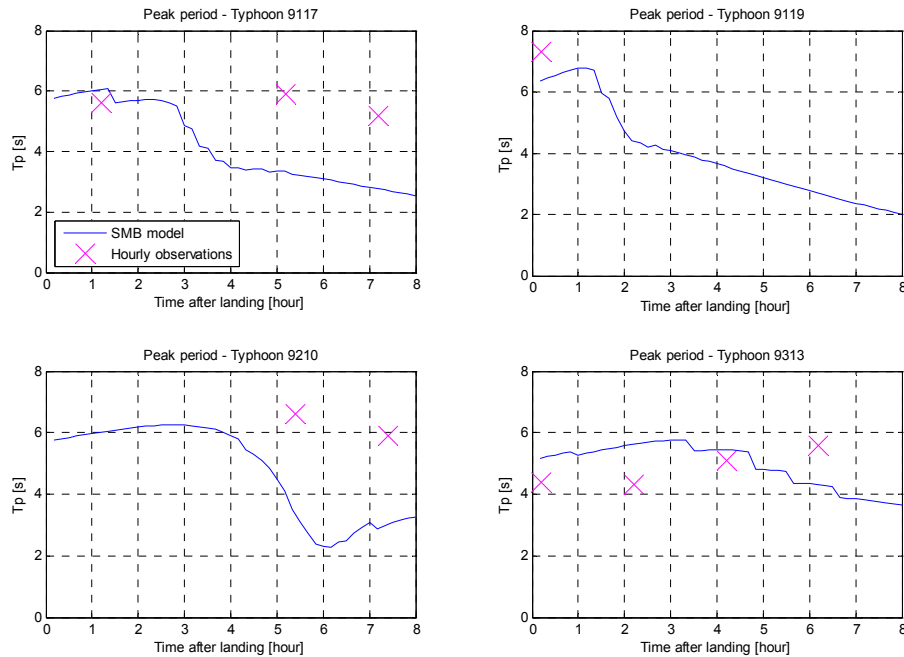
Figure 5-11: Observed wave period and calculated (SMB) wave period with calibrated coefficient v (=1.0)

5.6.2 Discussion of calibrated values for the SMB wave height and period model

The hourly fit of the computed values for the wave height and period is poor. The model under predicts the observational data points after the occurrence of the maximum. This is because the inertia of the wave field is not accounted for properly. Since only the maximum wave height is needed in the probabilistic analysis, that value should be compared to the computed wave height. The maximum is estimated reasonably with the model. A point of consideration is that the given observed maximum could not have been the actual maximum that occurred, since some observational data during typhoons are missing. The malfunctioning of the observation instrument under extreme conditions has impact on the quality of information for a statistical analysis. The total number of maxima of wave characteristics during historical typhoons is small; only four typhoons can be compared.

The computed maxima for the wave height deviate on average about 20% (0.3m) from the observed values. The fit parameter that has been added is calibrated to the value of 0.9. This implies that the SMB wave height model predicts the significant wave height in the right order of magnitude. The maxima of the computed SMB peak wave period deviate in the order of 5% (0.4s) from the observed wave periods. The constant used determined by the calibration is 1.0.

5.7 Deterministic determination of the wave steepness for wave period

The wave period is determined in two ways: with the SMB model for the wave period and with the wave steepness model. In this paragraph the wave steepness is determined from which the wave period can be computed. The model is based on the joint observations of T_p and H_s. The observations are used to calibrate the model.

5.7.1   The determination of the wave steepness

The wave steepness is calibrated in another way than the storm surge level and the SMB wave height and period model. The steepness of the observed typhoons is derived from an analysis of the observed wave height and wave period during the same historical typhoons as used for the calibration of the SMB model (i.e. no 9117, 9119, 9210, 9313). The wave steepness relation is given in the following equation:

$$T_p(H_s, s_p) = \sqrt{\frac{H_s \cdot 2\pi}{g \cdot s_p}}$$

T_p	Peak wave period	[s]
H_s	Significant wave height	[m]
s_p	Wave steepness	[-]
g	Gravity acceleration	[m/s^2]

The values of the wave steepness can be found in Figure 5-12 and Figure 5-13 (also shown in chapter 3). The values of the wave steepness are independent to the wave height above wave heights of 0.5m and prove to be normally distributed. The parameters of the normal distribution are determined with a maximum likelihood analysis. Since the wave steepness is already determined based on the observed wave height and wave period, a calibration step is not useful.
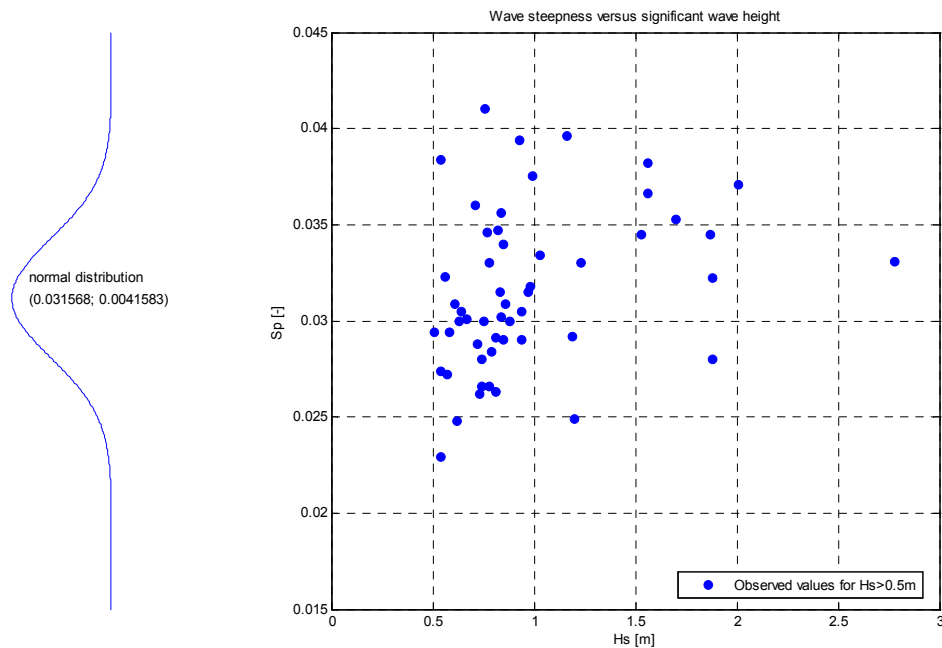
Figure 5-12: Independent wave steepness and wave height for wave heights above 0.5m with normal distribution of the wave steepness (typhoons 9117, 9119, 9210, 9313)
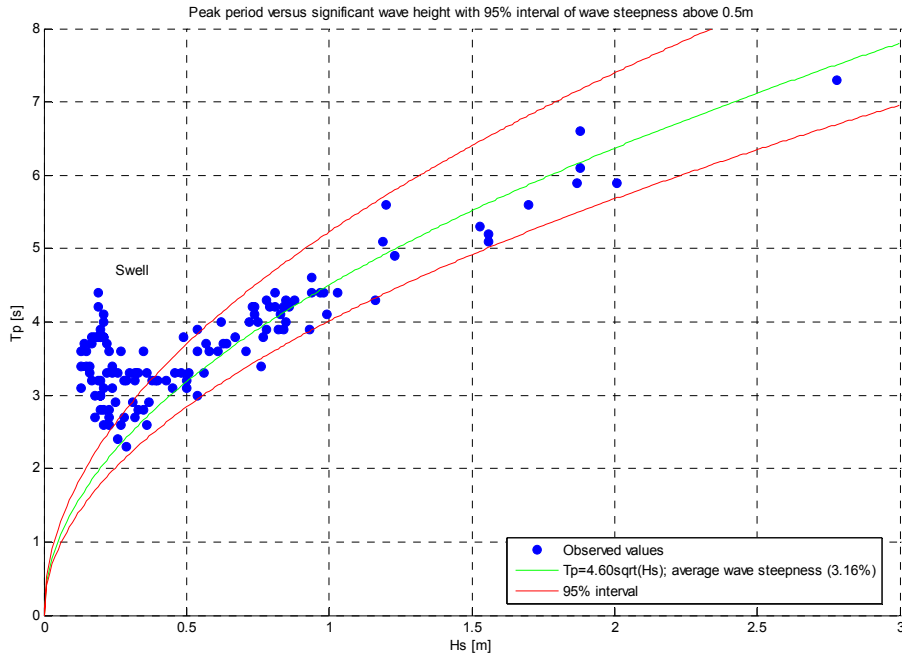
Figure 5-13: Observed peak period plotted against observed significant wave height (no. 9117, 9119, 9210, 9313)

The wave periods that are observed with a wave height under 0.5m are less interesting for the research because the research focuses on extreme values. If the values of the wave steepness are plotted above this threshold level, it can be seen that there is no clear relation between the wave height and the wave steepness. A normal distribution is found for the wave steepness and the values of the normal distribution are given in Figure 5-12. The model predicts the values of the wave height and period reasonably.

The average wave steepness (i.e. 3.16%) is used in the deterministic hindcasting of historical typhoons and is plotted as the green line in Figure 5-13. The properties of the normal distribution are used in the probabilistic analysis. The computed peak wave periods and the wave periods computed with the calibrated wave steepness model are given in Figure 5-14. Again, for the probabilistic analysis, the maxima of the wave period are of interest and not the hourly fit of the observation to the computed wave period.
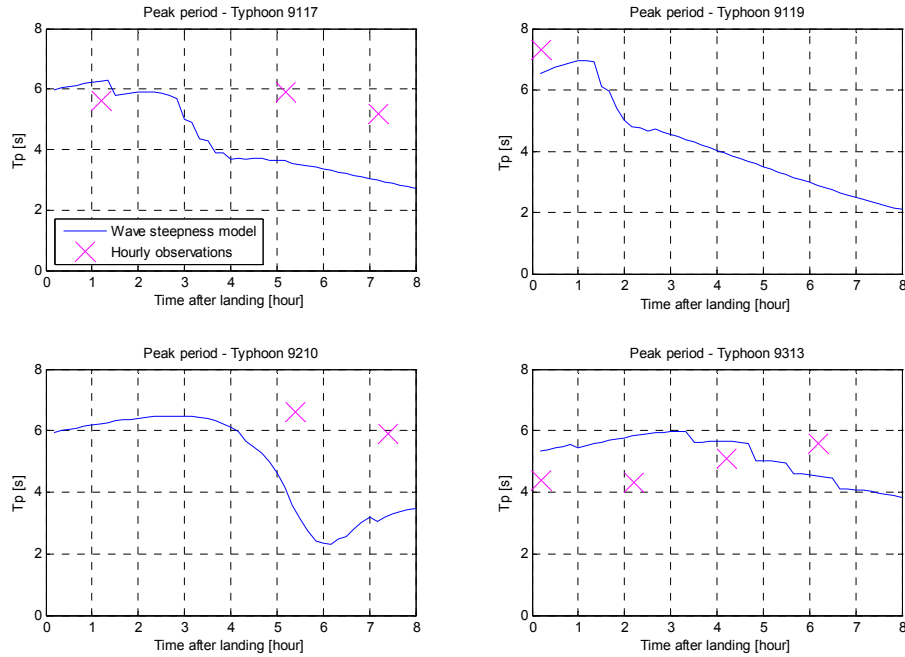
Figure 5-14: Observed wave period and calculated (wave steepness) wave period using an average wave steepness of 3.16%

5.7.2   Discussion of the two models for the determination of the wave period

The wave period computed with the steepness model differs only slightly from the wave period computed with the SMB wave period model. The computed maxima deviate in both cases 0.3 seconds (5%) of the observed maxima. The plotted lines of the wave height and the two wave period models have the same curvature. This can be explained by the fact that the wave steepness is dependent on the SMB wave height. The SMB wave period formula is the same as the SMB wave height formula (only different constants). The calibrated wave period with the wave steepness model implies an average wave steepness of 3.16%. For the statistical analysis in chapter 6 the wave steepness model has got advantages over the SMB wave period model. Therefore the wave steepness model is further used in the research.

5.8   Conclusions about the calibrated model

The models for the storm surge, wave height and wave period have been calibrated. For the statistical analysis, the estimation of the maxima of the observations is of importance. The total storm surge level is calculated and calibrated with two constants (c_1 and c_2). The hourly values of the storm surge are used because both constants have to be fitted. If evaluated with respect to other studies using the same kind of formulae, the calibrated constants seem to be in the order of magnitude of the constants used in that model.

The hourly prediction of the wave height and wave period is poor. The model underestimates the observed wave characteristics after the computed maximum. This is because the inertia of the travelling waves and water level inclination is not accounted for properly. For the statistical analysis, the estimation of the maxima of the observations is of importance. This maximum is estimated reasonably well. The calibration of the wave height and period model with respect to the maximum observed value however is questionable because some observations during extreme conditions failed.

The difference in the SMB wave period model in comparison with the wave steepness model is not significant. In the further research the wave steepness model will be used because of advantages in the statistical analysis. In Table 5-6 the results of this chapter are summarised.

Table 5-6: Overview of calibrated constants and the average errors between observation and the model

Hydraulic variable	Fit constant	Error relative	Error absolute
Pressure set-up	c_1 of 0.03	25 %	0.3m
Wind set-up	c_2 of $0.5*10^{-6}$		
Wave height SMB	fit parameter 0.9	20 %	0.3m
Wave period SMB	fit parameter 1.0	5 %	0.3s
Wave period steepness	steepness of 3.16%	5 %	0.3s

A validation step is needed to determine the uncertainty of the model. The calibrated values can actually not be used for this purpose because the observations may be reproduced better since they were used in the calibration process. Still the calibrated observations are used as to give a rough indication of the model uncertainty.

5.9   Hindcasted typhoons with computed hydraulic variables

The calibrated models are now used for estimating the storm surge level, wave height and peak period for historical typhoons. All historical typhoons are plotted with the modelled water level, wave height and wave period after typhoon landing (Figure 5-15). Also the typhoon tracks over the Kyushu area and Suo-nada Bay are plotted.
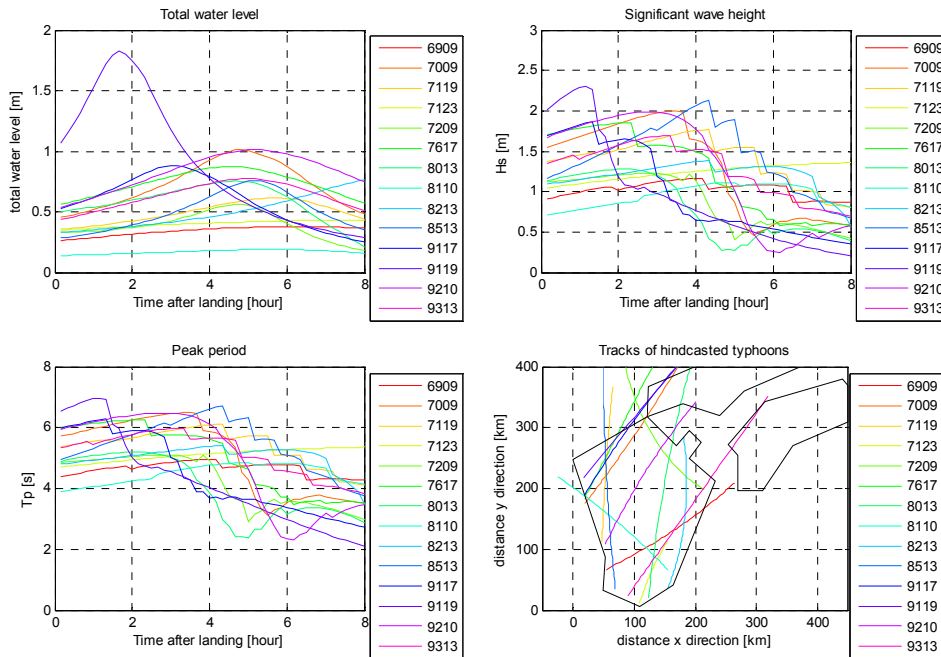
Figure 5-15: Water level, wave height, wave period relative to time of landing and position of historical typhoons

Figure 5-15 shows that the prediction of wave height and period is not smooth but stepwise. This can be explained because the bay is schematised in a discrete number of fetches with accompanying fetch lengths and water depths in order to use the SMB model (see Appendix H). If the wind changes from one of the 16 fetches into the other, a sudden bend in the graph can be seen. In analogy with Figure 5-15 the statistical properties of the hydraulic variables will be determined in the next chapter.

6 Probabilistic analysis of typhoon related hydraulic boundary conditions

In this chapter the probabilistic properties of the hydraulic boundary conditions are determined. The distributions of water level and wave conditions can be obtained via the input probability distributions of typhoon characteristics and the calibrated dependence model from the previous chapter. The marginal and the joint probability density functions of the hydraulic variables are derived. The marginal and joint probability distributions are statistically validated afterwards. Finally, an application of the joint probability density function is given with respect to a failure mode.

6.1 An overall model for probabilistic analysis of hydraulic loads

The overall model for the probabilistic analysis of hydraulic loads depends on different input variables. The input distributions are the typhoon characteristics, the astronomical tide and the basin geometry and bathymetry. Dependence models have been presented in the previous chapter, resulting in the determination of the hydraulic boundary conditions. The variables and the models necessary to describe the JPDF of the hydraulic boundary conditions are stated in Table 6-1.

Table 6-1: Models necessary to describe the JPDF of hydraulic conditions

Variable	Type of variable	Model describing variable
Typhoon parameters	Input	Probability model
Tide level	Input	Probability model
Basin geometry / bathymetry	Input	Probability model (deterministic)
Pressure field	Intermediate	Dependence model
Pressure set-up	Intermediate	Dependence model
Wind field	Intermediate	Dependence model
Wind set-up	Intermediate	Dependence model
Water depth	Intermediate	Dependence model
Total water level	Output / Intermediate	Dependence model
Wave height	Output / Intermediate	Dependence model
Wave period	Output	Dependence model

The joint probability density function of a set of variables can be written as the multiplication of a set of conditional probability density functions and the probability density functions of the input variables. The conditional distribution of any hydraulic variable is obtained by combining a physical dependence model with the probability density functions of the input variables. The behaviour of the physical model depends on the geometry and bathymetry of the basin. In the description of the hydraulic conditions, the following elements need to be established:
- Probability density functions of the typhoon characteristics
- Distribution of the tide level

- Deterministic values of basin geometry and bathymetry

The following models are used as dependence model:
- Dependence model for pressure set-up as a function of atmospheric pressure
- Dependence model for wind set-up as a function of wind speed and the tide level
- Dependence model for wave conditions (wave height, wave period) as a function of the wind speed and total water level

6.2   Probabilistic input parameters for typhoon modelling

In order to perform a Monte Carlo analysis, the input variables (typhoon characteristics, tide level and geometry/bathymetry) have to be described with probability distributions[10]. The probability distributions of the typhoon characteristics are given by Mitsuta and Fujii (1979, 1986). For the average change rates of characteristics after typhoon landing values given by Fujii (1998) are used. Both analyses have the same method of analysing the typhoons and determining the typhoon characteristics. Therefore, the deterministic typhoon characteristics (Fujii, 1998) and the statistical properties of typhoon characteristics (Mitsuta and Fujii, 1979, 1986) can both be used. The modelled typhoons have statistical characteristics similar to the historical typhoons that struck the Japanese main islands between 1951 and 1984.

6.2.1   Number of typhoon landings in a year and position of landing
- Number of landings in a year

The number of landings in a year is estimated with a Poisson distribution. The mean value for the Poisson distribution is 1.04 for area A. To get an insight in this distribution function, the PDF is given in Figure 6-1.
- Location of landing on the boundary of the area

The direction of forward movement is unchanged throughout the path (see next sub paragraph). Therefore the course of the typhoon can be generated starting from the position of landing in each area. This position is generated assuming a uniform probability in the width of the area, seen in the direction of motion of the typhoon (Mitsuta and Fujii, 1986a). An example of the uniform distribution for an arbitrary width of 200 km is given in Figure 6-1).
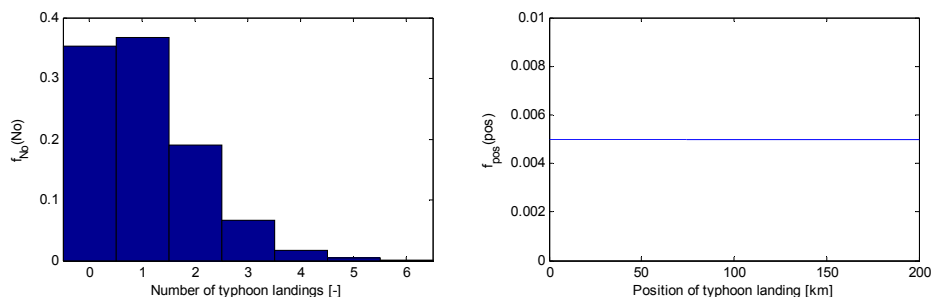
Figure 6-1: Poisson distribution for the number of landings in a year and uniform distribution of position of landing

6.2.2   Probabilistic typhoon characteristics at time of landing
The probabilistic typhoon characteristics at the time of landing are assumed to be lognormally distributed (according to the analysis of Mitsuta and Fujii, 1986). The distributions of central pressure depth, radius to maximum cyclostrophic wind speed, speed of forward movement and direction of forward movement are given in Figure 6-2. The accompanying cumulative lognormal values for the distributions are given in Table 6-2. The radius to maximum cyclostrophic wind speed differs with value of

---

[10] Deterministic variables used for geometry and bathymetry are special cases of probability distributions

the pressure depth. Therefore the typhoons are divided in three classes of pressure depth at the time of landing. The direction of forward movement is defined as the direction of forward movement relative to the east. The use of the lognormal distribution for the direction of forward movement seems to have no physical background, but is still adopted in the probabilistic analysis.

Table 6-2: Typhoon characteristics and the values that describe their cumulative lognormal distributions

Typhoon characteristic	Symbol	Dim.	Application	Lognormal parameter μ	Lognormal parameter σ
Central pressure depth	Δp	[hPa]	Area A	3.60	0.38
Forward movement of typhoon	C_{fm}	[km/h]	Area A	3.40	0.38
Direction of forward movement	γ	[deg]	Area A	4.20	0.45
Radius to maximum cyclostrophic wind seed			0 < Δp < 30	4.61	0.31
	r_m	[km]	30< Δp < 45	4.39	0.59
			45< Δp	4.26	0.41

For the typhoon characteristics the PDFs are plotted in Figure 6-2.
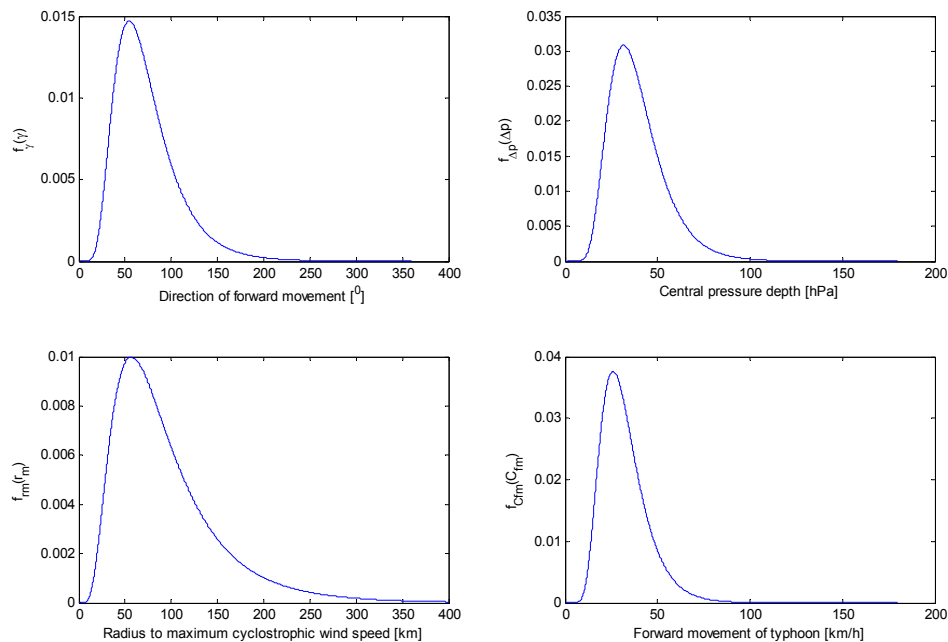
Figure 6-2: Probabilistic typhoon characteristics used as input variables for the Monte Carlo analysis

6.2.3   Changes of typhoon characteristics after landing

The changes in typhoon characteristics after landing are not defined as input variables in the total model. However they are influenced by these values and therefore described here. In the analyses used (Mitsuta and Fujii, 1979, 1986), the characteristics are determined at the moment of typhoon eye landing. The change rates are determined starting from that moment. The change rates are derived from the analysis of Fujii (1998), because that analysis states the values more accurately than the analyses by Misuta and Fujii (1979, 1986). The change in typhoon centre direction is mostly within ±5º/h and is therefore assumed not to change for several hours after landfall. The values of the change of typhoon characteristics are stated in Table 6-3.

Table 6-3: Change rates after landfall for different areas and parameters

Change of characteristic	Symbol	Dimension	Value
Central pressure depth	a_p	[h^{-1}]	0.065
Radius to maximum wind	a_r	[km/h]	4.9
Forward movement	a_c	[km/h^2]	1.4
Direction of forward movement	a_d	[°/h]	0.0

6.2.4   Input variables of tide level and basin geometry

For the analysis of the water level the tidal level has to be computed. To determine the tidal level during the passing of the typhoon, a database of two years of tidal levels has been constructed with the astronomical tide calculated at Aohama (near Kanda) for every 10 minutes (www.mobilegeographics.com). From this database (Figure 6-3), the tide at the time of typhoon landing is drawn randomly (uniform over the total number of individual tide levels). The following tide levels are consecutively drawn from the database in the time steps afterwards to account for the natural tide pattern. Extreme circumstances are however not included in this approach, since only two years of tide levels have been used. Also, the seasonal variation in tidal level is not taken into account in this method, because the tide level is based on a whole year of predicted tide levels. The tidal level is thus slightly underestimated (ca. 0.1m) for the typhoon season.
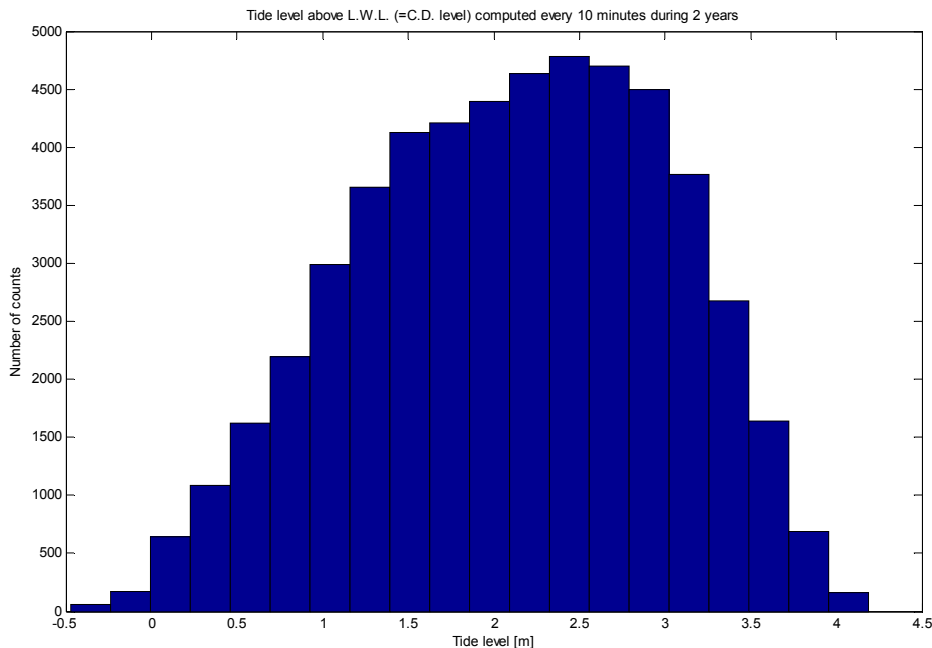
Figure 6-3: Database of tides relative to low water level at Aohama as used in modelling (divided in 20 classes)

The proportion of the tidal water level relative to the storm surge level has got a major influence on the maximum total water level that may occur. If one of the phenomena has got a duration that is much larger than the other, the combined maximum can be estimated to happen approximately around the maximum of the variable of which the period is an order of magnitude bigger. If the magnitude differs considerably, the influence of the dominant variable will play a big role in the combined maximum.

In the case of the storm surge and the tidal level at Suo-nada Bay, the period of the storm surge is slightly longer than the tidal period, but approximately in the same order of magnitude (see Figure 6-4). The maximum value of the tidal level is bigger than the maximum of the storm surge level, but often in the same order of magnitude. Both phenomena and their individual probability of occurrence have to be taken into

account. The tidal level will also have a stronger influence on the total water level because the magnitude exceeds the magnitude of the storm surge level for lower wind speeds.
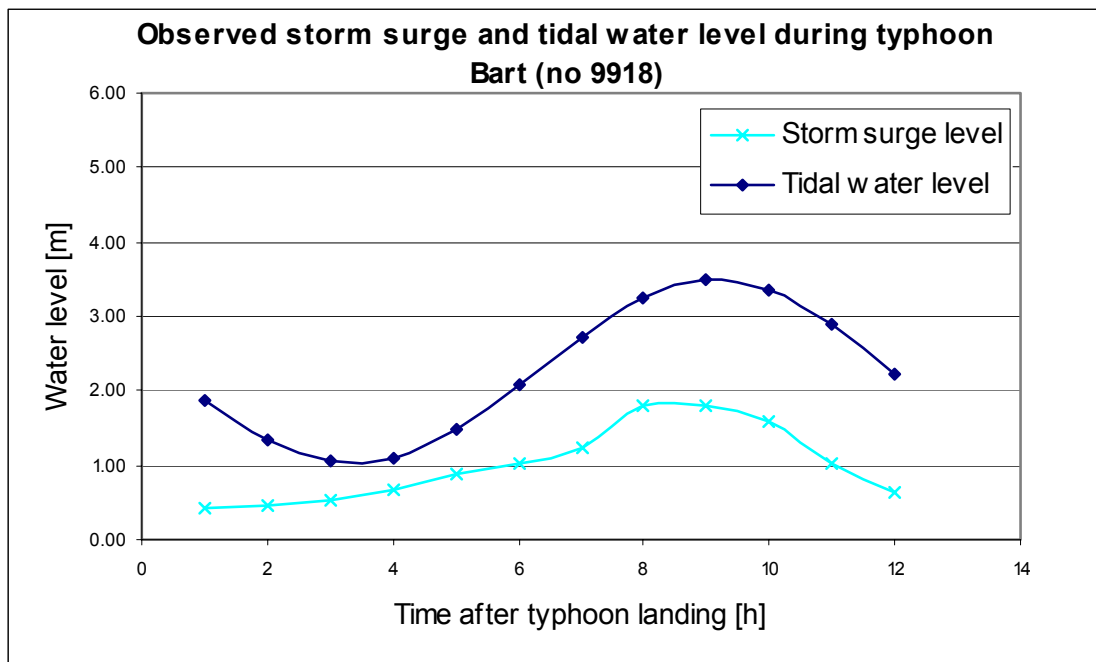
Figure 6-4: Comparison of storm surge level and tidal water level during typhoon Bart (9918)

The deterministic basin geometry and bathymetry as determined in chapter 4 are used as input parameters.

6.3 Marginal distributions and exceedance curves of hydraulic loads

With the randomly drawn typhoon parameters, the tidal water level and the deterministic geometry/bathymetry, the hydraulic boundary conditions can be computed for every typhoon with the use of the combined model as derived in chapter 3. The maxima of every water level, wave height and period can be placed in increasing order to compose a complementary cumulative distribution function[11].

6.3.1 Simultaneous occurrence of maxima

As stated before, the maximum value of every hydraulic variable will be derived for every typhoon. During a typhoon, the occurrence of the extreme water level does not have to occur simultaneously with the maximum wave height or wave period. Since only the maxima and not the hourly values of the hydraulic variables were reasonably estimated, the exact joint occurrence of the maxima is not accounted for; there may in practice be a deviation of an hour between the values. They are conservatively estimated to occur simultaneously because only the maxima of the hydraulic variables are used in the statistical analysis. The joint values (of the maxima) of the hydraulic variables are taken into account and will be used in the analysis of the joint probability density functions.

---

[11] A descending cumulative distribution function, further stated as CCDF

6.3.2   Positions of calculated maxima in exceedance plot

To determine the parameters of the cumulative probability distribution, the observations are put in order of increasing magnitude. There are several conditions that the plot positions have to meet. Different methods are used for plot positions in statistical analyses. The following approximation of the ordinate of the plot position given by Bernard / Bos – Levenbach is used (see Vrijling et al., 2002).

$$\frac{i - 0.3}{N + 0.4}$$

(6-1)

i	Position of data point in increasing order	[-]
N	The number of data points	[-]

Further, the maxima are determined per typhoon and not per year. Since the exceedance probability of hydraulic boundary conditions per year is of interest and not per typhoon, the ratio between these two has to be taken into account. The probability is therefore multiplied by the ratio of the number of typhoons and the number of years. This results in an exceedance probability per year.

6.3.3 Number of years of simulations

To calculate the maxima of the hydraulic variables, a number of simulations has to be executed to get stable results. Three times simulations for the same number of years have been done and plotted in the same graph (for 10 years, 100 years and 1000 years of simulation). The results for the maxima of the peak period are plotted in Appendix I. It can be seen that the CCDF converges with the number of years of simulation. Since the level of probabilities of exceedance is dependent on the (not yet determined) level of protection, the exact number of years of simulation is not known. Because of capacity limits in computation, 10000 years of simulations will be done.

6.3.4   Types of distributions of hydraulic variables

The exceedance curves for the water level, the wave height and the wave period are obtained together with the track of the typhoons over Kyushu Island and Suo-nada Bay (Appendix J). The typhoon tracks all start at the boundary of area A.

A distribution type is fitted to the dataset of 10000 maxima for the total water level, storm surge level, the wave height and the wave period. The choice of the distributions was done visually[12]. The parameters were determined with ML estimation. The computed parameters for the probability distributions are given in Table 6-4 for the total water level, the tidal water level, the storm surge level, the wave height and the wave period. Further, intermediate variables are fitted that are used later in this chapter.

Table 6-4: MLE values of parameters of fitted distributions

Typhoon characteristic	Symbol used	Distribution type	Distribution parameter	Distribution parameter
Total water level (increase)	deltah	Lognormal	1.31 (μ)	0.124 (σ)
Tidal water level*	dhtide	Weibull	3.49 (a)	9.53 (b)
Storm surge level*	dhwp	Lognormal	-0.606 (μ)	0.522 (σ)
Significant wave height	Hs	Normal	1.45 (μ)	0.452 (σ)
Peak period	Tp	Normal	5.39 (μ)	0.947 (σ)

* Intermediate hydraulic variables used later in the research

6.3.5   Derived marginal probability density functions of hydraulic variables

The dataset calculated with the Monte Carlo analysis is plotted together with the probability distributions in Figure 6-5.

---

[12] The computer program Bestfit (Bestfit, 1993) was used, but the program appeared to give erroneous results
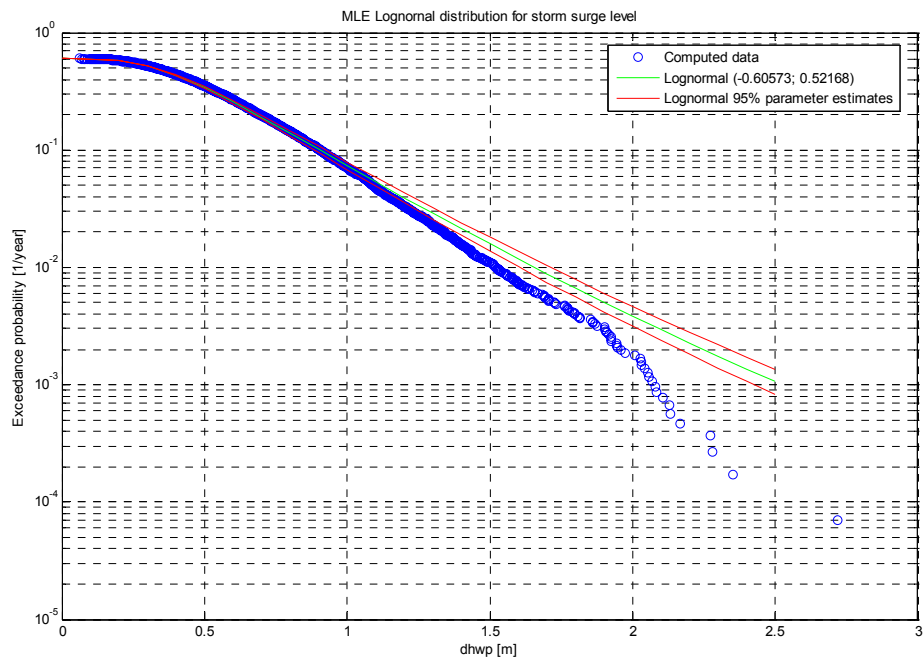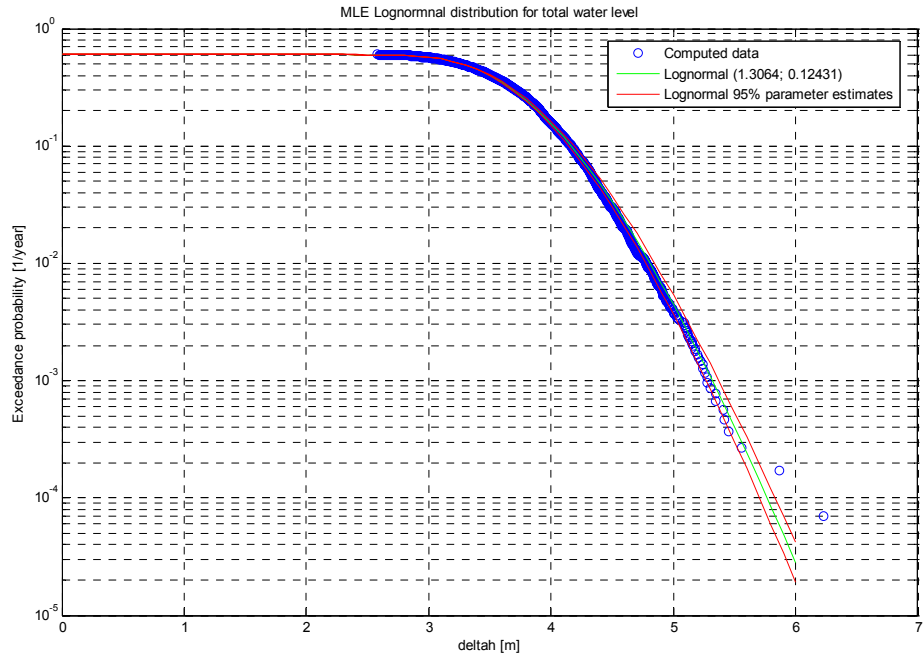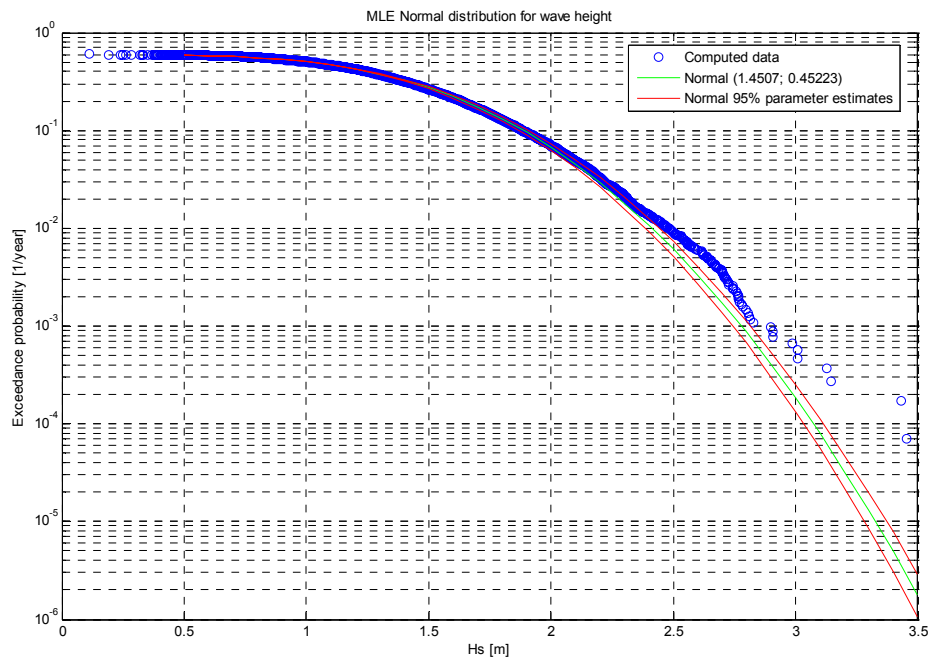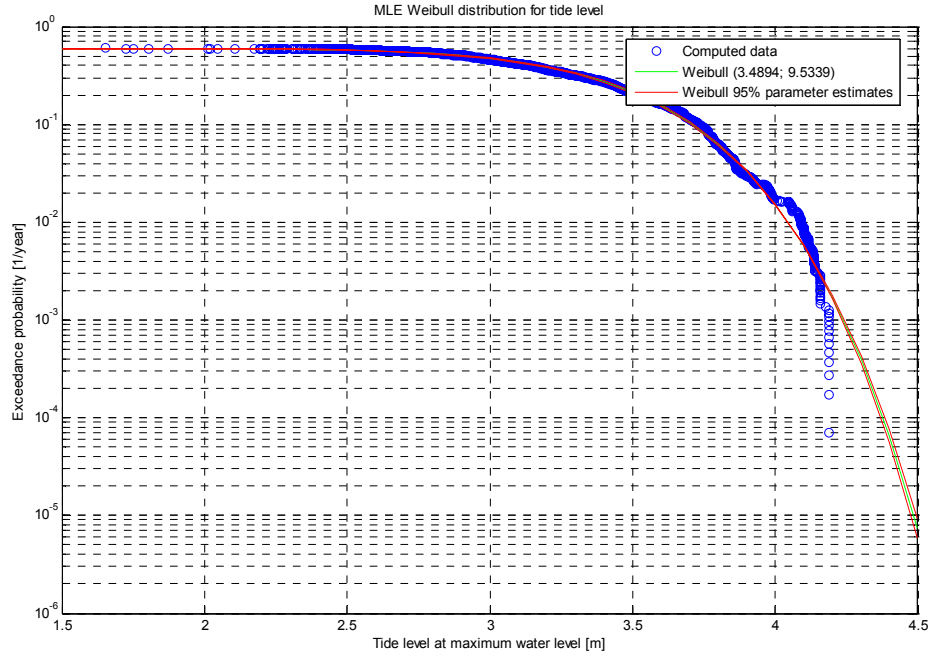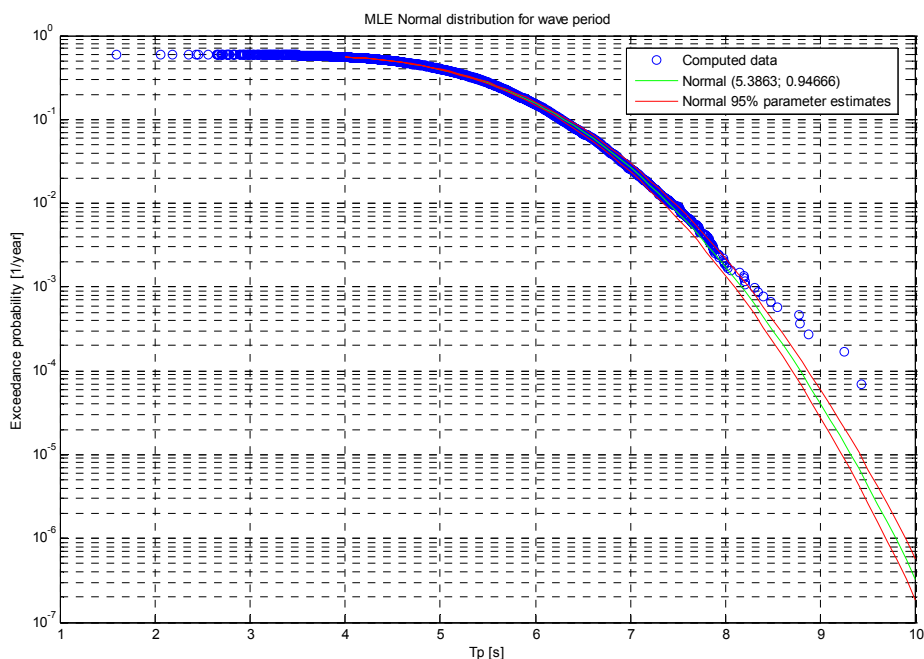
Figure 6-5: Exceedance plots for the hydraulic variables for 10000 simulations

- Discussion of results

The marginal probability distributions fit to the average values of the computed (Figure 6-5). The tail of the distributions however deviates from the fitted distributions.

6.3.6 Fitting the tails of the marginal probability density functions

The tails are analysed separately to obtain better results for the distributions of the hydraulic variables. Only the highest values (the top 10 data points, or 0,1%) of the dataset are used to determine the distribution function of the tail. With a high threshold level, the distribution function of exceedance may be approximated by the Generalized Pareto Distribution (according to the limit theorem of Balkema and de Haan (de Wit et al., 2003)). The Generalized Pareto Distribution is fitted to the tail of the hydraulic variables using a least square analysis, resulting in the parameters as stated in Table 6-5. The results are plotted in Figure 6-6.

Table 6-5: Parameters of fitted GPD on the top 10 simulation points

Typhoon characteristic	Symbol	GPV parameter θ	GPV parameter a
Total water level	dh	26.1	5.279
Significant wave height	Hs	15.0	2.897
Peak period	Tp	17.9	8.300

LS Pareto distribution for extreme total water levels

LS Pareto distribution for extreme wave heights
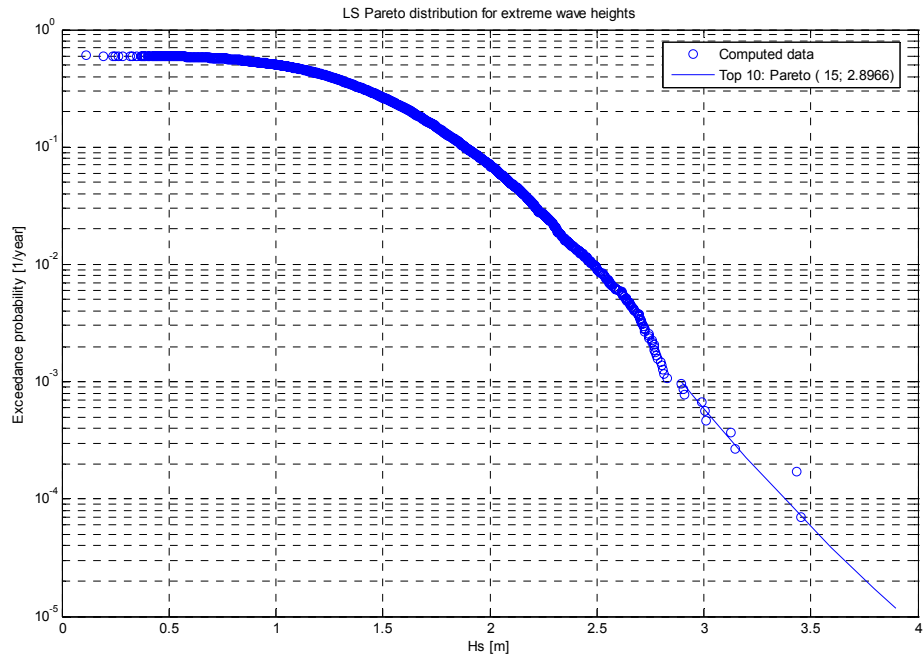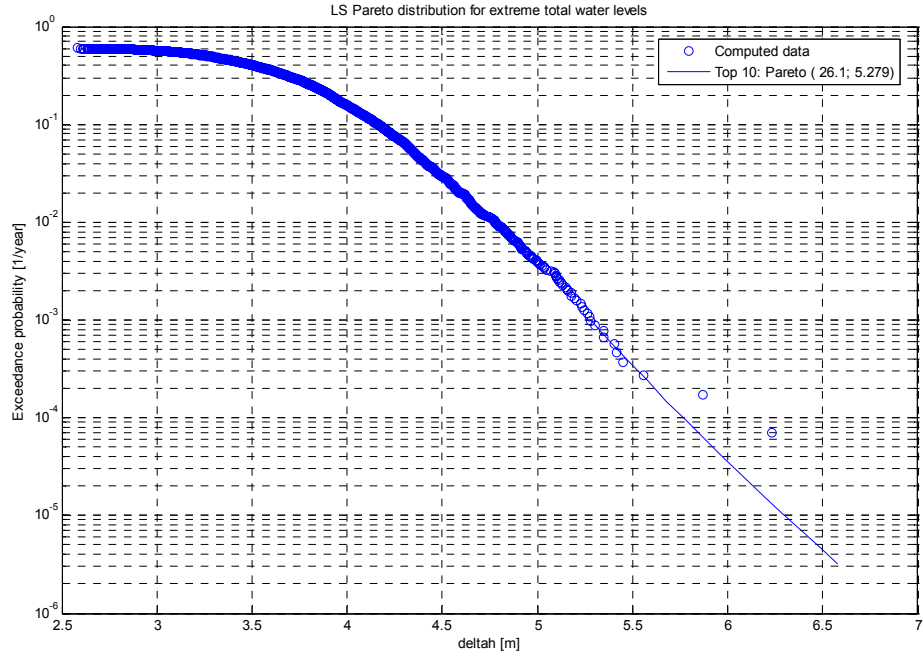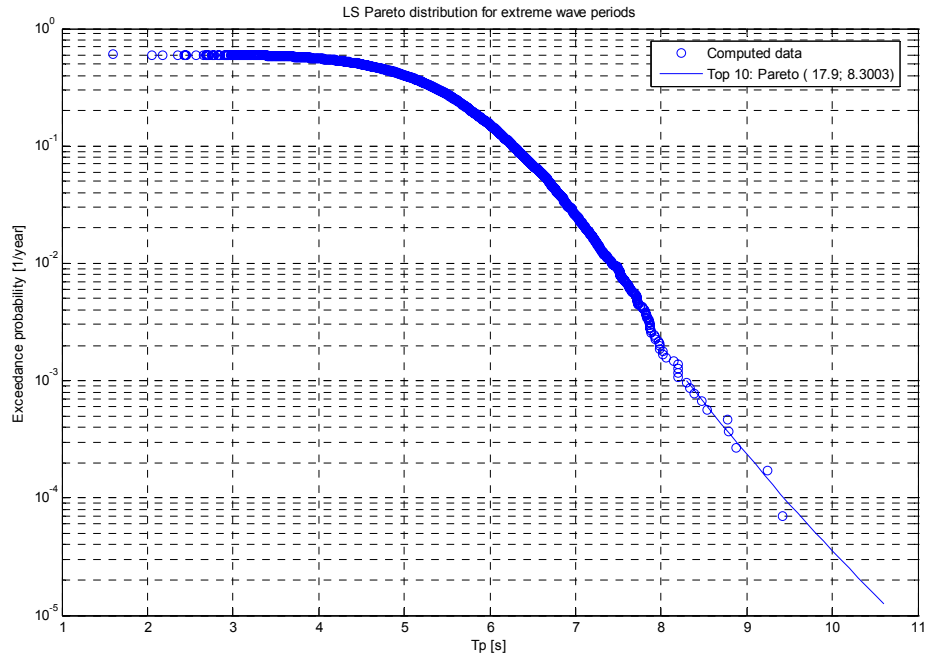
Figure 6-6: Tail of exceedance probability functions derived from the top 10 simulated data points

- Conclusions about marginal probability distributions

The optimal marginal probability distributions of the hydraulic variables are obtained. The package Bestfit was used to obtain the best distributions. However the results appeared to be erroneous. The visual determination of the best distribution should be replaced by a Chi-square test to obtain the distribution type that fits the data points best. The distribution of the total water level and the storm surge level can be described with a lognormal distribution. The tidal water level can be described with a Weibull distribution. The wave height and the wave period can be described with a normal distribution. The tails of the marginal probability density functions however deviate form the fitted distributions to the complete dataset. Therefore a threshold is used to fit only the top 10 data points, to obtain the tail distribution. The Generalized Pareto Distribution was fitted according to the theorem of Balkema and de Haan. This distribution type is applied to describe the tail of the hydraulic variables. If more simulations are done, the tail can be estimated better. The following values of the hydraulic parameters can be estimated with different return periods (Table 6-6).

Table 6-6: Return periods of hydraulic variables

Return period [1/year]	Dimension	10^{-3}	10^{-4}	10^{-5}
Total water level	[m]	5.5	5.7	6.3
Significant wave height	[m]	2.9	3.4	3.9
Peak wave period	[s]	8.3	9.4	10.8

6.4   Joint probability density functions of hydraulic variables

The marginal probability density functions have been derived for the hydraulic variables. For several reliability functions, more than one hydraulic variable have to be taken into account as pointed out in chapter 2. In that case, the JPDFs have to be used instead of the marginal PDFs. The hydraulic variables that have to be taken into account are the total water level, the wave height and the peak wave period (Chapter 2). The JPDFs of different combinations of the variables are determined. The correlation between two variables needs to be investigated and, if possible, explained by the physical relations between the variables. From the JPDFs, the conditional PDFs are determined.

6.4.1   Comparison correlated versus not correlated
The difference between hydraulic variables that are independent and hydraulic variables that are dependent is pointed out in this paragraph as an example (Figure 6-7). The distribution of the independent hydraulic variables is derived from random plotting of the marginal distribution functions. The other figure states the actual derived joint values of hydraulic variables (wave height and storm surge level).
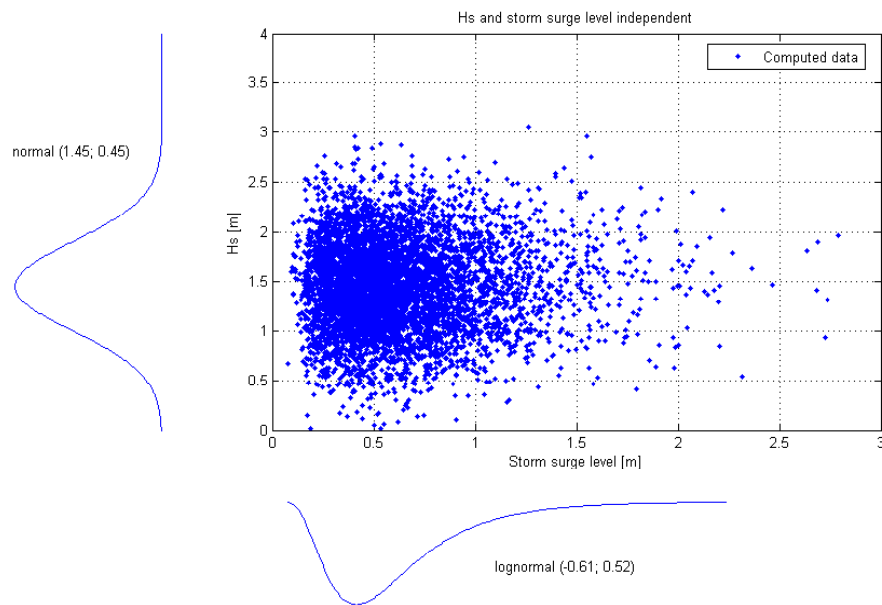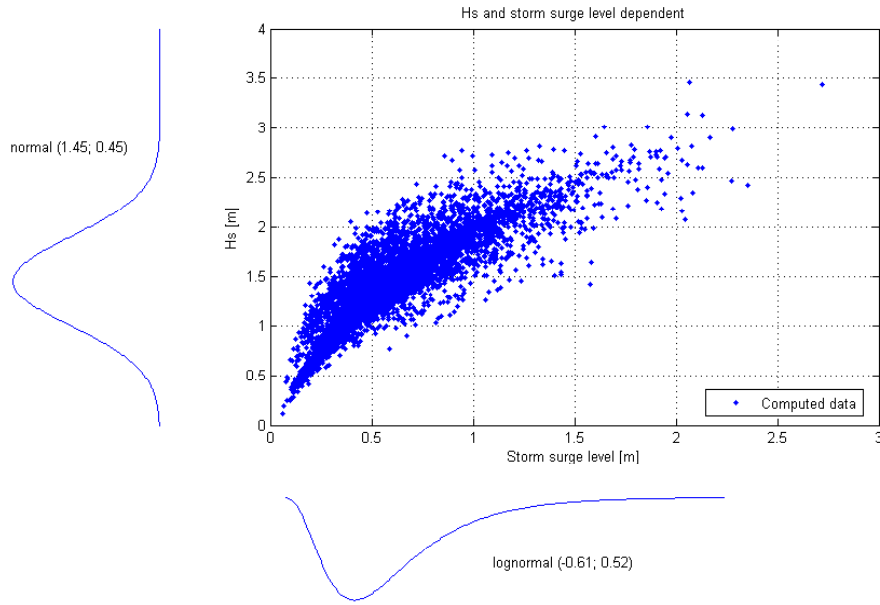
Figure 6-7: Figure with independence (top) and dependence (bottom) between wave height and storm surge level

The correlation coefficient R^2 is often used to describe the correlation between two variables. For this example the correlation coefficient is derived. In the first case the value of R^2 is 0 because of the independence. In the second case the correlation coefficient is 0.75. If the values were fully correlated the value would be 1.0. A strong correlation appears to be present in the relation between the storm surge and the wave height and may not be neglected in analysing the JPDFs.

6.4.2   JPDFs of peak wave period versus wave height
In the case of two independent variables the JPDF of the variables can simply be obtained by multiplying their marginal probability density functions (as could be seen in the previous sub paragraph). However, since there is dependence between the hydraulic variables this approach cannot be used. The joint distribution can be obtained via independent variables that are related to the hydraulic variables (that have to be described with the JPDF).

For the derivation of the JPDF of the wave period and the wave height, the independence of the wave steepness and the wave height can be used. The marginal probability density functions of the wave height and the wave steepness can be multiplied. The following transformation of the independent marginal probability density functions has to be done (after Vrijling et al., 2002):

$$f_{H_s,T_p} = f_{H_s} \cdot f_{s_p} |J| \qquad (6\text{-}2)$$

$$|J| = \begin{vmatrix} \dfrac{\partial H_s}{\partial H_s} & \dfrac{\partial H_s}{\partial T_p} \\[2mm] \dfrac{\partial s_p}{\partial H_s} & \dfrac{\partial s_p}{\partial T_p} \end{vmatrix} \Rightarrow \begin{vmatrix} \dfrac{\partial H_s}{\partial H_s} & \dfrac{\partial H_s}{\partial T_p} \\[2mm] \dfrac{\partial s_p}{\partial H_s} & \dfrac{\partial s_p}{\partial T_p} \end{vmatrix} = \begin{vmatrix} 1 & \dfrac{\partial H_s}{\partial T_p} \\[2mm] 0 & \dfrac{\partial s_p}{\partial T_p} \end{vmatrix} = \begin{vmatrix} \dfrac{\partial s_p}{\partial T_p} \end{vmatrix} \qquad (6\text{-}3)$$

$$s_p = \frac{H_s \cdot 2\pi}{g \cdot T_p^2} \Rightarrow \left| \frac{\partial s_p}{\partial T_p} \right| = \left| \frac{-4\pi \cdot H_s}{g \cdot T_p^3} \right| = \left| \frac{-4\pi \cdot H_s}{g \cdot \sqrt[3]{\dfrac{H_s \cdot 2\pi}{s_p \cdot g}}} \right|$$

$f_{x,y}$	Joint probability density function of variables x and y	[-]
f_x	Marginal probability density function of variable x	[-]
J	Jacobian	
$\dfrac{\partial y}{\partial x}$	Derivative of variable y with respect to variable x	

The joint probability density function and the simulated dataset are both plotted in Figure 6-8
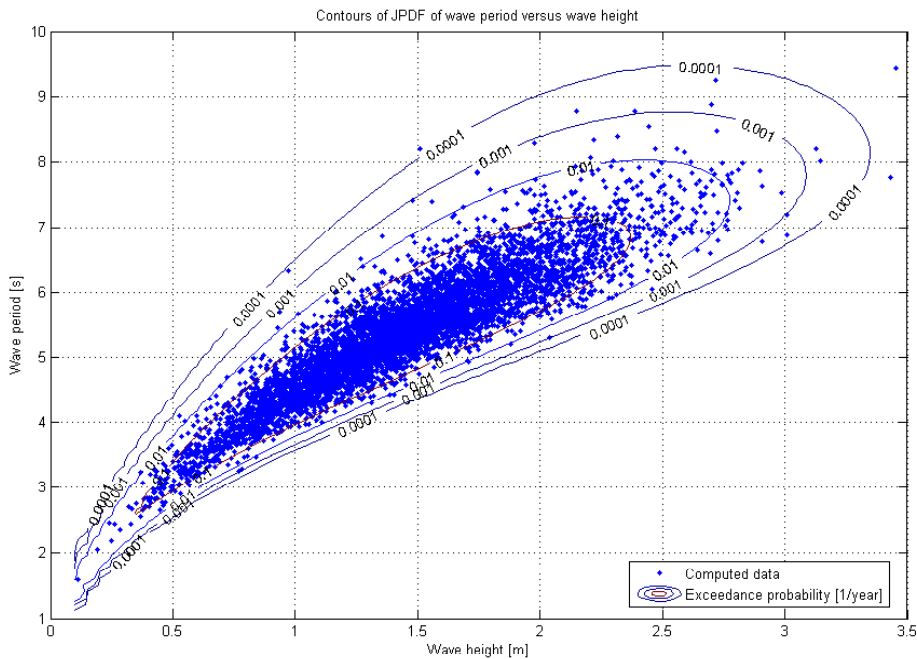
Figure 6-8: Joint probability density function and computed dataset of peak period and wave height

A good agreement between the simulated dataset and the JPDF can be seen. The tails of the marginal probability density functions do not properly describe the extreme computed data points. Therefore in the highest region the model does not cover the computed values completely.

With the JPDF of wave height and wave period, the conditional PDF can easily be derived (Vrijling et al., 2002):

$$f_{(T_p|H_s)} = \frac{f_{H_s,s_p}}{f_{H_s}} = \frac{f_{H_s} \cdot f_{s_p}}{f_{H_s}} \cdot |J| \tag{6-4}$$

$$|J| = \left| \frac{\partial s_p}{\partial T_p} \right| \tag{6-5}$$

$f_{x|y}$	Conditional probability density function of variable x with respect to variable y	[-]

f_x	Marginal probability density function of variable x	[-]
J	Jacobian	

The result is plotted in Figure 6-9 and is in line with the JPDF and the simulated dataset.
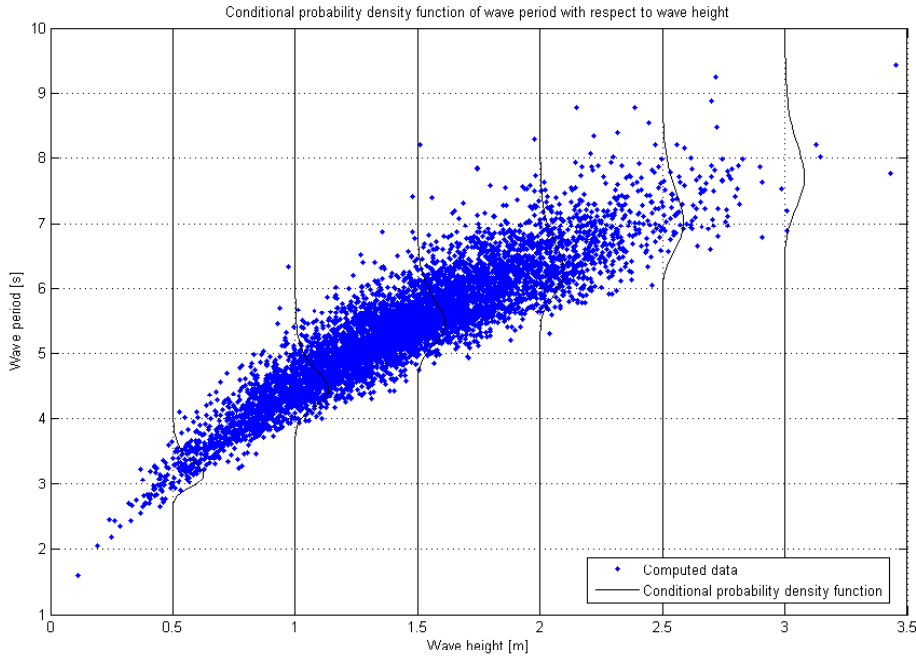
Figure 6-9: Conditional PDF with computed data of wave period dependent on wave height

6.4.3   JPDF's of wave height and total water level

From the previous section it can be concluded that two independent variables are needed to describe the JPDF and that these variables must be related to the hydraulic variables that are described with the JPDF. The total water level is the sum of two independent contributions: the tidal water level and the storm surge level (sum of wind and pressure set-up)

$$\Delta h = \Delta h_{tide} + \Delta h_p + \Delta h_w \qquad (6-6)$$

$$\Delta h_{wp} = \Delta h_p + \Delta h_w \qquad (6-7)$$

And therefore:

$$\Delta h_{tide} = \Delta h - \Delta h_{wp} \qquad (6-8)$$

Δh	Total water level increase	[m]
Δh_{tide}	Tidal water level	[m]
Δh_p	Pressure set-up	[m]
Δh_w	Wind set-up	[m]
Δh_{wp}	Storm surge level	[m]

The relation between the tidal water level, the storm surge and the wave height needs to be derived to use the independence between tidal water level and storm surge in the determination of the JPDF of the total water level and the wave height. The relation between wave height and storm surge level can be found via the wind speed. The wind speed is explicitly included in the wind set-up and the wave height and implicitly in the pressure set-up.

First of all is the tidal water level is independent of the wind speed. This can be seen in Figure 6-10:
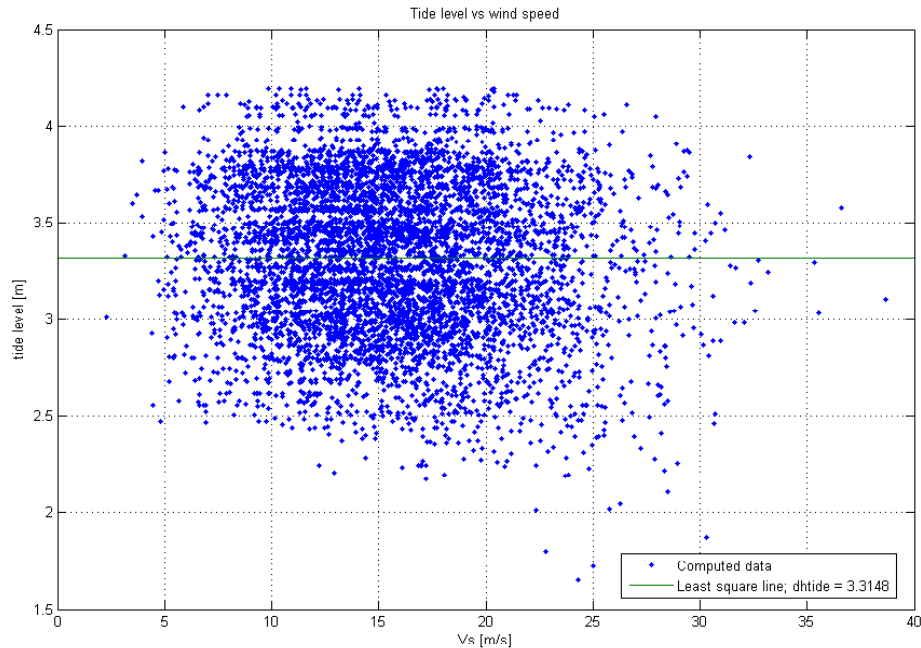
Figure 6-10: Relation between tidal water level and wind speed
Because of the classes used for the tidal water level regularity seems to appear

A number of lower values of tide level are found in regions of higher wind speeds. This is because the total maximum water level is then built up of larger values of the storm surge.

Now the relation of the storm surge level and the wind speed has to be determined. The storm surge is the sum of the pressure set-up and the wind set-up. The relation between the pressure set-up and the wind speed is given in Appendix K and is found via the central pressure depth which determines the wind speed:

$$\Delta h_p :: aV_s^2 + bV_s + c$$

Δh_p	Pressure set-up	[m]
V_s	Surface wind speed	[m/s]
a	Constant	[s²/m]
b	Constant	[s]
c	Constant	[m]

The wind set-up is explicitly related to the quadratic wind speed. The following relations hold:

$$\Delta h_w :: c \cdot V_s^2$$

Δh_w	Wind set-up	[m]
V_s	Surface wind speed	[m/s]
c	Constant	[s²/m]

With respect to the storm surge level and the wind speed, the following relation is valid:

$$\Delta h_{wp} :: aV_s^2 + bV_s + c$$

Δh_{wp} Storm surge level (wind and pressure set-up)   [m]

V_s Surface wind speed   [m/s]

a,b,c Constants of a not yet determined value

This relation is confirmed by to the simulated dataset (Figure 6-11)
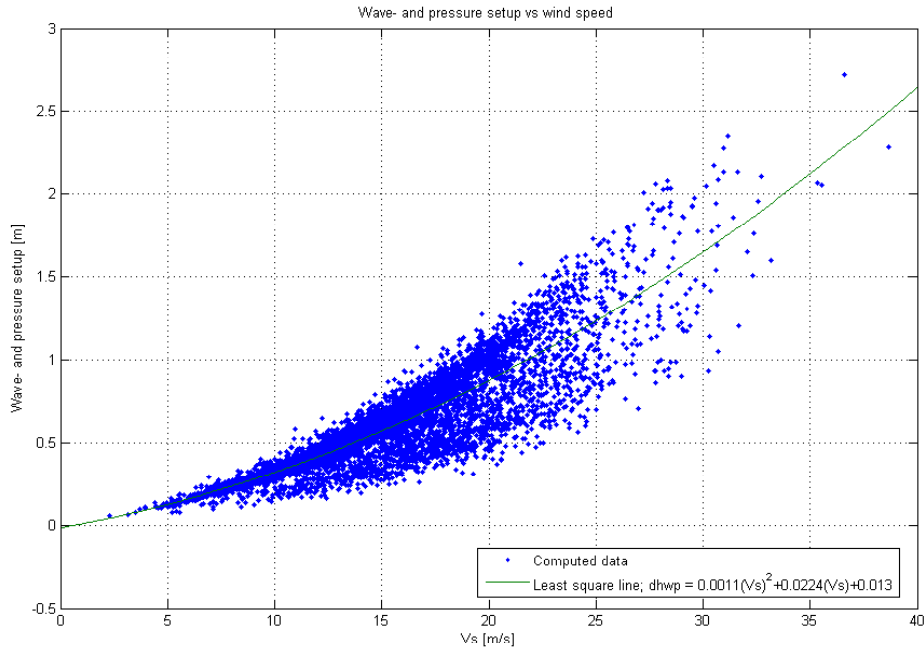
Figure 6-11: Quadratic relation between storm surge and wind speed, fitted with least square line

The wave height is related to the wind speed via the SMB model. The expression however cannot be stated explicitly. Therefore, the simulated dataset is used to derive the relation between wave height and wind speed. The wave height appears to be proportional to the wind speed (Figure 6-12).

$$H_s :: V_s$$

This relation is confirmed if the SMB model is analysed more in depth. The upper boundary of wave heights is determined by the limitation of the fetch length (Appendix L).
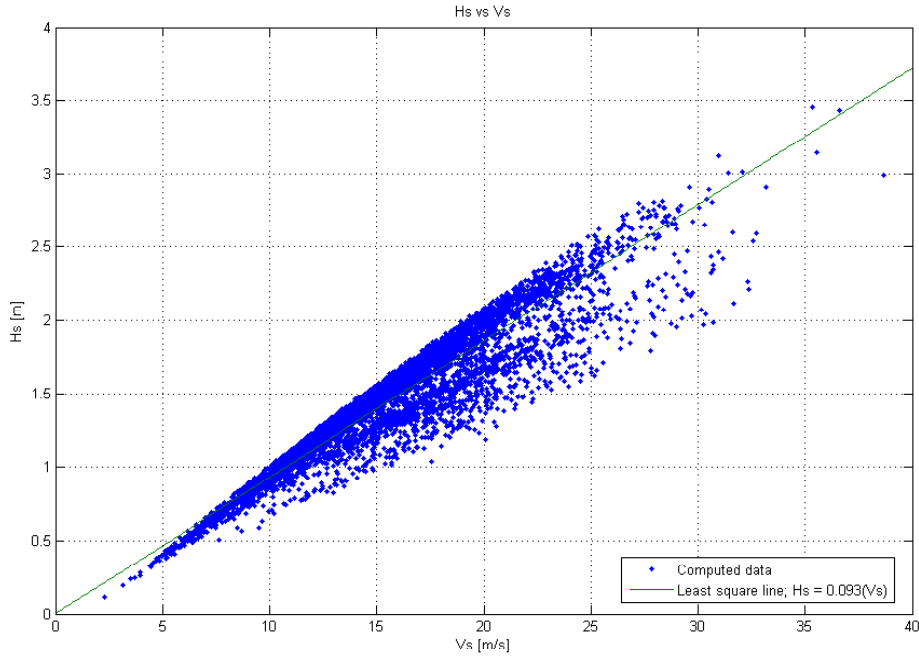
Figure 6-12: Relation between wave height and wind speed with least square line

The derived relation between storm surge and wind speed could be defined as:

$$\Delta h_{wp} :: aV_s^2 + bV_s + c$$

The interest however is the inverse dependence of wind speed on storm surge level. From physical point of view, the storm surge level is zero if there is no wind speed. The following inverse expression can therefore be stated:

$$V_s :: b\sqrt{\Delta h_{wp}}$$

The relation between the wave height and the storm surge can now be derived. In this case it should also be taken into account that both variables have no value if there is no wind speed:

$$H_s :: b\sqrt{\Delta h_{wp}}$$

The shape of the derived physical relation is confirmed by the simulated dataset. The value for the constant in the formula can be obtained from the simulated dataset and appears to be 1.96 (see Figure 6-13).

$$H_s = 1.96\sqrt{\Delta h_{wp}} \tag{6-9}$$

H_s Significant wave height   [m]
Δh_{wp} Storm surge level   [m]
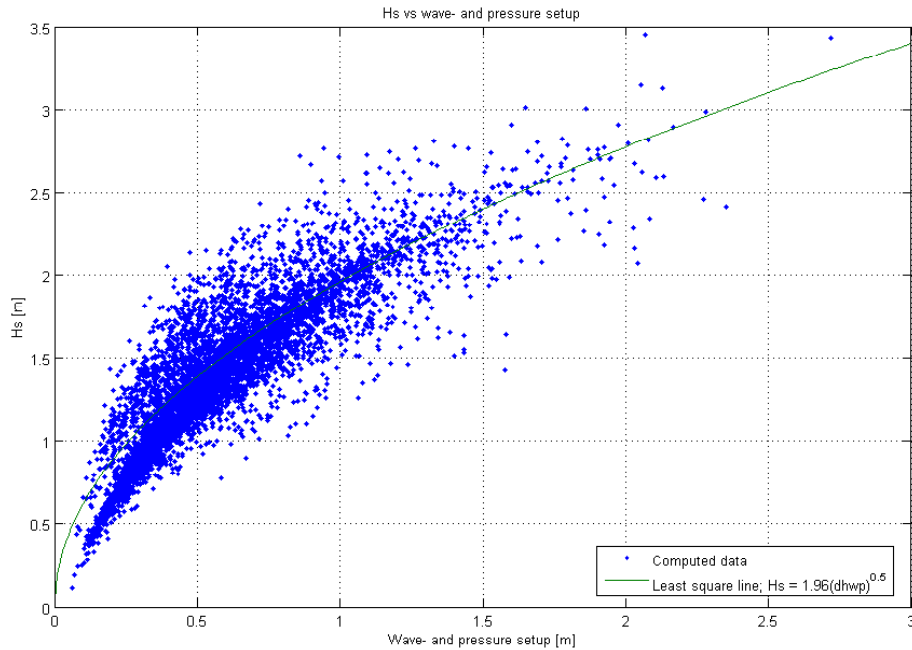
Figure 6-13: Relation between wave height and storm surge with least square line

The tide level is related to the wave height in the SMB wave height model. The relation is however very weak as can be seen in Figure 6-14. The variables may therefore be assumed to be independent.
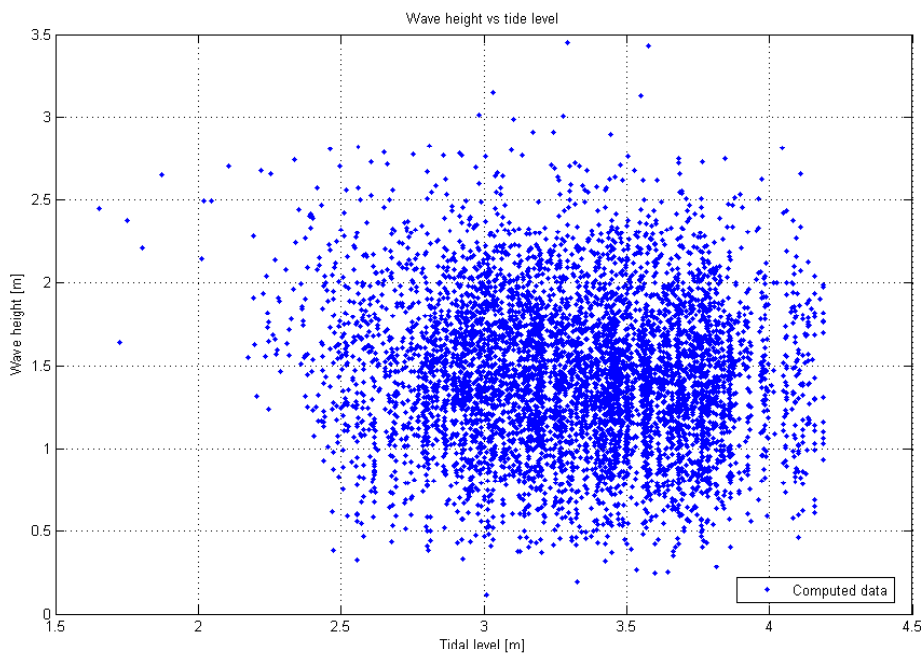
Figure 6-14: Relation between wave height and tidal water level

The same phenomenon occurs as could be seen in the relation between tidal water level and wind speeds (Figure 6-10). In the regions where the high values of the storm surge determine the maximum water level, the wave height will have larger values and the tidal water level will be lower.

The following expression can now be stated:

$$f_{dh,H_s} = f_{dh_{tide}} \cdot f_{dh_{wp}} \cdot |J| \qquad (6\text{-}10)$$

$$|J| = \begin{vmatrix} \dfrac{\partial dh_{tide}}{\partial dh} & \dfrac{\partial dh_{tide}}{\partial H_s} \\[2mm] \dfrac{\partial dh_{pw}}{\partial dh} & \dfrac{\partial dh_{pw}}{\partial H_s} \end{vmatrix} \Rightarrow \begin{vmatrix} \dfrac{\partial dh_{tide}}{\partial dh} & \dfrac{\partial dh_{tide}}{\partial H_s} \\[2mm] \dfrac{\partial dh_{pw}}{\partial dh} & \dfrac{\partial dh_{pw}}{\partial H_s} \end{vmatrix} = \begin{vmatrix} 1 & 0 \\[2mm] 1 & \dfrac{\partial dh_{wp}}{\partial H_s} \end{vmatrix} = \left| \dfrac{\partial dh_{wp}}{\partial H_s} \right| \qquad (6\text{-}11)$$

$$H_s = 1.96\sqrt{dh_{wp}} \Rightarrow \left| \frac{\partial dh_{wp}}{\partial H_s} \right| = \frac{2H_s}{1.96}$$

dh	Total water level increase	[m]
dh_{wp}	Storm surge level	[m]
dh_{tide}	Tidal water level	[m]
H_s	Significant wave height	[m]
J	Jacobian	

The results are plotted in Figure 6-15
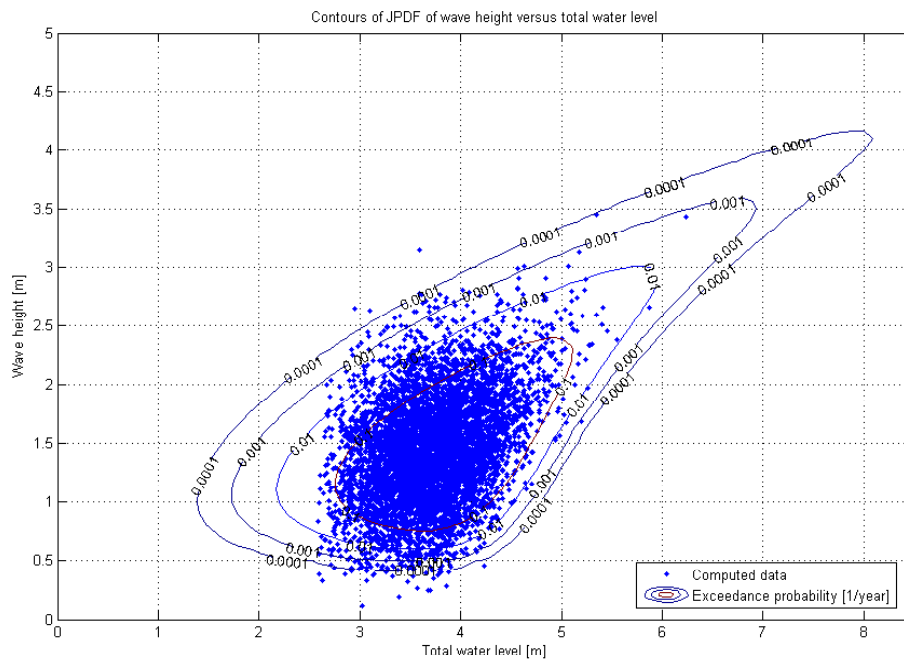
Figure 6-15: Contour plot and computed dataset of wave height versus total water level

The simulated dataset is in line with the JPDF. The values should be within the limits of the contours because the simulation is done for 10000 years. The extreme tail is reasonably estimated by the JPDF

Again, with the obtained JPDF the conditional PDF can be obtained. The hydraulic variables are now given in another order so the Jacobian changes:

$$f_{(H_s|dh)} = \frac{f_{dh_{tide}} \cdot f_{dh_{wp}}}{f_{dh}} \cdot |J| \tag{6-12}$$

$$f_{(H_s|dh)} \Rightarrow |J| = \begin{vmatrix} \dfrac{\partial dh_{tide}}{\partial dh} & \dfrac{\partial dh_{tide}}{\partial H_s} \\ \dfrac{\partial dh_{wp}}{\partial dh} & \dfrac{\partial dh_{wp}}{\partial H_s} \end{vmatrix} = \begin{vmatrix} 0 & 1 \\ \dfrac{\partial dh_{wp}}{\partial H_s} & 1 \end{vmatrix} = \left| -\dfrac{\partial dh_{wp}}{\partial H_s} \right| \tag{6-13}$$

$$H_s = 1.96\sqrt{dh_{wp}} \Rightarrow \left| -\frac{\partial dh_{wp}}{\partial H_s} \right| = \frac{2H_s}{1.96}$$

dh	Total water level increase	[m]
dh_{wp}	Storm surge	[m]
dh_{tide}	Tidal water level	[m]
H_s	Significant wave height	[m]
J	Jacobian	

The relations can be plotted and the results are given in Figure 6-16
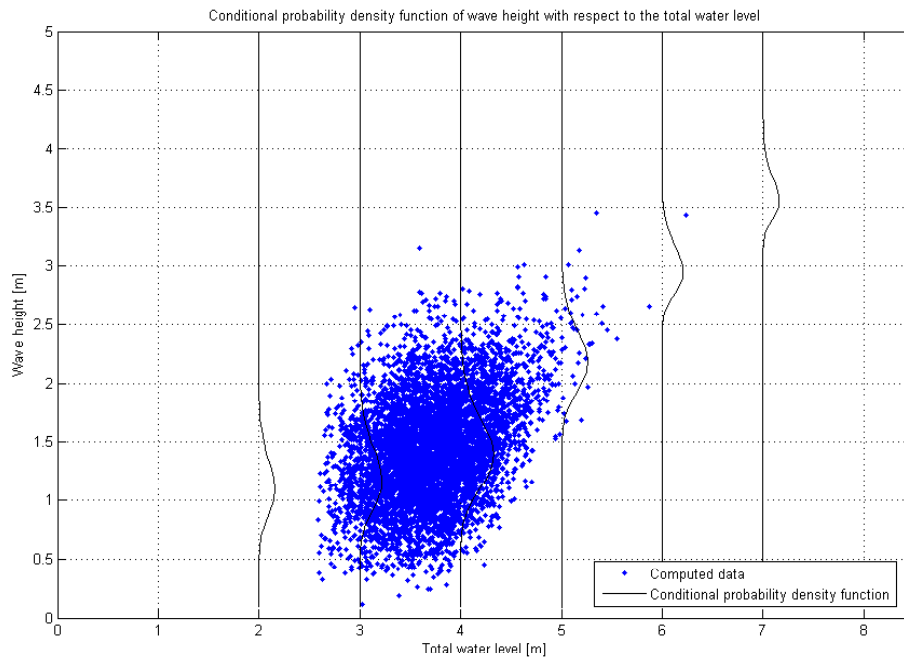
Figure 6-16: Conditional PDF and computed data of wave height dependent on the total water level

The results are in line with the presented JPDF.

6.4.4 JPDFs of wave period and total water level

In analogy with the derived JPDF of the total water level and the wave height, the JPDF of the total water level and the wave period can be determined. The following relation between wave height and wave period holds according to the wave steepness model:

$$T_p :: \sqrt{H_s}$$

Therefore the following relation between wave period and wind speed can be stated, because the wave height is proportional to the wind speed:

$$T_p :: \sqrt{V_s}$$

This is confirmed by the simulated dataset (Figure 6-17)
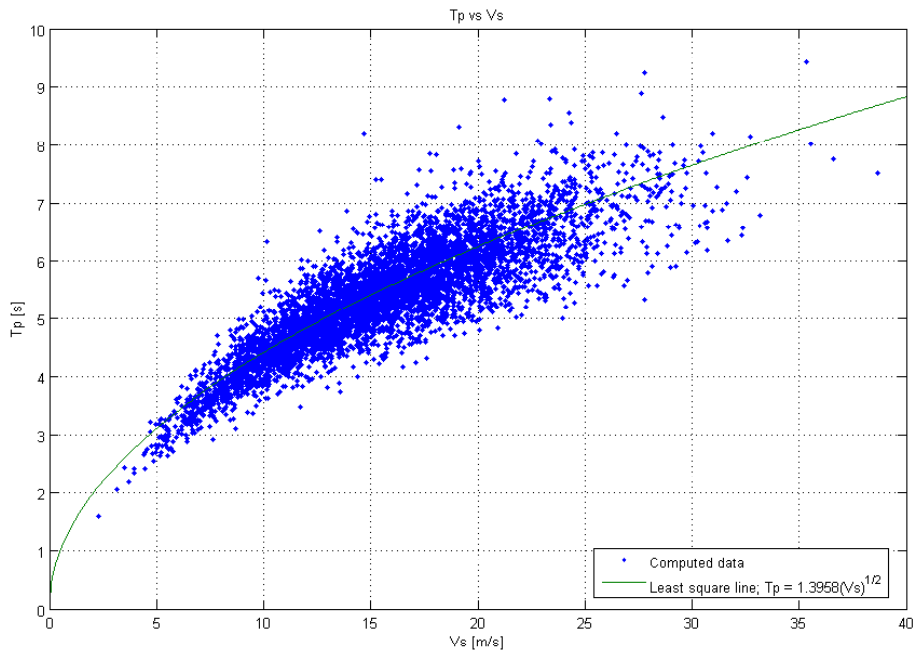
Figure 6-17: Relation between wave period and wind speed with least square line

The relation between wave period and storm surge can now be derived. Taking into account that both variables have no value, if there is no wind speed the following holds:

$$T_p :: b\sqrt[4]{\Delta h_{wp}}$$

The constant in the formula is obtained wit h the least square method fitting the simulated dataset with this physical relation. The constant in the formula is 6.32:

$$T_p = 6.32\sqrt[4]{\Delta h_{wp}} \tag{6-14}$$

T_p	Peak wave period	[s]
Δh_{wp}	Storm surge level	[m]

The shape of the physical line is confirmed by the simulated dataset (Figure 6-18).
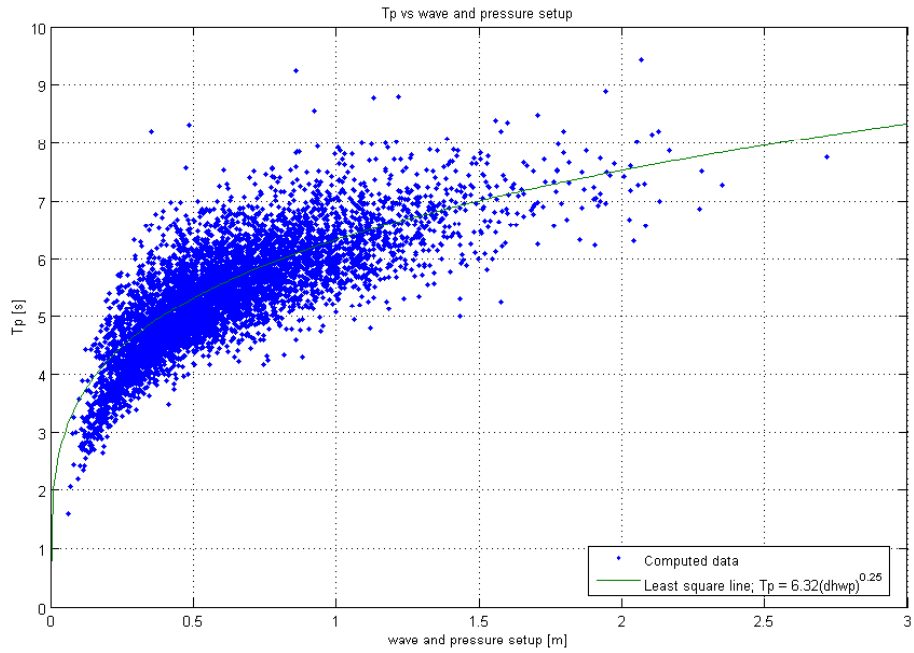
Figure 6-18: Relation between wave period and storm surge with least square line

The relation between wave period and tidal water level is also very weak. The same holds as in the previous analysis of wind speed and tidal water level and wave height and tidal water level in regions of lower tidal water levels (Figure 6-10 and Figure 6-14).
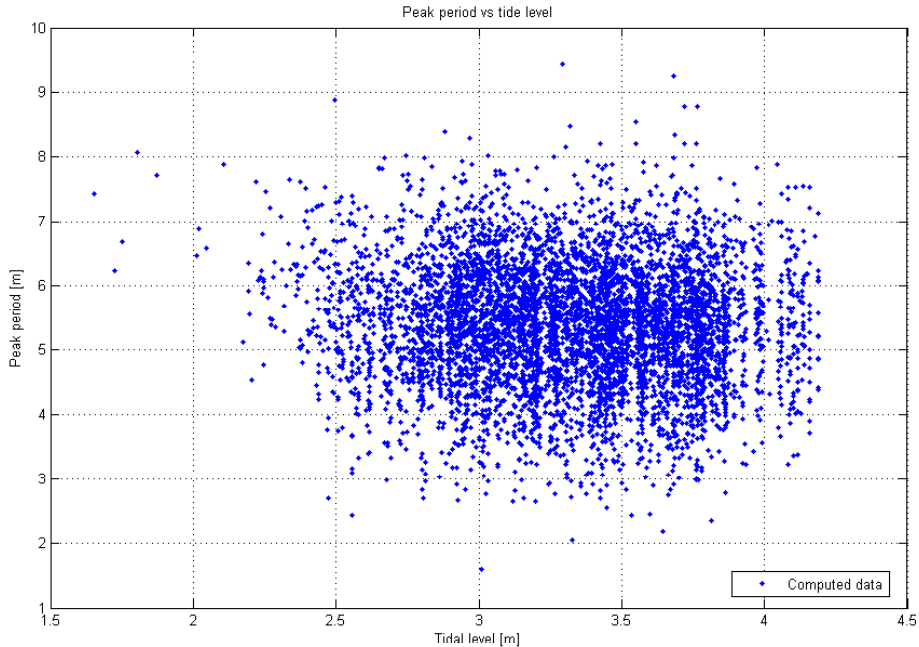
Figure 6-19: Relation between peak period and tidal water level

This results in the following JPDF.

$$f_{dh,T_p} = f_{dh_{tide}} \cdot f_{dh_{wp}} \cdot |J| \qquad (6\text{-}15)$$

$$|J| = \begin{vmatrix} \dfrac{\partial dh_{tide}}{\partial dh} & \dfrac{\partial dh_{tide}}{\partial T_p} \\ \dfrac{\partial dh_{wp}}{\partial dh} & \dfrac{\partial dh_{wp}}{\partial T_p} \end{vmatrix} \Rightarrow \begin{vmatrix} \dfrac{\partial dh_{tide}}{\partial dh} & \dfrac{\partial dh_{tide}}{\partial T_p} \\ \dfrac{\partial dh_{wp}}{\partial dh} & \dfrac{\partial dh_{wp}}{\partial T_p} \end{vmatrix} = \begin{vmatrix} 1 & 0 \\ 1 & \dfrac{\partial dh_{wp}}{\partial T_p} \end{vmatrix} = \begin{vmatrix} \dfrac{\partial dh_{wp}}{\partial T_p} \end{vmatrix} \qquad (6\text{-}16)$$

$$T_p = 6.32 \sqrt[4]{dh_{wp}} \Rightarrow \left| \frac{\partial dh_{wp}}{\partial T_p} \right| = \frac{4T_p}{6.32}$$

dh	Total water level increase	[m]
dh_{wp}	Storm surge level	[m]
dh_{tide}	Tidal water level	[m]
T_p	Peak period	[s]
J	Jacobian	

The JPDF is given in Figure 6-20 together with the computed data
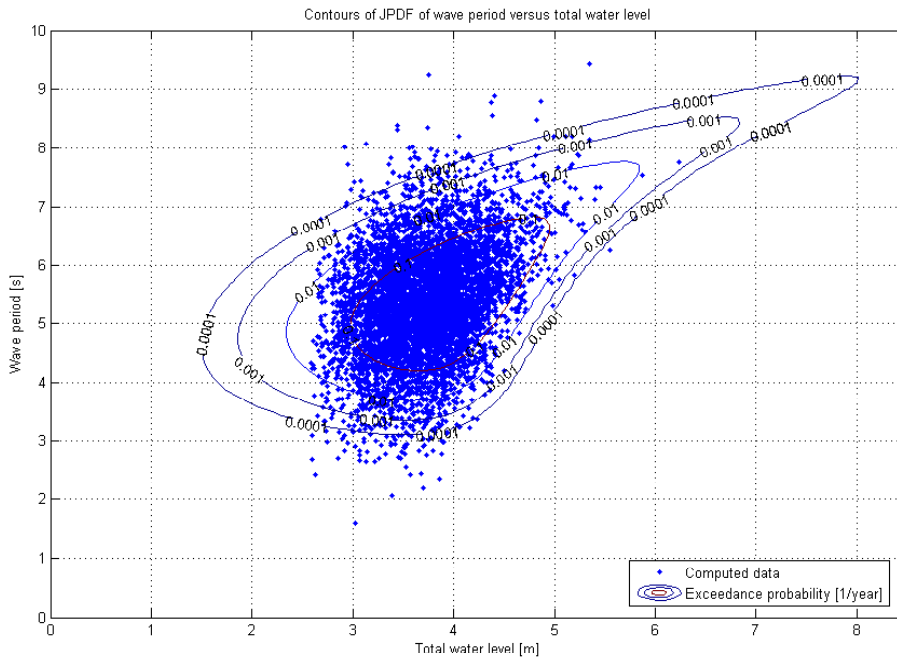
Figure 6-20: Contour plot wave period versus total water level

The distribution is not completely in line with the dataset. Some extreme wave periods are present in the region of lower total water levels.

The conditional PDF can also be obtained for the peak period dependent on the total water level The Jacobian changes with respect to the Jacobian used for the JPDF:

$$f_{T_p|dh} = \frac{f_{dh_{tide}} \cdot f_{dh_{wp}}}{f_{dh}} \cdot |J| \tag{6-17}$$

$$f_{T_p|dh} \Rightarrow |J| = \begin{vmatrix} \dfrac{\partial dh_{tide}}{\partial dh} & \dfrac{\partial dh_{tide}}{\partial T_p} \\ \dfrac{\partial dh_{wp}}{\partial dh} & \dfrac{\partial dh_{wp}}{\partial T_p} \end{vmatrix} = \begin{vmatrix} 0 & 1 \\ \dfrac{\partial dh_{wp}}{\partial T_p} & 1 \end{vmatrix} = \left| -\dfrac{\partial dh_{wp}}{\partial T_p} \right| \tag{6-18}$$

$$T_p = 6.32 \sqrt[4]{dh_{wp}} \Rightarrow \left| -\frac{\partial dh_{wp}}{\partial T_p} \right| = \frac{4T_p}{6.32}$$

dh	Total water level increase	[m]
dh_{wp}	Storm surge level	[m]
dh_{tide}	Tidal water level	[m]
T_p	Peak wave period	[s]
J	Jacobian	

The result is plotted in Figure 6-21
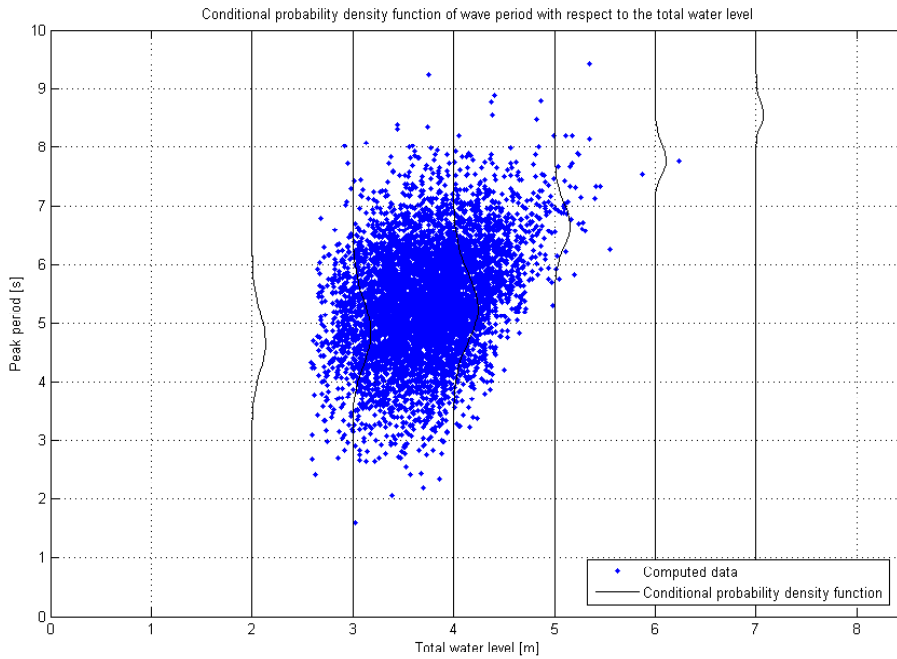
Figure 6-21: Conditional PDF and computed data set of peak period dependent on the total water level

The conditional PDF is in line with the derived JPDF.

6.4.5   Conclusions concerning the Joint probability density functions

The JPDF of the hydraulic variables and the conditional PDF have been presented. For the JPDF independent variables related to the hydraulic variables that are described with the JPDF were needed. The relation between the wave height and the wave period was determined via the independent relation between wave steepness and the wave height above a threshold level of 0,5m. The relation between the total water level and the wave height and period is found via the independence between the storm surge level and the tidal water level. The relation between the wave height and period and the storm surge level is derived with the joint relation with the wind speed. The derived physical relations are confirmed by the simulated dataset and the constants needed for the description are determined with the least square method, fitting the computed dataset.

Agreement of the JPDF and the computed data set of the wave height and total water level is good. The agreement of the JPDF and the computed data set of the wave period and the total water level is reasonable. In regions of lower total water levels some extreme wave periods seem to occur. A better fit of the marginal probability density functions to the tail could lead to slightly but not significantly better results. The input distribution of the tidal water level should be accounted for properly in a further analysis.

6.5   Statistical validation of hydraulic boundary conditions

The marginal PDFs and the joint PDFs can be evaluated with a small number of observations of the total water level, the wave height and the wave period. The values available for statistical validation are compared to the probability distributions as derived in the previous paragraphs.

6.5.1   Data available for statistical validation
The observations that are used for the calibration of the model cannot be used for the statistic validation, because the results may be positively affected by calibration. The typhoons after 1994 have to be submitted to the same selection criteria as the typhoons selected by Mitsuta and Fujii (1979, 1986) and Fujii (1998). If not, the statistic properties are not applicable to these typhoons, and the statistical validation cannot be done. The area of landing (Area A) and the central pressures (below 980hPa) of the historical typhoons after 1994 have to be identical to the analyses of Mitsuta and Fujii (1979, 1986) and Fujii (1998). This results in the typhoons that are stated in Table 6-7. Whether observations are available or not is also stated in the table.

Table 6-7: Overview of typhoons and observations that can be used for statistical validation

Year	Typhoon Name	Typhoon Number	Total water level [m]	Wave height [m]	Wave period [s]
1995	Ryan	9514	3.80	1.46	5.67
1996	Eve	9606	n.a.*	n.a.	n.a.
1996	Kirk	9612	n.a.	n.a.	n.a.
1997	Peter	9708	n.a.	1.62	6.11
1997	Oliwa	9719	4.39	1.90	6.33
1998	Zeb	9810	3.97	n.a.	n.a.
1999	Bart	9918	5.29	3.46	9.00
2004	Chaba	0416	4.75	1.58	5.33
2004	Songda	0418	4.09	2.00	6.33
2004	Meari	0421	4.24	1.23	4.78

* not available

To compare the marginal PDFs with the observations, the observed values are also put in increasing order and compared to the exceedance curve (Bernard, Bos Levenbach, see paragraph 6.3.2). The ration between the number of observations and the number of years in which the observations have been done must also be taken into account.

6.5.2   Statistic validation marginal distributions of hydraulic variables
The marginal PDFs of the computed maxima of total water level, wave height and period are used in this paragraph to statistically validate the model. In Table 6-7, the typhoons are given with the observations. The distributions and the observed values are plotted together in Figure 6-22 for the total water level, Figure 6-23 for the wave height and Figure 6-24 for the wave period.
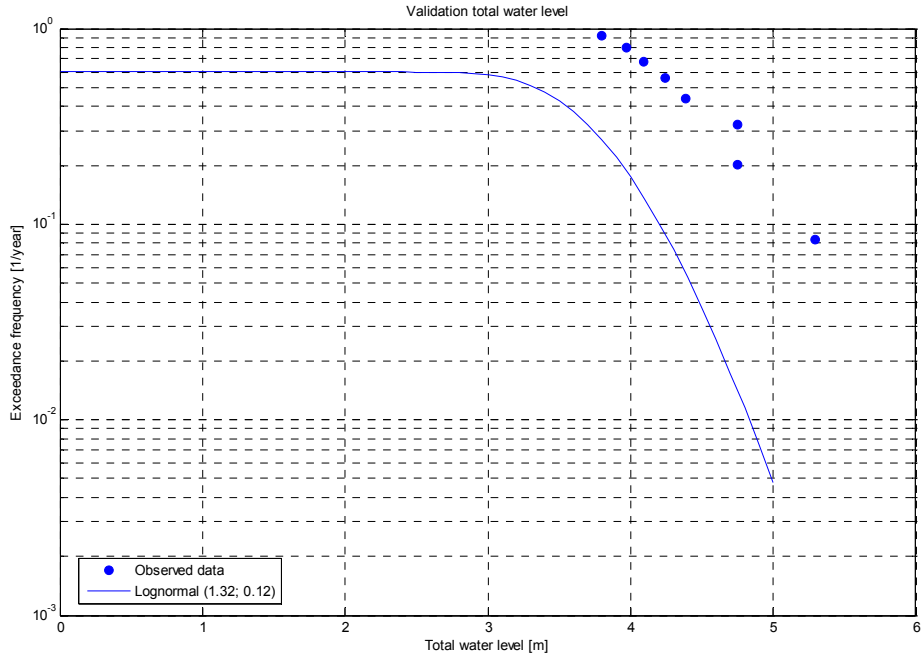
Figure 6-22: Statistical validation of the exceedance probability function of the total water level
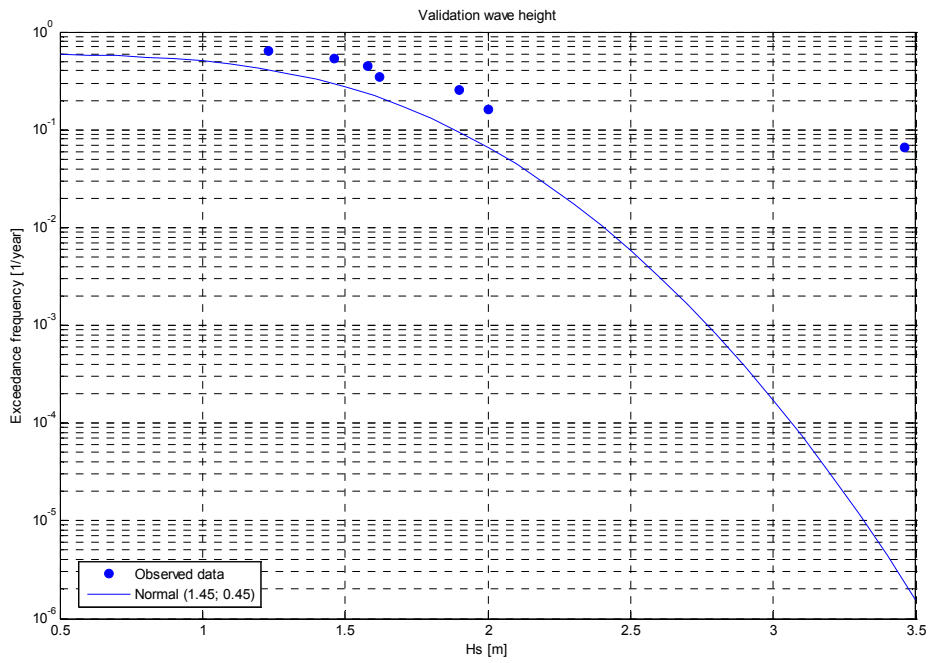
Figure 6-23: Statistical validation of the exceedance probability function of the wave height
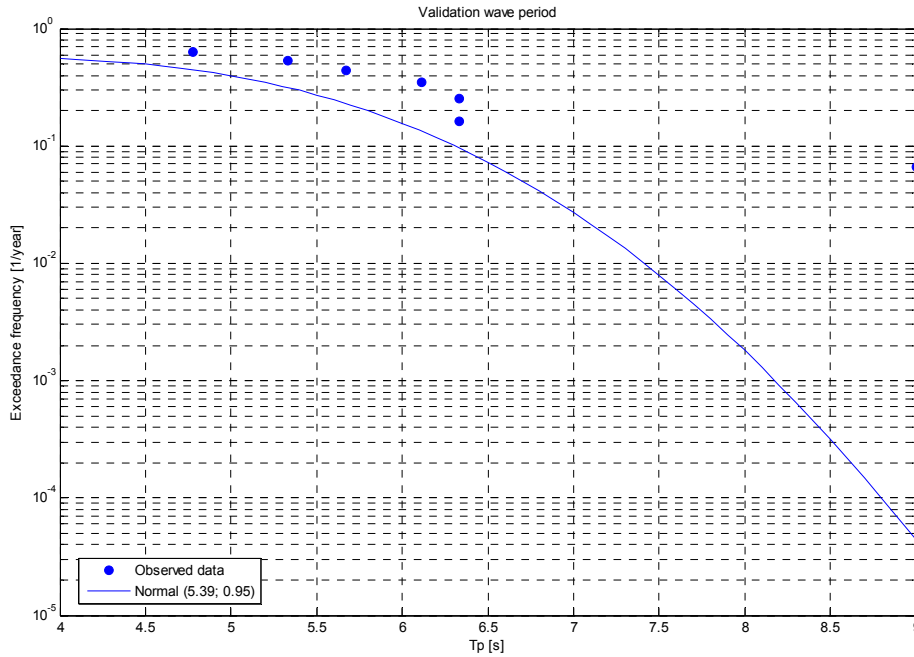
Figure 6-24: Statistical validation of the exceedance probability function of the wave period

- Discussion of statistical validation of marginal PDFs

There is agreement between theory and the historical data but conclusions on the extrapolation cannot be drawn based on this material. The set of data is far too small to be a reliable base for extrapolation into the region of small probabilities of exceedance.

The exceedance probability of the total water level seems to be underestimated by the model with a constant deviation (i.e. 0.7m). This deviation could not be explained, but may be found in a difference in observation point of the total water level with respect to the used input distribution of the tidal water level. The observations of the wave height and the wave period seem to be reasonably estimated, but also an underestimation of the exceedance probability can be seen. According to the derived distributions the data point of the wave height and period of one of the typhoons (i.e. typhoon Bart, no. 9918) is an outlier. According to the model this observation has got a return period of 10^{-4} for the wave height and 10^{-3} for the wave period.

6.5.3   Statistical validation of the joint probability density functions

The same statistical validation as done for the marginal probability density functions can be done for the joint probability density functions. The JPDF will be used and not the conditional PDFs, because these functions give a better overview of the distribution. The observed values can be potted in the derived contour plots (Figure 6-25, Figure 6-26 and Figure 6-27).
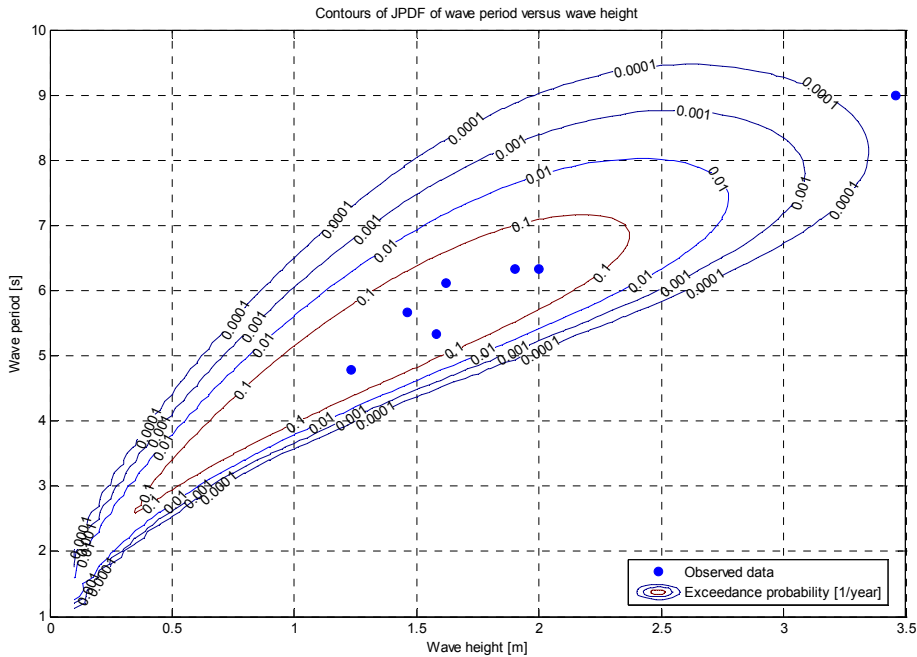
Figure 6-25: Statistical validation of the contour plot of wave period and wave height
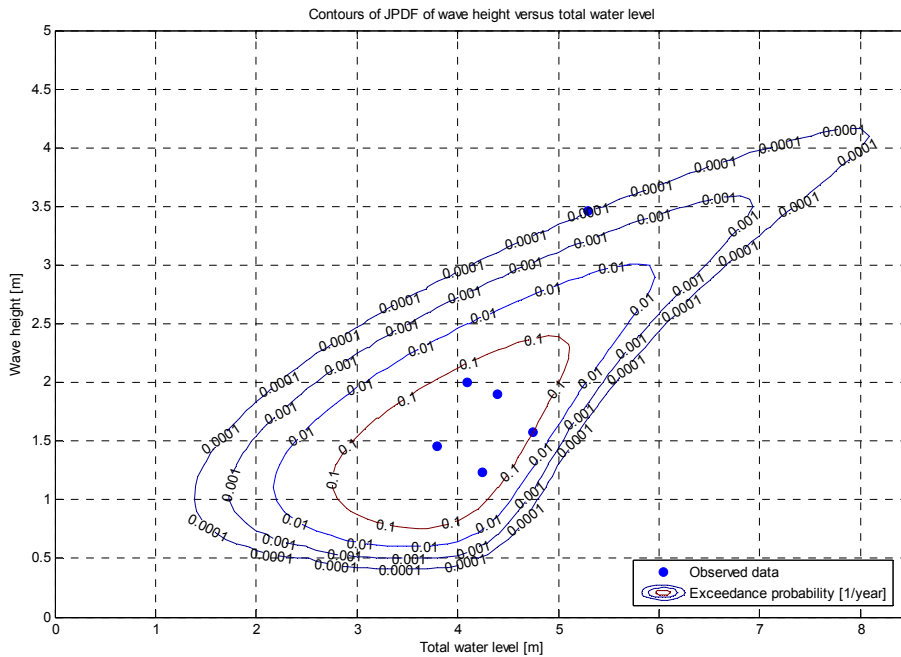
Figure 6-26: Statistical validation of the contour plot of wave height and total water level

Contours of JPDF of wave period versus total water level
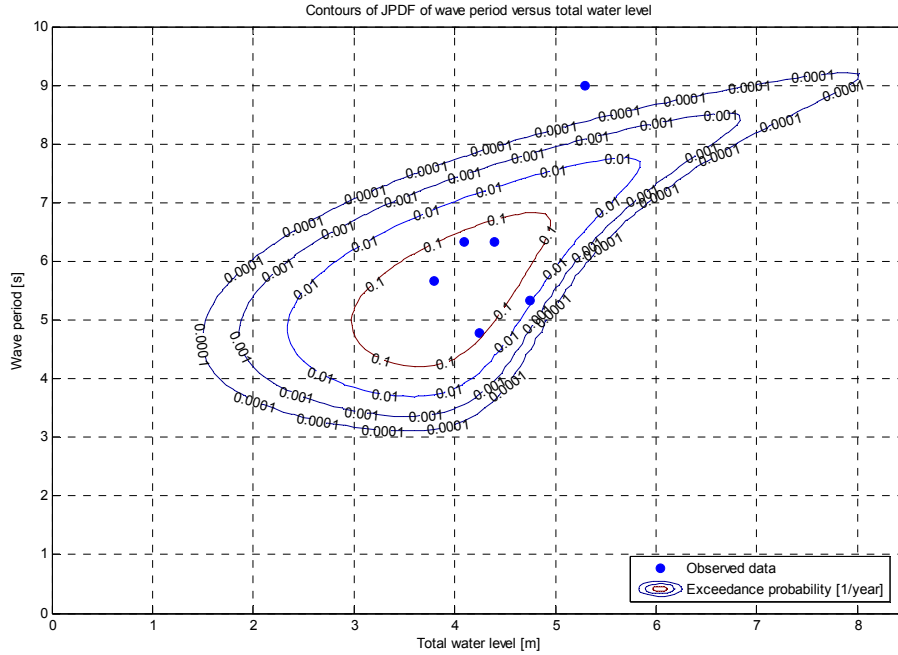
Figure 6-27: Statistical validation of the contour plot of wave period and total water level

- Discussion of statistical validation of contour JPDFs

The joint observed values are not contradicting the derived distributions. Only one outlier with a very small probability of exceedance would have occurred during one of the typhoons (i.e. no. 9918). This was also found in the marginal probability density functions. These functions have been used to obtain the joint probability density functions and therefore it is logical to find this also in this analysis. Adjusting the JPDF with the derived functions for the tails will not result in major changes of the JPDF. The deviation of T_p from the total water level is also found in the observations and should be analysed in further research.

6.6   An application of a joint probability density function

The failure mode of overtopping is analysed in order to illustrate the use of the JPDF in the analysis of the flood defence system. The overtopping can be found via the wave run-up. The following formula can be used to determine the 2% exceeded wave run up (TAW, 2002):

$$\xi_0 = \frac{\tan \alpha}{\sqrt{s_o}} \tag{6-19}$$

ξ_0	Breaker parameter	[-]
α	Angle of slope of flood defence	[deg]
s_0	Wave steepness related to the wave spectrum	[-]

In which:

$$s_0 = \frac{2\pi H_{m0}}{g T_{m-1,0}^2} \tag{6-20}$$

s_0	Wave steepness related to the wave spectrum	[-]
H_{m0}	Wave height (related to zero moment of spectrum)	[m]
g	Gravity acceleration	[m/s^2]

$T_{m-1,0}$ Spectral wave period   [s]

In which:

$$H_{m0} = 4\sqrt{m_0}$$ (6-21)

$$T_{m-1,0} = \frac{1}{1.1} T_p$$ (6-22)

m_0 Zero moment of spectrum   [m²]
$T_{m-1,0}$ Spectral wave period   [s]
T_p Peak wave period   [s]
m_{-1} First negative moment of spectrum   [m²s]

Further:

$$H_s = 3.8\sqrt{m_0}$$ (6-23)

H_s Significant wave height   [m]
m_0 Zero moment of spectrum   [m²]

To be able to use the formula the cross section of a flood defence system should be known. A cross section of a typical flood defence in Suo-nada Bay was estimated (from Takahashi et al., 2004) and is given in Figure 6-28.
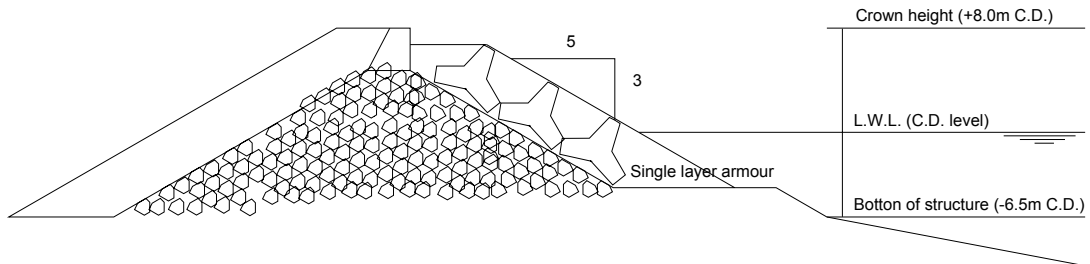
Figure 6-28: Cross section of a typical dike section in Suo-nada Bay

With this cross section, the following value of the breaker parameter can be derived:

$$\xi_0 = \frac{\tan\alpha}{\sqrt{s_o}} = \frac{\tan\alpha}{\sqrt{\dfrac{2\pi H_{m0}}{g T_{m-1,0}^2}}}$$

$$\frac{\tan\alpha}{\sqrt{\dfrac{2\pi \cdot \dfrac{1}{0.95} H_s}{g \cdot \left(\dfrac{1}{1.1} T_p\right)^2}}} = \frac{\tan\alpha}{\sqrt{1.27 \dfrac{2\pi \cdot H_s}{g \cdot T_p^2}}} = 3.02$$

Variables as stated before (with average wave steepness of 3.16%)

With this breaker parameter a formula for the wave run-up can be stated. It is advised not to follow the average trend. A safety margin of one standard deviation is used to calculate the wave run-up. The following formula should then be used assuming perpendicular attack of waves and single layer armour rock (TAW, 2002):

$$\frac{z_{2\%}}{H_{m0}} = \gamma_f \cdot \gamma_\beta \left(4.0 - 1.5/\sqrt{\xi_0}\right)$$ (6-24)

$$\frac{z_{2\%}}{H_s} = 0.7 \cdot 1.0 \left(4.0 - 1.5 / \sqrt{3.02} \right) \frac{1}{0.95} = 2.31 \Rightarrow z_{2\%} = 2.31 \cdot H_s$$

$z_{2\%}$	2% wave run-up level above still water line	[m]
H_{m0}	Wave height (related to zero moment of spectrum)	[m]
H_s	Significant wave height	[m]
γ_f	Influence factor for roughness elements on slope	[-]
γ_β	Influence factor for angled wave attack	[-]

A simple formula for wave run-up is the following:

$$z_{2\%} = 8 \cdot \tan \alpha \cdot H_s = 4.8 \cdot H_s \tag{6-25}$$

$z_{2\%}$	2% wave run-up level above still water line	[m]
H_s	Significant wave height	[m]
α	Angle of slope of flood defence	[deg]

This deviated from the previous derived value. The factor 2.31 is therefore assumed in the further research.

In order to obtain the reliability function of the overtopping, a statement of failure should be made: the statement of failure due to overtopping is if the 2% wave run-up would reach above the crown of the dike. So:

$$z_{2\%} \geq h_{dike} - dh_{tot} - L.W.L \tag{6-26}$$

$z_{2\%}$	2% wave run-up level above still water line	[m]
h_{dike}	Height of dike (crown height minus bottom of structure)	[m]
dh_{tot}	Height of total water level increase	[m]
$L.W.L.$	Low water level (=C.D. level) above bottom of structure	[m]

With the previous equation the following relation can be derived:

$$2.31 \cdot H_s \geq h_{dike} - dh_{tot} - L.W.L$$

$$H_s \geq \frac{h_{dike} - dh_{tot} - L.W.L}{2.31} = \frac{14.5m - dh_{tot} - 6.5m}{2.31} = 3.46 - \frac{dh_{tot}}{2.31}$$

The reliability function is plotted in Figure 6-29:
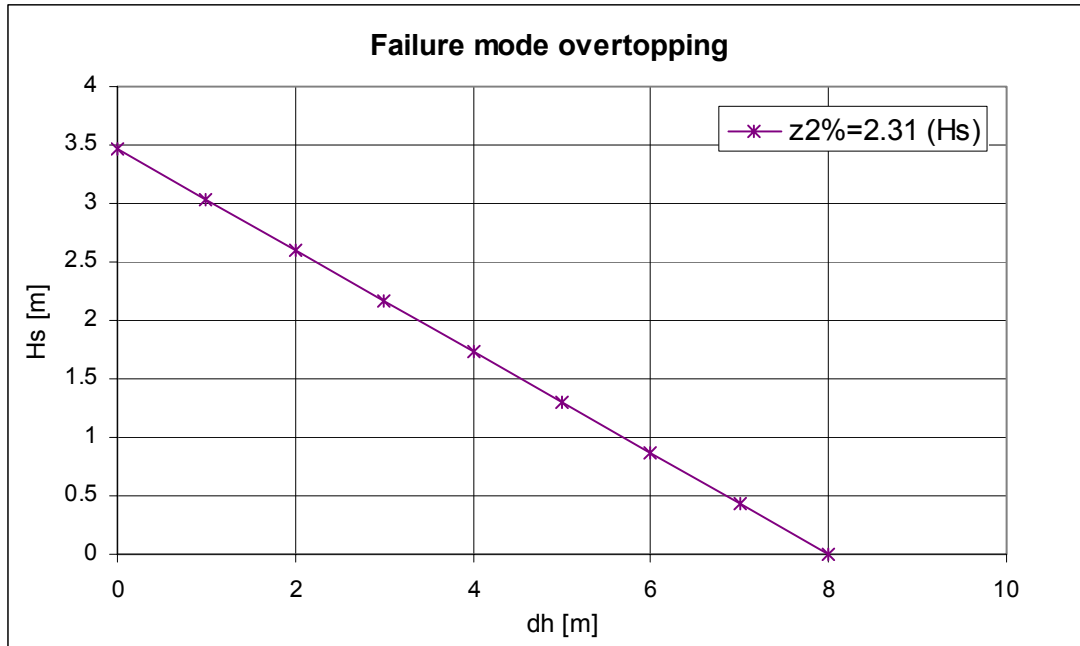
Figure 6-29: Reliability functions for wave overtopping

The definition of the failure does not directly lead to inundation of the hinterland. A better statement has to be subject of further research. The reliability function can also be plotted in the same figure as the JPDF of the total water level and the wave height. This can be seen in Figure 6-30.
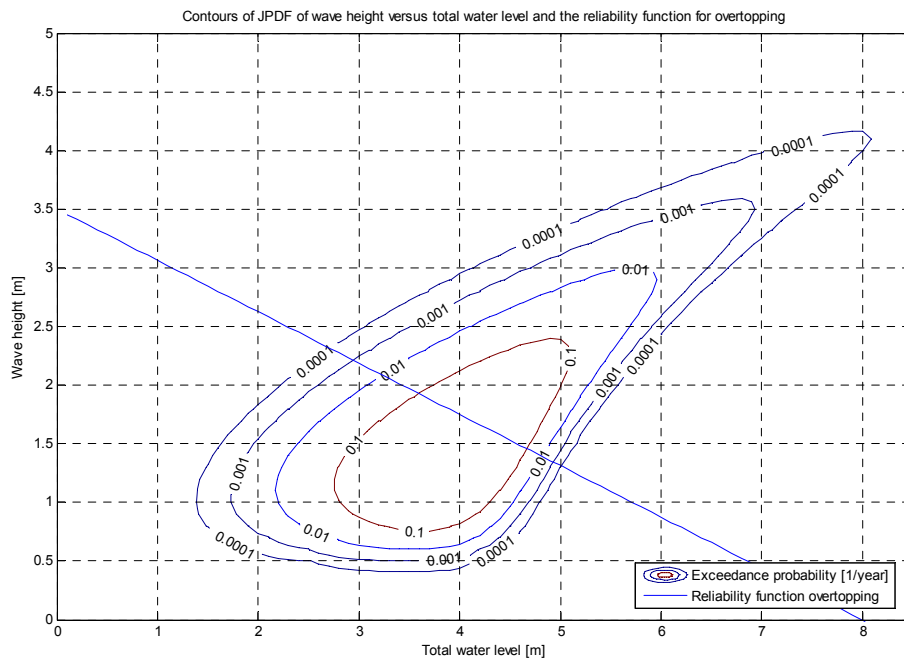
Figure 6-30: JPDF of wave height and total water level and the reliability function of overtopping

In order to obtain the probability of failure of a failure mode, the volume of the JPDF-mountain that is within the failure area has to be computed. The volume = 0.27 so the probability of failure due to overtopping as defined in this paragraph is 27%. Once every three years the dike will fail according to this failure criterion.

The failure probability can also be computed with the Monte Carlo analysis. This is done by counting the number of simulated data points located in the failure area. The probability would then be 0.22, so slightly smaller than in the case of the derived joint probability density function.
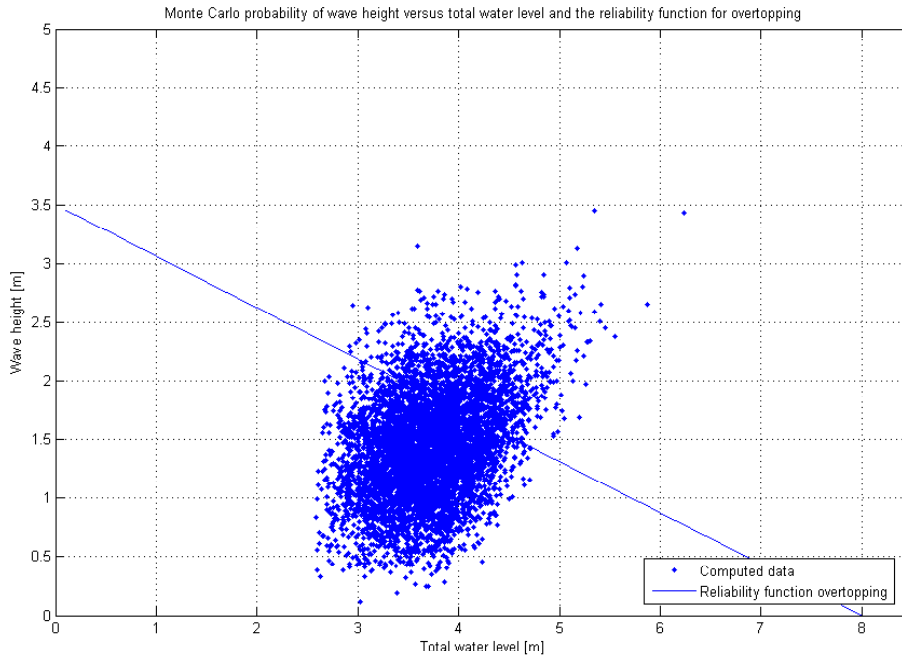
Figure 6-31: Computed data of wave height and total water level and the reliability function of overtopping

7 Conclusions and recommendations

In this chapter the conclusions and recommendations are stated. The objective of the research was to obtain the marginal and joint probability density functions of the hydraulic boundary conditions for Suo-nada Bay.

7.1 Conclusions

7.1.1 General conclusions

With respect to the derived model that determines the hydraulic boundary conditions

The research has demonstrated that with the derived model it is possible to:

- Hindcast the maxima of the hydraulic boundary conditions induced by historical typhoons reasonably
- Derive the marginal and joint probability distributions of the hydraulic boundary conditions based on the dependence model and probabilistic input distributions

With respect to the method that derives the probability distributions

A method that includes both statistics and physical relations makes it possible to:

- Use input distributions of physical variables related to the hydraulic variables that have a broader statistical basis than the hydraulic variables.
- Extrapolate the hydraulic boundary conditions into regions where no observations are available and taking physical boundaries and limitations into account
- Include knowledge of physical relations that are found and observed all over the world in the model

With respect to the obtained probability density functions

From the derived marginal and joint probability density functions it can be concluded:

- The observed values that are used for statistical validation are reasonable in line with the derived marginal and joint probability density functions
- The number of observations is far too small to statistically validate the model in the regions of low probabilities of exceedance

With respect to the current design method of flood defences in Japan

The design method should be extended with:

- A reliability-based design method, to be able to judge the safety of the flood design in an objective way
- The dependence between hydraulic variables in the assessment of failure probabilities of failure modes, especially in the regions of extreme values it is of major influence on the joint probability distributions

7.1.2   Other conclusions

A number of conclusions can be stated, not directly related to the objective of the research:

Relevant hydraulic variables in the Suo-nada Bay case

A research into the relevance of physical phenomena that could occur during typhoons in Suo-nada Bay pointed out that:
-   The total water level is influenced by the storm surge level mainly in the extreme cases; in normal cases the tidal water level is of more influence on the total water level
-   The magnitude and the period of the storm surges and the tidal water level are approximately the same. Therefore both variables have to be taken into account
-   The wave steepness is independent of the wave height for waves higher than 0.5m and is on average 3.16%, which points out that swell penetrates into the bay

Derived combined model

To derive the combined total model that is used in the deterministic and probabilistic analysis of typhoons, the typhoon characteristics play a central role
-   The use of input distributions of typhoon characteristics is preferred because the characteristics are observed for a longer period and because most hydraulic loads lead back to this driving mechanism
-   An objective analysis of pressure patterns of historical typhoons by Mistuta and Fujii gives the best description of the typhoon characteristics
-   Deterministic and probabilistic typhoon characteristics are given and the total model can therefore be used for the deterministic calibration and the statistical analysis
-   The wave steepness model is preferred over the SMB wave period model, because of the advantages in the probabilistic analysis with respect to the independence to the wave height.

Deterministic calibration

A range of constants is given for the formulae for wind set-up and pressure set-up and also the schematisations make it necessary to calibrate the models.
-   The resulting calibrated models are in line with the values of constants used in other analyses.

The following phenomena are calibrated and their average deviation from the maximum observed values is given:
-   Storm surge: 25% (0.3m) deviation (above and under). The constant for the wind set-up is determined to be $0.5*10^{-6}$. The constant for the pressure set-up is 0.03m/hPa.
-   Wave height: 20% (0.3m) deviation (above and under). A fit parameter over the wave height model of 0.9 (instead of 1.0) is adopted to obtain the best results.
-   Wave period: 5% (0.3s) deviation (above and under). The wave period is fitted with the values of the wave height and the wave steepness.

The marginal probability density functions

Marginal probability density functions of the hydraulic variables can be derived from the simulated dataset.
-   The fitted distributions are mainly determined by the average values of hydraulic variables and therefore deviate in the region of extreme values
-   Generalized Pareto Distributions have to be fitted to the tails of the distributions in order to obtain the correct distributions for the tail

- The marginal distribution of the total water level seems to deviate from the observations. The deviation could not be explained.
- Statistical validation proves that the other derived distributions are in line with the observed values. Conclusions on the extrapolation however cannot be drawn
- There seems to be an outlier according to the derived marginal probability density functions: typhoon Bart. According to the derived distribution the hydraulic loads have a return period of 1000 years

The joint probability density functions
Via independent physical variables, related to the hydraulic variables of interest, the joint probability density functions can be obtained.
- To derive the joint wave height and wave period distribution, the independence between the wave steepness and the wave height can be used.
- In the case of the joint total water level and the wave height, the independence between the tidal water level and the storm surge can be used. The relation between the storm surge level and the wave height can be derived from the wind speed (the same analysis holds for the wave period and the total water level).
- The JPDF of the wave height and the wave period are reasonably in line with the computed dataset and the observations. Conclusions on the extrapolation can however not be drawn
- The JPDF of the wave height and the total water level are reasonably in line with the computed dataset and the observations. Conclusions on the extrapolation can however not be drawn
- The JPDF of the wave period and the total water level seems to predict the computed data set completely. This is also found in the statistical validation
- Typhoon Bart seems to be an outlier if compared to the results of the joint probability density functions. The joint hydraulic conditions seem to have a return period of 10000 year.

Failure of the coastal defence system
Insight is obtained in how to apply the joint probability density functions in the analysis of failure modes.
- The reliability functions of failure modes can directly be applied in the model and the failure probability can be obtained easily from integrating the probability area outside the reliability line
- Another easy tool is to obtain the failure probability with the dataset generated by the Monte Carlo analysis
- In the example of overtopping, the failure of the dike if defined as water running over the defence system can be estimated to have a return period of three years

7.2   Recommendations

Several recommendations can be stated with respect to the research. First the possible improvements of the method are given. Then the general application of the model and the application of the model in reliability-based design is stated. Finally recommendations for further research in Japan are given.

Improvement of the presented method
- The ignored physical phenomena in the first order approximation of the hydraulic boundary conditions should be analysed more in detail and possibly be taken into account
- More sophisticated models can be used to predict the maxima and the hourly values of the hydraulic variables with more accuracy. The model as derived in this research could be used as a framework to implement the sophisticated models.
- The observations are at the time not all available for the research. With these observations a validation step should be included to be able to get better insight in the model uncertainty. The observations
- The marginal distribution functions derived for the hydraulic variables should be fitted more to the extreme values. The extreme values will be better predicted and the distributions in that region will be more accurate
- The tidal water level is constructed with a database of 2 years of tidal water levels. A better estimation of extreme tidal water levels should be done in order to obtain the tidal water levels with low probabilities of exceedance.
- The deviation of the marginal probability density function and the observed total water level could not be explained. An analysis of the uniformity of the observed total water levels should be done
- The input distributions for typhoon characteristics are directly adopted from an analysis done by Fujii and Mitsuta. The distribution types are assumed. This should be checked with a more objective method (e.g. Chi square test)
- Distribution types of the hydraulic variables are currently determined visually. An objective test should be done (using Chi square test)
- The exact joint occurrence of the hydraulic boundary conditions in time should be taken into account. In this research only the maxima are taken into account.

General application of the model
- The model should be applied to other bays in Japan and other basins in general. This would give insight in the applicability and the reliability of the model
- Extension of the model is needed if it is applied to other bays with a bay axis in the direction of the typhoon path. Shoaling is then more important
- The model is derived for one case site within Suo-nada Bay. The predictions for other sites within the bay should also be evaluated
- The approach presented in this research can be used as a first check of results of more sophisticated analyses

Application of the model in reliability-based design
- The desired level of protection should be derived. This can be done based on an economic consideration, but also the value human life etc.
- An analysis of failure modes should be made. A failure tree and the reliability functions should be stated for the flood defence system. The joint probability density functions can then be used for the analysis of the individual failure modes

- The Monte Carlo approach can easily be extended with the reliability functions to obtain probabilities of exceedance via the Monte Carlo method instead of via the probability density functions
- The dike system and the geometry is currently not accurately described. The failure modes should be analysed with more reliable information about cross sections etc.

Research in Japan
- More observations of waves should be done in the bay in order to calibrate the model for other case sites and to have a backup if instruments fail
- The analysis of the pressure pattern as derived by Mitsuta and Fujii is currently not available for the past decades. The deterministic and statistic characteristics of typhoons should be extended until now to obtain a better basis for the derived distributions of typhoon parameters
- Information about wave spectra will give more insight in the properties of the wind-generated waves and should be obtained or included.

References

Bakker, W.T., Vrijling, J.K. (1980)
> *Probabilistic design of sea defences.* Proceedings of the International Conference on Coastal Engineering 1980 (*)[13]

Banton, J.D., Smith, D.A.Y., Warner, P.S. (2002)
> *Long term variability of hurricane trends and a Monte Carlo approach to design.* International Conference on Coastal Engineering 2002

Battjes, J.A., (1974)
> *A Computation of Set-Up, Longshore Currents, Run-Up and Overtopping Due to Wind-Generated Waves.* Ph.D. Dissertation, Delft University of Technology, The Netherlands

Battjes, J.A. (1984)
> *Synthesis of design climate, Breakwaters, Design and Construction.* Proceedings of the Conference by the Institution of Civil Engineers, Thomas Telford Limited London

Battjes, J.A. and Stive, M.J.F., (1985)
> *Calibration and Verification of a Dissipation Model for Random Breaking Waves.* J. Geophys. Res., Vol 90, No. C5, pp. 569-568 (*)

Battjes, J.A. (2001)
> *Short waves* (Lecture notes Ct4320). Delft University of Technology

Bretschneider, C.L. (1952)
> *Revised wave forecasting relationships.* Proceedings of the second conference on coastal engineering, ASCE (*)

Bretschneider, C.L. (1958)
> *Revisions in wave forecasting, Deep and shallow water.* Proceedings of the International Conference on Coastal Engineering 1958, Ch. 3, pp. 20-67 (*)

Brunt, D. (1939)
> *Physical and Dynamical Meteorology.* Cambridge University Press, Cambridge, pp. 261

Burcharth, H.F., Dalsgaard, Sorensen, J., Christiani, E. (1995)
> *Application of reliability analysis for optimal design of vertical wall breakwaters.* Proceedings of the International Conference on Coastal and Port Engineering in Developing Countries (*)

Coastal Engineering Manual (2002-2003)
> Meteorology and wave climate. Part II, pp. II-2-28-II-2-50

Cooper, C.K. (1988)
> *Parametric Models of Hurricane-Generated Winds, Waves and Currents in Deep Water.* Proceedings of 20th Annual OTC, Houston, Texas USA, May, pp. 475-484

Fujii, T. (1998)
> *Statistical analysis of the Characteristics of Severe Typhoons Hitting the Japanese Main Islands.* Monthly weather review, April 1998, Vol 126, no. 4

Fujii, T., Maeda, J., Ishida, N., Hayashi, T. (2002)
> *An analysis of a pressure pattern in severe Typhoon Bart hitting the Japanese Islands in 1999 and a comparison of the gradient wind with the observed surface wind.* Journal of Wind Engineering and Industrial Aerodynamics 90 (2002), pp. 1555-1568

Goda, Y (1988)
> *On the methodology of selection design wave height.* Proceedings of the 21st International Conference on Coastal Engineering, pp. 899-913 (*)

---

[13] The publications stated with an (*) are referred to in other literature and not studied during this research

Goda, Y. (2000)
    Population distribution of extreme wave heights estimated through regional analysis. Proceedings International Conference on Coastal Engineering 2000
De Haan, L., De Ronde, J.G. (1997)
    Sea and wind: multivariate extremes at word. Extremes 1 (1), pp. 7-45 (*)
Harris, D.L., (1958)
    The hurricane surge. International Conference on Coastal Engineering 1958, Ch. 5, pp. 96-114
Harris, D. L., (1963)
    Characteristics of the Hurricane Storm Surge. U. S. Weather Bureau, Technical Data Report No. 48, U. S. Department of Commerce, Washington, DC.
Hashimoto, N., Kawai, H., Kuniaki, M., Kawaguchi, K. (2004)
    Development of stochastic typhoon model for performance design of coastal structures. Proceedings of the International Conference on Coastal Engineering 2004
Holland, G. (1980)
    An analytical Model of the Wind and Pressure Profiles in Hurricanes. Monthly Weather review. Vol 108, pp. 1212-1218 (*)
Japan Meteorological Agency (1999)
    Tide table for the year 2000, pp. 283 (in Japanese) (*)
Kato, F., Torii, K. (2002)
    Risk assessment on storm surge floods. Proceedings of the 2nd Workshop on the Development of Integrated Disaster Reduction Systems on Compound Urban Floodings, 2003, pp. 20-31
Kato, F., and Torii, K., (2002a)
    Damages to general properties due to a storm surge in Japan. Solutions to Coastal disasters Conference 2002.
Kawai, H., Takemura, S. (2002)
    Simultaneity of maximum storm surge and wave caused by typhoon in Tokyo bay, Japan. Proceedings International Conference on Coastal Engineering 2002
Kawai, H., Kawaguchi, K., Hashimoto, N. (2004)
    Development of storm surge model coupled with wave model and hindcasting of storm wave and surges caused by Typhoon 9918. Proceedings of 14th ISOPE, conference paper No 2004-NM-9, p.8
Kawai, H., (2004a)
    Presentation for ISOPE 2004 conference (Internal CD)
Kawai, H., Tomita, T., Hiraishi, T., Kim, D. Kang, Y., (2004b)
    Hindcasting of storm surge by Typhoon 0314 (Maemi). Workshop on Waves an Storm surges around Korean Peninsula 2004, pp. 67-73
Kim, K., Yamashita, T., (2003)
    Parallel computation of coupled atmosphere and ocean model - The case study of typhoon 9918 in the Yatsushiro Sea. Workshop on Hydro environmental Impacts of Large Coastal Developments, 2003
Komaguchi, T., Tsuchiya, Y., Shiraishi, N., (1990)
    Generation mechanism of abnormal waves along the Japan coast. Proceedings of the International Conference on Coastal Engineering 1990, Ch. 59, pp. 769-782
KSRGW, Kasumigaseki Society for Research on Global Warming (1991)
    Summary of the report of the intergovernmental panel on climate chance. Chuo Houki, pp. 75-78 (in Japanese) (*)
Matano, H. (1956)
    On the role of the lateral mixing in the cyclostrophic flow pattern in the atmosphere. Journal of Meteorological Society Japan, 34, pp. 125-136 (*)

Miche, R., (1944)
> *Mouvements Ondulatoires des Mers en Profondeur Constante ou Decroissante, Annales des Ponts et Chaussees.* pp. 25-78, 131-164, 270-292, 369-406 (*)

Mitsuta, Y., Standard Project Typoon (1) (1965)
> *Annual Disaster Prevention.* Res. Inst., Kyoto Univ., Vol 8, pp. 605-612 (Japanese) (*)

Mitsuta, Y., Fujii, T., Kawahira, K., (1979)
> *Analysis of typhoon pressure patterns over Japanese islands.* Journal of Natural Disaster Science, Vol 1, No. 1, 1979, pp. 3-19

Mitsuta, Y., Fujii, T., (1986)
> *Analysis of typhoon pressure patterns over Japanese islands (II).* Journal of Natural Disaster Science, Vol 8, No. 2, 1986, pp. 19-28

Mitsuta, Y., Fujii, T., (1986a)
> *Synthesis of typhoon wind patterns by numerical simulation.* Journal of Natural Disaster Science. Vol 8, No. 2, 1986, pp. 49-61

Mitsuta, Y. Fujii, T., (1987)
> *Analysis and synthesis of typhoon wind pattern over Japan.* Bulletin disaster Prevention Research Institute, Kyoto University, Vol 37, Part 4, No. 329, pp. 169-185 (in Japanese) (*)

Mitsuyasu, H. Tasai, F., Suhara, T., Mizuno, S., Ohkusu, M., Honda, T., Rikiishi, K. (1980)
> *Observation of the power spectrum of ocean waves using a cloverleaf buoy.* Journal of Physical Oceanography, Vol 10, pp. 286-296 (*)

Myers, V.A., Malkin, W., (1961)
> *Some Properties of Hurricane Wind Fields as Deduced from Trajectories.* U.S. Weather Bureau, National Hurricane Research Project, Rept. 49 (*)

Nakagawa, H., Inoue, K., Shimamoto, K., Uetsuka, T., (1995)
> *Storm surge flooding in cities in the Osaka bay area.* Journal of Natural Disaster Science, Vol. 17, No. 1, 1995, pp. 13-27

Repko, A., Van Gelder, P.H.A.J.M., Voortman H.G., Vrijling J.K., (2001)
> *Bivariate statistical analysis of wave climates*, Proceedings of International Conference on Coastal Engineering 2001

Schalkwijk, W.F. (1947)
> *A contribution to the study of storm surges on the Dutch coast.* KNMI, Med. en Verg. B part 2, No. 7 (*)

Schloemer, R.W. (1954)
> *Analysis and synthesis of hurricane wind patterns over Lake Okeechobee, Florida.* Hydrometeorological Report, USWB, No. 31, pp. 1-49

Shore Protection Manual (1977 and 1984)
> U.S. Army Coastal Research Center

Shultz, J.M., Russel, J. Espinel, Z. (2005)
> *Epidemiology of Tropical Cyclones. The Dynamics of Disaster Disease and Development.* Epidemiologic Review, Vol 27, 2005

Smith Warner International Ltd. (1999)
> *Storm surge mapping for Montego Bay, Jamaica.* Organization of American States General Secretariat Unit for Sustainable Development and Environment, USAID-OAS Caribbean Disaster Mitigation Project, September 1999, Kingston Jamaica

Sverdrupp, H.U., Munk, W.H. (1947)
> *Wind, Sea and Swell: Theory of relations for forecasting.* Publication no. 601, U.S. Navy Hydrographic Office, Washington D.C.

Takahashi, S., Kawai, H., Takayama, T., Tomita, T. (2004)
> *Performance design concept for storm surge defences.* Proceedings of International Conference on Coastal Engineering 2004

Takahashi, S., Kawai, H., Tomita, T., Takayama, T. (2004a)
> *A Basic Concept for Scenario Based Real Time Prediction of Storm Surge Disasters* (Internal CD)

Takahashi, S., Kawai, H., Takayama, T. (2005)
> *Storm surge disaster by typhoon no 9918, performance design of coastal defense.* (Internal CD)

TAW (2002)
> *Technical Report Wave Run-up and Wave Overtopping at Dike.* Technical Advisory Committee for Water Defences, The Hague, May 2002

Torii, K., Hitomi, H. and Fukushima, M. (2001)
> *Study on evaluation of tide in Kochi Coast by frequency analysis.* Proceedings of Coastal Engineering 48, pp. 296-300 (in Japanese) (*)

Tsuchiya, Y. Yasuda, T., (1980)
> *High tide and life risk, refuge warning in relation to the Ise Bay typhoon.* Journal of Natural Disaster Science, Vol 2, No. 2, 1980, pp. 27-60

Tsuchiya, Y., Kawata, Y., (1986)
> *Historical study of changes in storm surge disasters in the Osaka area.* Journal of Natural Disaster Science, Vol. 8, No. 2, 1986, pp. 1-18

Tsuchiya, Y., Kawata, Y. (1981)
> *Risk to life warning systems and protective construction against past storm surges in Osaka bay.* Journal of Natural Disaster Science, Vol 3, No. 1, 1981, pp. 33-55

Tsuruta, S., Goda, Y. (1960)
> *Damage on structures due to Ise Bay Typhoon.* Proceedings of Coastal Engineering 7, pp. 195-199 (*)

Vincent, C.L. (1985)
> *Depth-Controlled Wave Height.* J. Waterway, Port, Coastal and Ocean Eng., Vol 111, No. 3, pp. 459-475 (*)

Voortman, H.G., Vrijling, J.K. (1998)
> *Economic optimal design of vertical breakwaters.* Proceedings 26th International Conference on Coastal Engineering (*)

Voortman, H.G., Vrijling, J.K., Boer, S., Kortlever, W.C.D. (1999)
> *Optimal breakwater design for the Rotterdam Harbour Extension.* Proceedings of the 9th annual Conference of the Society for Risk Analysis Europe (*)

Voortman, H.G., van Gelder, P.H.A.J.M., Vrijling, J.K. (2002)
> *Joint probability distributions for wave height and wind set-up* (preliminary report)

Voortman, H.G., (2002a)
> *Risk-based design of large-scale flood defence systems.* Ph.D. dissertation, Delft University of Technology, The Netherlands

Vrijling, J.K., Bruinsma, J. (1980)
> *Hydraulic Boundary Conditions.* Symposium on Hydraulic Aspects of Coastal Structures pp. 109-132

Vrijling, J.K., Hengel, W. van, Houben, R.J. (1998)
> *Acceptable risk as a basis for design.* Reliability Engineering and System Safety 59, pp. 141-150 (*)

Vrijling, J.K., Gopalan, S., Laboyrie, J.H., Plate, S.E. (1998a)
> *Probabilistic Optimisation of the Ennore Coal Port.* Proceedings of the International Conference on Coastlines, Structures and Breakwaters, pp. 135-147, Thomas Telford, London (*)

Vrijling, J.K., Van Gelder, P.H.A.J.M. (2002)
> *Probabilistic design in hydraulic engineering* (Lecture notes Ct5310). Delft University of Technology

WAMDI (1988)
The WAM Model - A third Generation Ocean Wave Prediction Model. J Physical Oceanography, Vol. 18, pp. 1775-1810 (*)

Webbers, P.B., (2000)
A model for the hydraulic climate of the 2nd Maasvlakte. MSc thesis, Delft University of Technology

Webbers, P.B., Voortman, H.G., Van Gelder, P.H.A.J.M., Vrijling, J.K. (2000)
Multi-variate statistics of hydraulic boundary conditions for the Rotterdam harbour extension. Proceedings of the International Conference on Coastal Engineering

Weenink, M.P.H. (1958)
A theory and method of calculation of wind effects on sea levels in a partly-enclosed sea, with special application to the southern coast of the North Sea. Staatsdrukkerij en Uitgeverijbedrijf 's Gravenhage (*)

De Wit, M.S., Van Gelder, P.H.A.J.M., (2003)
Extreme Value Applications. Presentation Esrel 2003

Yamaguchi, M., Hatada, Y., Nakamura, Y. (1994)
Probabilistic typhoon model and its application to extreme value estimation of storm surges and waves. Proceedings of Annual Conference of Japan Society for Natural Disaster Science, pp. 135-138 (in Japanese) (*)

Yamaguchi, M., Ohfuku, M., Hatada, Y. (1998)
Some considerations on extreme statistics of storm surge height. Journal of Natural Disaster Science, Vol 17, No. 1, pp.57-66 (in Japanese) (*)

Young, I.R. (1988)
Parametric Hurricane Wave Prediction Model. J. of waterway, Port Coastal and Ocean Engineering, Vol 114, No.5, September 1988

Internet sites

www.gsj.go.jp/~kiyo/new_1km/index0.html	(February 2005)
www.cnmoc.navy.mil/nmosw/thh_nc/japan/otaru/text/sect5.htm	(March 2005)
www.cnmoc.navy.mil/nmosw/thh_nc/korea/pohang/text/sect5.htm	(March 2005)
www1.kaiho.mlit.go.jp	(March 2005)
www.oas.org/CDMP/document/kma/mobay/mobay.htm	(March 2005)
www.city.sendai.jp/.../ bousai-e/taihu_kiso.html	(April 2005)
www.agora.ex.nii.ac.jp	(May-October 2005)
www.marineharbors.com	(August 2005)
www.aoml.nooa.gov	(August 2005)
www.bocc.citrus.fl.us/ disaster/hurricane/anat...	(September 2005)
www.gsfc.nasa.gov	(November 2005)

Computer programs

Bestfit, 1993, Version 1.0, Palisade Corporation, Newfield, NY
Matlab, 2005, Version 7.01, Mathworks Company,

Appendices

Appendix A   Beaufort scale

Cat.	Winds [km/h]		Effects
0	0-2	Calm	Land- Smoke rises vertically Water- Like a mirror
1	2-6	Light Air	L- Rising smoke drifts W- Small ripples
2	7-11	Light Breeze	L- Leaves rustle W- Small wavelets, wind fills sail
3	12-19	Gentle Breeze	L- Light flags extend W- Large wavelets, sailboats heel
4	20-30	Moderate Breeze	L- Moves thin branches W- Working breeze, sailboats at hull speed
5	31-39	Fresh Breeze	L- Small trees sway W- Numerous whitecaps, time to shorten sails
6	40-50	Strong Breeze	L- Large tree branches move W- Whitecaps everywhere, sailboats head ashore, large waves
7	51-61	Moderate Gale	L- Large trees begin to sway W- Much bigger waves, some foam, sailboats at harbour
8	62-74	Fresh Gale	L- Small branches are broken from trees W- Foam in well marked streaks, larger waves, edges of crests break off
9	75-87	Strong Gale	L- Slight damage occurs to buildings W- High waves, dense spray, visibility affected
10	88-102	Whole Gale	L- Large trees uprooted, considerable building damage W- Very high waves, heavy sea roll, surface white with spray and foam, visibility impaired
11	103-117	Storm	L- Extensive widespread damage W- Exceptionally high waves, small to medium ships obscured, visibility poor
12	117+	Hurricane	L- Extreme destruction W- Waves 40+', air filled with foam and spray, visibility restricted

(www. marineharbors.com)

Appendix B   Storm surges and shoaling
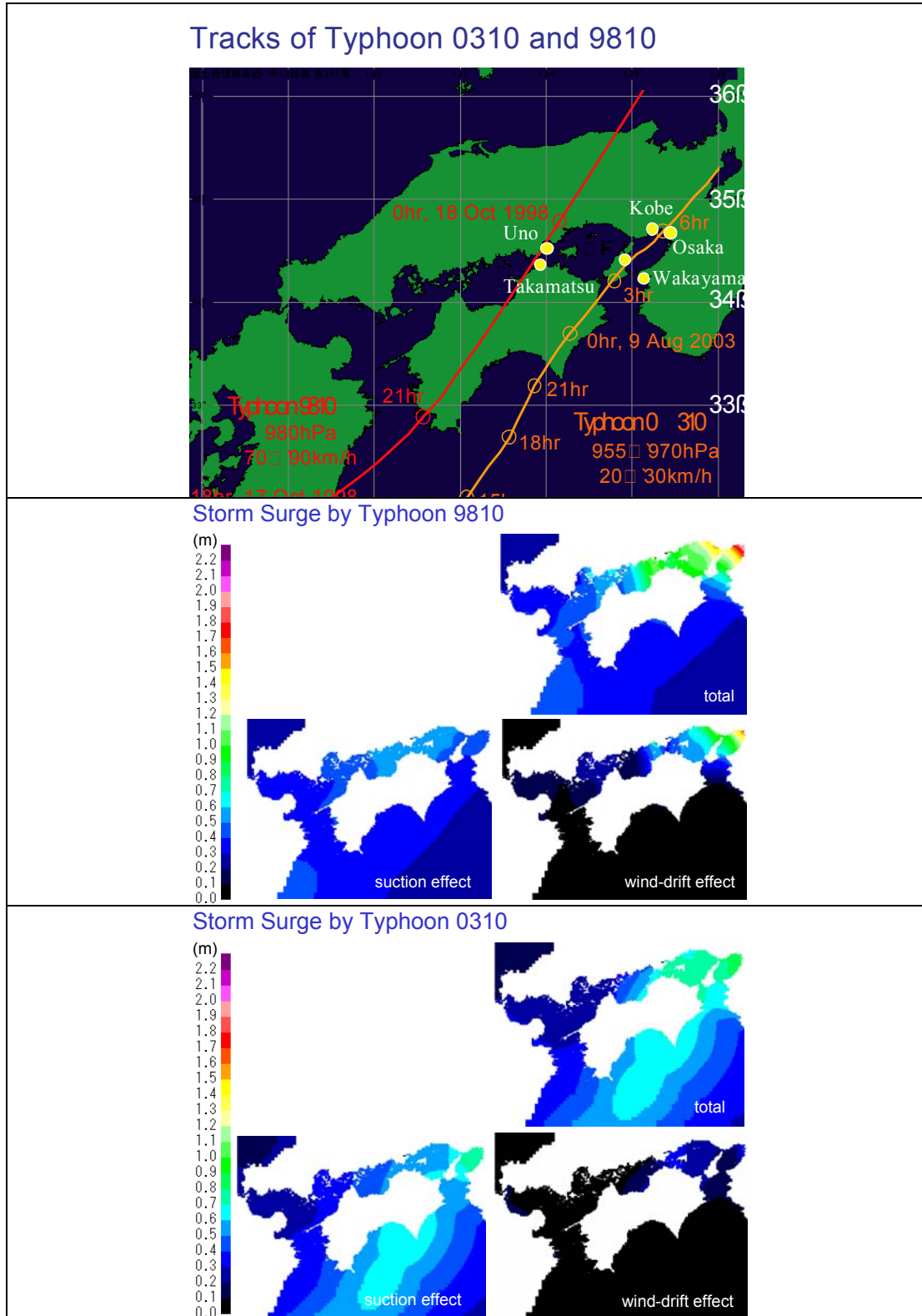
Hindcasted typhoons 0310 and 9810 with resulting total- wind- and pressure set-up (Kawai, personal communication)

Appendix C   Various models for the description of physical phenomena

Shore Protection Manual '77 and '84

Atmospheric pressure field
The SPM'84 states first of all a mathematical model to use for the typhoon pressure field

$$\frac{p - p_0}{p_n - p_0} = e^{-\frac{R}{r}} \text{ (After Myers (1954) and Harris (1958)}$$

p   Pressure at point at distance r from storm centre   [millimetres of mercury]
p_0 Central pressure [millimetres of mercury]
p_n Pressure at outskirts of storm [millimetres of mercury]
R   Radius of maximum wind [km]

Wave height and peak period
The wave height and peak period can be calculated with the following formulae

$$H_0 = 5.03 e^{\frac{R\Delta p}{4700}} \left[1 + \frac{0.29\alpha V_f}{\sqrt{U_r}} \right] \text{ (After Brettschneider (1958)}$$

$$T_s = 8.6 e^{\frac{R\Delta p}{9400}} \left[1 + \frac{0.104\alpha V_f}{\sqrt{U_r}} \right]$$

H_0 Deepwater significant wave height [m]
T_s Significant wave period [s]
R   Radius of maximum wind [km]
V_f Forward speed of hurricane [m/s]
U_r Maximum sustained wind speed (10m above water level) [m/s]
    $U_r = 0.865 U_{max} + 0.5 V_f$ (moving hurricanes)
U_{max} Maximum gradient wind speed (10m above water level) [m/s]
    $U_{max} = 0.447[14.5(p_n - p_0)^{1/2} - R(0.31f)]$
f   Coriolis parameter (Latitude 33.8°: f=0.290)
α   Coefficient (~1.0)

Coastal Engineering Manual (2003)

Atmospheric pressure field
The model of Holland provides a good fit to observed wind fields in early stages of storms. The hurricane pressure profiles are normalised:

$$\beta = \frac{p - p_c}{p_n - p_c}$$

p   pressure at radius r [mb]
p_c central pressure in the storm [mb]
p_n ambient pressure at the periphery of the storm mb]

The beta curves resembled a family of rectangular hyperbolas

$$\beta = \exp\left(\frac{-A}{r^B} \right)$$

A   scaling parameter [m]
B   parameter that controls the peakedness of wind speed [-]
r   arbitrary radius [m]

This leads to a pressure profile:

$$p = p_c + (p_n - p_c)\exp\left(\frac{-A}{r^B}\right)$$

Winds in hurricanes

$$U_c = \left[\frac{AB(p_n - p_c)\exp\left(\frac{-A}{r^B}\right)}{\rho_a r^B} + \frac{r^2 f^2}{4}\right]^{1/2}$$

For the radius to maximum winds as

$$R_{\max} = A^{\frac{1}{B}}$$

The maximum wind speed can then be approximated as

$$U_{\max}\left(\frac{B}{\rho_a e}\right)^{1/2}(p_n - p_c)^{1/2}$$

Assumptions in simplified wave predictions
Recent studies in shallow water (Jensen 1993) indicate that fetch limited wave growth in shallow water appears to follow growth laws that are quite close to deepwater wave growth for the same wind speeds up to a point where an asymptotic depth dependent wave height is attained. In light of this evidence is seems prudent to disregard bottom friction effect on wave growth in shallow water

Recommended for estimation waves in shallow basins:
  - Determine the straight line fetch and over water wind speed
  - Using fetch and wind speed from fetch limited growth equations to estimate the wave height and period from the deepwater nomograms
  - Compare the predicted peak wave period from to the shallow water limit given in

$$T_p = 9,78\left(\frac{d}{g}\right)^{1/2}$$

T_p Peak period
d   water depth
g   gravity acceleration
- If wave height exceeds 0.6 times the depth, wave height should be limited to 0.6 times the depth

Wave predictions
Recent studies in shallow water (Jensen 1993) indicate that fetch limited wave growth in shallow water follow growth laws that are close to deepwater wave growth for the same wind speeds up to a point where an asymptotic depth dependent wave height is attained. The only constraint is that no wave period can grow past a limiting value (Vincent 1985) given in the relationship:

$$T_p \approx 9.78\left(\frac{d}{g}\right)^{\frac{1}{2}}$$

Hurricane wind fields can be well represented by a small number of parameters, since winds in a hurricane tend to remain very close to a dynamic balance with certain driving mechanisms. Waves also depend next to the present wind fields on earlier wind fields, bathymetric effects, pre existing waves and the entire wave

generation process over the last 12 to 24 h. The following conditions have to be met before applying parametric models:
- Hurricane intensity is relatively constant
- Hurricane track is relatively straight
- Hurricane forward speed is relatively constant
- Hurricane is not affected by land or bathymetric effects
- No strong secondary wind and wave systems affect the area
The CEM introduces the parametric hurricane model of Young (1987)

Wave set-up
The wave set-up can be calculated by

$$\bar{\eta}_{max} = \bar{\eta}_s + \frac{d\bar{\eta}}{dx}\Delta x$$

$$\Delta x = \frac{\bar{\eta}_s}{\tan\beta - \frac{d\bar{\eta}}{dx}}$$

s to be filled in

Δx Shoreward displacement of the shoreline [m]
η_{max} set-up at the mean shoreline [m]

Seiches
For an open rectangular basin the free oscillation period can be calculated by:

$$T_n = \frac{4l_B}{(1+2n)\sqrt{gh}}$$

T_n natural period of the basin [s]
l_B Bay length [m]
n Number of frequency [-]
g Gravity acceleration [m/s^2]
h water depth [m]

The fundamental mode corresponds to n=0.

Model used by the PARI

Atmospheric pressure field
Kawai (2004) predicts the storm pressure in the same manner with the Myers and Malkin (1961) formula:

$$p = p_c + (p_\infty - p_c)e^{\left(-\frac{r_0}{r}\right)}$$

p_c Central pressure [mb]
Δp pressure differential [mb]
r radial distance from typhoon centre [km]
r_0 radius of maximum wind speed [km]

According to pressure data the pressure of Typhoon 9918 was deformed after its landfall. The radius r_o is a function of angle θ (Veltcheva and Kawai, 2002).

$$r_0 = r + r_{01}\cos(\theta - \alpha_1) + r_{02}\cos(2\theta - \alpha_2)$$

  r   radius [m]
  θ   angle [deg]
  α   angle [deg]
The five quantities are determined from the pressure data measured around the typhoon with the least square method.

The wind speed reduction coefficient is normally 0.7 at the right quarter of the typhoon. Mitsuta and Fujii (1987) proposed the following equation:

$$C_1(X) = C_1(\infty) + \left[C_1(X_p) - C_1(\infty)\right]\left(\frac{X}{X_p}\right)^{k-1}\exp\left\{\left(1 - \frac{1}{k}\right)\left[1 - \left(\frac{X}{X_p}\right)^{k}\right]\right\}$$

  X   radius relative to radius to maximum wind speed [-]
  k   parameter [-]
  $C_1(\infty)$ coefficient at remote point from typhoon centre [-]
  X_p distance of maximum coefficient [m]
  $C_1(X_p)$ maximum coefficient [-]
They use a wave model called WAM to calculate the waves and storm surges.

Typhoon analyses in Natural Disaster Science (1979-now)

Atmospheric Pressure field
Mitsuta and Fujii stated for typhoons with central pressures of 980 mb or less from 1979 to 1984 that landed on the Japanese Main Islands, the main characteristics. The pressure patterns o the typhoons were assumed to be represented by concentric circular isobars and the pressure profile by the formula of Schloemer (1954).

$$p = p_c + \Delta p e^{-(r_m/r)}$$

  p_c Central sea level pressure [mb]
  Δp central pressure depth [mb]
  r_m Radius to maximum cyclostrophic wind speed [m]
  r   Radius [m]

Mitsuta et al. (1979) studied three different pressure profiles for typhoons:
  - Pressure profile by Fujita
  - Schloemer formula by USACE
  - Bjerkness formula
The formulae are of the same accuracy in describing pressure profiles, but the cyclostrophic wind speed profile balancing to the pressure profile of Schloemer was more realistic than for the other ones so that formula was chosen.
Most typhoons move toward north-northeast or northeast. The return period of the pressure differential is given for three different areas (A,B and C).
They chose the profile from the three most frequently used profiles in the analysis of pressure patters of tropical cyclones (Mitsuta et al, 1979 and 1986).

Wind speed

The wind distribution in a synthesised typhoon pressure pattern is constructed from the gradient wind speed distribution balanced with the moving circular pressure pattern. The friction free wind speed is given by (Mitsuta et al 1986b)

$$\frac{V_{gr}^2}{r_t} + fV_{gr} = \frac{1}{\rho}\frac{\partial p}{\partial r}$$

V_{gr} gradient wind speed [m/s]
r_t radius of the curvature of trajectory [m]
f Coriolis parameter []
ρ Air density (1.1) [kg/m^3]

The isobars are assumed to be circular but when it moves wt constant speed the radius of the trajectory of the air parcel differs from the radius of an isobar. The relation is described by Blaton

$$\frac{1}{r_t} = \frac{1}{r}(1 + \frac{C}{V_{gr}}\sin\theta)$$

r radios of an isobar [m]
θ Direction angle of radius vector from direction of typhoon movement [deg]

The surface wind can be deflected from the friction free wind by

$$V_s = V_g(\cos\alpha - \sin\alpha)$$

V_s Surface wind speed [m/s]
V_g Geostrophic wind speed [m/s]
α Deflection angle [deg]

Surface lifting

Nakagawa calculated the water surface being lifted by the drop in atmospheric pressure:

$$\Delta h_p = 0.991(p_\infty - p)$$

p_∞ Peripheral pressure
p Pressure

Wind set-up

Further for the wind set up he calculated

$$\Delta h_w = \beta\Delta h_p$$

Δh_p increment in water level caused by drop in pressure [cm]
p_∞ peripheral pressure [mb]
Δh_w increment in water level caused by wind drift [cm]
β numerical constant (~1.0) [-]

Sea level rise

Nakagawa sketches an increase of 3 C in temperature and 65 cm in sea level by the end of the 21st century because of global greenhouse effects (KSRGW, 1991)

Risk assessment on Storm Surge Floods by Kato (2002)

Atmospheric pressure field combined with wind speed

Kato predicted the storm surge for different bays in Japan (Tokyo, Ise, Osaka, Tosa). Kato determines the pressure near the typhoon with Myers' Model. The storm tides is calculated from a combination of pressure and wind set-up were calculated according to the Japan Meteorological Agency (1999) as

$$s = a(1010 - P) + bW^2\cos\theta$$

s   Maximum storm tide [cm]
P   lowest atmospheric pressure [hPa]
W   maximum wind speed [m/s]
θ   difference between critical direction wind and wind at wind peak [deg]
a,b   constants given by the Japan Meteorological Agency (1999)

The estimated storm tides were corrected based on the relationship between estimated values and observed values for the actual typhoons.

<u>Wave height and peak period</u>
Kato predicted the wave heights for different bays in Japan (Tokyo, Ise, Osaka, Tosa). The wave heights were estimated with the SMB method by

$$\frac{gH_{1/3}}{U_{10}^2} = 0.30 \left[1 - \left\{ 1 + 0.004 \left(\frac{gF}{U_{10}^2} \right)^{1/2} \right\}^{-2} \right]$$

$$\frac{gT_{1/3}}{2\pi U_{10}} = 1.37 \left[1 - \left\{ 1 + 0.008 \left(\frac{gF}{U_{10}^2} \right)^{1/3} \right\}^{-5} \right]$$

$H_{1/3}$ Significant wave height [m]
$T_{1/3}$ Significant wave period [s]
U_{10} Wind speed 10m above sea surface [m/s]
F   Fetch [m]
g   Gravity acceleration [m/s^2]

Parametric Hurricane model by Cooper (1988)

Cooper developed a parametric model to estimate winds, waves and currents generated by hurricanes in water depths greater than 100m. The need for parametric models still exists for initial design and investigations of joint statistics. Models for Hurricane generated currents are limited and still theoretical. The simple parametric models are derived from advanced numerical models. This implies that the accuracy of parametric model can be no better than the accuracy of the numerical model.

<u>Wind speed</u>
A parametric equation for wind speed at 20m above mean sea level averaged for one minute at r greater than R is

$$W = W_m (r / R)^a$$

$$a = -0.38 + 0.08 \cos \theta$$

$$W_m = 0.885(5.6 \sqrt{\Delta p} - 0.5 R \cdot f) + V_f \cos \theta$$

W   Wind speed [m/s]
W_m Maximum wind speed [m/s]
r   arbitrary radius [m]
R   Radius to maximum wind [m]
a   Angle [deg]
Δp   Central pressure depth [mb]
f   Coriolis parameter [-]
V_f Forward movement of typhoon [m/s]

All units are MKS except pressure, which is in mb.
The wind at r<R is found by multiplying W_m by

$$(1 - \exp(-3.1 \cdot r / R))$$

<u>Wind direction</u>
The wind direction in polar coordinates is

$$\beta = \theta + \alpha + 90°$$
$$\alpha = 22.0 + 10.0\cos\theta$$

Wave height
The parametric equation for significant wave height Hs is expressed as a '25% rule':

$$H_s = 0.25 \cdot W$$

    W   Local wind speed given by previous equation [m/s]

Peak period

$$T_p = a \cdot W^b$$
$$a = 8.0 - 3.5\cos\theta + 2.7\sin\theta$$
$$b = 0.143 + 0.138\cos\theta - 0.074\sin\theta$$

Wave direction
The average wave direction is given by:

$$\phi = \alpha + a(r/R)^b + \theta - 90°$$
$$a = 144 + 39\cos\theta - 25\sin\theta - 15\cos 2\theta$$
$$b = -0.08$$

Current model
The derivation of a current model is executed. The model is quite complicated and more based on theoretical background. Therefore it is at this time not interesting to use in the Japanese case.

Parametric Hurricane model by Young (1988)

Young created a synthetic database on wave conditions within hurricanes suitable for wave prediction in deep water. The results indicated that both the velocity of forward movement (V_{fm}) and maximum wind velocity within the storm (V_{max}) play an important role in determining both the magnitude of the waves and the spatial distribution of these waves. The synthetic database consisted of V_{fm} [0 - 12.5 m/s], V_{max} [15 - 60m/s] and the radius R [15 - 60km]. If V_{fm} is relatively fast the waves will be left behind the storm and no swell will be present ahead of the storm. An equivalent Fetch is used to apply the wave growth relationships. Given the parameters V_{max}, V_{fm} and R the following steps can be performed
Determine effective radius to maximum winds R' from

$$R' = 22.5 \cdot 10^3 \log R - 70.8 \cdot 10^3$$

    R'   Effective radius [m]
Determine F/R' and thus F by substitution of V_{max} an V_{fm}

$$F/R' = aV_{max}^2 + bV_{max}V_{fm} + cV_{fm}^2 + dV_{max} + eV_{fm} + f$$

    F   Equivalent fetch [m]

$$a = -2.175 \cdot 10^{-3} \text{ [s}^2/\text{m}^2]$$
$$b = 1.506 \cdot 10^{-2} \text{ [s}^2/\text{m}^2]$$
$$c = -1.223 \cdot 10^{-1} \text{ [s}^2/\text{m}^2]$$
$$d = 2.190 \cdot 10^{-1} \text{ [s/m]}$$
$$e = 6.737 \cdot 10^{-1} \text{ [s/m]}$$
$$f = 7.980 \cdot 10^{-1}$$

Substitute V_{max} and F to obtain H_s max and f_m(max)

$$\frac{gH_s(\text{max})}{V_{max}^2} = 0.0016\left(\frac{gF}{V_{max}^2}\right)^{0.5}$$

$$\frac{g}{2\pi f_m(\max)V_{\max}} = 0.045\left(\frac{gF}{V_{\max}^2}\right)^{0.33}$$

Parameters the same as mentioned above.
Select the appropriate spatial distribution diagram for the values of V_{max} an V_{fm} and read $H_s/H_s(max)$ and fm/fm(max)

Young found in each of the spectra a relatively high frequency peak with a broad direction distribution centered about the local wind direction. The spatial distribution of significant wave heights is a function of both V_{fm} and V_{max}. Young presented spatial distribution diagrams where vectors are given; the direction of the mean wave direction obtained by integrating the directional spectrum. A crescent-shaped region on the right of the storm characterises typical distributions. This region occurs since the wind velocity is at a maximum here and also because the wind direction is approximately parallel with the storm track. Thus waves generated in this region move forward with the hurricane and maximise the time for which they experience strong winds. If V_{fm} is high the storm outruns the swell and the waves ahead of the storm are entirely locally generated and in the local wind direction. For rapidly moving storms waves generated directly ahead of the storm have not had sufficient time to propagate away from the region. As a result, conditions in the left rear quadrant are extremely confused with swell moving to the left and locally generated waves moving to the lower right.

Monte Carlo Approach in Hurricane design by Banton (2002)

A typical approach to derivate hurricane waves is there described as follows: (summarised by Goda (1988)):
- Use a parametric model (Young 1987 or Cooper 1988) to allow for the simulation of large numbers of storms.
- Select the appropriate data set (Annual maximum, Peak Value series)
- Fit the data set to a distribution (Fisher Tippett, Gumbel, Weibull)
- Extract the design wave for given return periods by data fitting (Least squares etc.)

Banton developed a hindcasting system to predict a design wave that corresponds to a particular return period. He uses a Monte Carlo simulation together with a purpose developed computer program, which incorporates a number of parametric wind and wave models and statistical procedures. He uses V_{max} [knots] as an input parameter.
Pressure field

$P_c = (a+\alpha) - bV_{\max}^{(c-\alpha/d)}$

P_c Central pressure [mb]
a, b, c, d   Given coefficients
α random variable uniformly distributed in the range [-10,10]
For the radius he gives
$R_{\max} = 3.10^{-6} e^{0.017Pc}$ radius to maximum wind [m]
He calculates the waves by the parametric model of Cooper (1988)

Storm surge mapping for Jamaica by Smith Warner (1999)

A storm surge is caused by interactions between hurricane, water body over which it passes and the nearby landmasses. It can be considered as the sum of three components (Smith Warner, 1999).
- Meteorological effects caused by low atmospheric pressure at the centre of the storm
- Wind effects caused by the wind stresses on the water surface
- Wave effects caused by breaking in the surf zone (wave set-up)

The different phenomena to calculate components of the storm surge are given below:

Surface lifting

The inverse Barometer Rise effect is the increase in water level under the low-pressure eye of a hurricane. The IBR can be calculated using a 2D model that assumes no flow normal to the shoreline, instantaneous water level response to the driving forces and a uniform sea surface. The following formula is found in the SPM'84.

$$\Delta h = 0.1(P_n - P_0)(1 - e^{-R/r})$$

Δh IBR [m]
P_n Ambient Pressure [hPa]
P_0 Pressure in eye of hurricane [hPa]
R Radius to maximum wind [km]
r Radius to a particular location [km]

Wind set-up

The onshore component of the hurricane wind leads to the wind set-up. Useful approximations of this phenomenon can be derived from the formula used for enclosed bays. The formula can be found in the SPM'77:

$$\Delta s = \frac{KW^2 F}{d}$$

Δs Wind set-up [m]
K empirical constant
W wind speed [m/s]
F Fetch length [m]
d water depth [m]

Wave set-up

Wave set-up can be considered as a static effect. It is the rise in mean sea level, which is caused by mass transport and the transfer of wave energy from a kinetic into a potential state. It occurs within the wave breaker zone. Assuming a frictionless planar beach, Battjes (1974) derived an equation for the average maximum wave set-up:

$$\eta_{max} = \frac{5}{16}\gamma_b H_b \approx \frac{H_b}{4}$$

η_{max} average maximum wave set-up [m]
γ_b ratio of breaker height to water depth [-]
H_b Breaking wave height [m]

Tides

Tides may be either diurnal or semi-diurnal in nature; a specific shoreline location may experience either one high and one low water per day, or two. For the sake of conservatism, it is recommended that a storm surge is calculated at mean high tide.

Long-term sea level rise

For future trends, and to allow for a possible "greenhouse effect' component, UNEP has predicted a rate for the Caribbean, of 5 mm/yr. Although somewhat conservative, it is recommended that this be figure be adopted until more site-specific, long-term water level data is obtained.

Battjes: wave set up

$$\frac{d\eta}{dx} = -\frac{\frac{3}{8}\gamma^2}{1+\frac{3}{8}\gamma^2}\frac{dh_b}{dx}$$

Method of Vrijling and Bruinsma

Vrijling and Bruinsma (1980) developed a model that describes the wave height as a function of the water level. The basis is formed by the model for wind set-up of Weenink (1958) and the model of significant wave height of Sverdrupp, Munk and Bretschneider (1958). Vrijling and Bruinsma found that the wind set-up of the Weenink model can be approximated by a quadratic function of the wind speed

$$h(u_9) = \alpha \frac{u_9^2}{g}$$

α   Empirical parameter [-]
u_9 Continuous Wind speed during 9 hours [m/s]
g   Gravity acceleration ['m/s^2]

Vrijling and Bruinsma restricted the analysis to storms between West and North and then derived the value α.
The astronomical tide and wind set-up were supposed to be independent so the water level is described by:

$$h_w(u_9, h_a) = h(u_9) + h_a$$

h_a Astronomical tide

Vrijling and Bruinsma found that the maximum water level during a storm can be found by using the astronomical high water. By using the above formulae the 9 hour wind speed for an observed water level can be found. The astronomical tide varies little so the wind set-up and the back-calculated wind speed also vary.
For a known wind speed and a known geometry of the bay a wave height can be calculated with the SMB formula:

$$H_s(u, d, F) = \frac{u^2}{g} H_\infty \tanh(k_3 \left(\frac{dg}{u^2}\right)^{m_3}) \tanh\left(\frac{k_1 \left(\frac{Fg}{u^2}\right)^{m_1}}{\tanh\left(k_3\left(\frac{dg}{u^2}\right)^{m_3}\right)}\right)$$

F   Fetch length [m]
d   Depth [m]
u   Wind speed [m/s]
g   Gravity acceleration [m/s^3]
$k_1, k_3, m_1, m_3, H_\infty$ Empirical parameters (CERC)

From the observe water level a wind speed can be derived. This wind speed put in the wave height model gives the wave height.

Method of Webbers

Webbers went back to the original method. The extension of Webbers compared with Vrijling and Bruinsma was the description of the peak period of the wave spectrum with the use of a method described by Repko et al (2001). Within a wave field the significant wave height and peak period of the spectrum are important parameters. Between them there exists a physical dependence. The parameter wave steepness is a function of wave height and peak period:

$$s_{0p} = \frac{H_s}{\frac{g}{2\pi}T_p^2}$$

s_{0p} Wave steepness [-]
H_s Significant wave Height [m]
T_p Peak period [s]
g Gravity acceleration [m/s^2]

From analysis of Repko (2001) it follows that from measurements over the world the wave height and steepness are statistically independent. That's why the peak period can be written as a function of two statistically independent variables by:

$$T_p = \sqrt{\frac{2\pi H_s}{s_{0p}g}}$$

Method of Voortman

In the methods of Vrijling and Bruinsma (1980) the distributions of the water level and the uncertainty of the maximum wind speed as function of the water level serve as input parameters. In the method of Webbers (2000) this set is extended with the wave steepness.

The method of Voortman (2002) is consistent with the previous models. The method is based on a parametric model that describes four hydraulic variables (water level, wind set-up, wave height and peak periods as a function of
- Characteristic wind speed
- Characteristic wind direction
- Direction dependent geometry of the North Sea
- Model insecurities

PDF's of the input parameters are bases on observations in the field and the choice of the distribution type is done on earlier research.

For the models the input and output variables are given and the field of application. The variables used for the different models are written with the same symbols.

Name	Subject	Variables for Input	Output	Field of application
Manuals by the USACE based on US hurricanes				
SPM '77 / '84	Pressure model by Myers	P_c; P_∞; r; R_m	P	Slowly moving typhoons
	Significant wave height	C_{fm}; V_r; V_{max}	H_s	Slowly moving typhoons
	Significant wave period	C_{fm}; V_r; V_{max}	T_s	Slowly moving typhoons
CEM '02 / '03	Wind speed model by Holland	P_∞; P_c	V_{max}	No forward movement
	Wave set-up	β;	η_{max}	Only in surf zone
Applications of studies in Japan				
PARI 2004	Pressure model by Myers	P_c; ΔP; r; R_m	P	Slowly moving typhoons
	WAM, wave prediction model			
Natural Disaster Science '79-now	Pressure model by Schloemer	P_c, Δp, r, r_m	P	No typhoon landfall
	Gradient wind speed	R_t, P, r	V_{gr}	Circular pressure field
	Blaton moving typhoon	R_t, r, θ	V_{gr}	Forward movement
	Surface wind speed	V_{gr}, α	V_s	R large; only land or water
	Surface lifting	P_∞; P	Δh_p	Typhoon pressure lift
	Wind set-up	Δh_p	Δh_w	Part of surface lifting
Kato 2002	Storm tide with JMA formula	P; V_{max}; θ	Δh_s	Other Japanese Bays
	Significant wave height with SMB	V_{10min}; F	H_s	Depth constant; Wind uniform
	Significant wave period with SMB	V_{10min}; F	T_s	Depth constant; Wind uniform
Parametric Hurricane models				
Cooper 1988	Wind speed	R_m; r; Δp; C_{fm}	V	Off coast, deep water only
	Wind direction	θ	β	Off coast, deep water only
	Wave height	V	H_s	Depth over 100m
	Peak period	V; θ	T_p	Depth over 100m
	Wave direction	θ; r; R_m	ϕ	Depth over 100m
Young 1988	Jonswap wave height	R_m; V_{max}; C_{fm}	H_s	Deep water only
	Jonswap mean period	R_m; V_{max}; C_{fm}	T_m	12.5m/s is maximum V_{fm}
Applications of studies in the Gulf of Mexico				
Banton 2002	Atmospheric pressure	V_{max}; α	P_c	Fitting Caribbean data
	Radius to maximum wind speed	P_c	R_{max}	Fitting Caribbean data
Smith Warner 1999	Pressure set-up from SPM'84	P_c; ΔP; r; R_m	Δh_p	No typhoon movement
	Wind set-up from SPM'84	V; F; d	Δh_w	Closed coast; lake
	Wave set-up by Battjes	H_b	η_{max}	No friction, planar beach
Applications to the Shallow North Sea				
Vrijling 1980	Astronomical tide	H_{HW}; T_0; φ	h	General applicable tide model
	Wind set-up by Weenink	V_{9hr}	Δh_w	Depth constant; Wind uniform
	Significant wave height with SMB	V; d; F	H_s	Depth constant; Wind uniform
Webbers 2000	Same as Vrijling; additional:			
	Wave steepness model	H_s; T_p	S_{0p}	Extreme values of T_p; H_s
Voortman 2002a	Same as Vrijling; difference:			
	Wind set-up model	V_{5hr}	Δh_w	Depth constant; Wind uniform

Appendix D   Deterministic and probabilistic typhoon characteristics

Table of Fujii (1998) with typhoon characteristics

Year	Typh. name	Typh. no.	Area land.	Δp [hPa]	r_m [km]	C_{fm} [km/h]	γ [°]	a_p [km/h]	a_r [km/h]	a_c [km/h²]	a_d [°/h]
1955	Louise	5522	A	63.8	97.5	29	-17	0.049	4.3	2.9	6.8
1956	Harriet	5615	C	30.9	67.0	54	55	-	-	-	-
1957	Bess	5710	A	48.2	84.5	35	44	0.064	5.0	-3.9	-5.6
1958	Helen	5821	C	46.5	118.0	47	45	0.035	5.3	5.0	2.9
1958	Ida	5822	C	42.8	44.0	34	52	0.212	8.0	5.7	-8.0
1959	Ellen	5906	B	21.6	146.0	26	40	0.012	4.5	1.9	3.9
1959	Vera	5915	B	85.2	10.5	45	12	0.119	12.3	6.9	2.1
1960	Della	6016	B	29.4	68.0	50	22	0.064	4.9	0.4	-3.2
1961	Nancy	6118	B	69.0	75.0	39	31	0.080	4.5	7.9	0.3
1961	Violet	6124	C	35.4	104.0	101	45	-	-	-	-
1963	Bess	6309	A	31.4	105.0	29	25	0.070	9.7	-3.9	-11.6
1964	Kathy	6414	A	40.0	77.5	13	-4	0.021	1.5	-0.3	3.5
1964	Wilda	6420	A	83.2	50.5	33	29	0.097	6.7	0.6	1.7
1965	Jean	6515	A	50.6	50.5	37	29	0.117	10.2	3.6	-3.4
1965	Lucy	6517	C	37.9	26.0	31	27	0.185	4.3	-5.7	4.0
1965	Shirley	6523	B	59.9	67.0	55	16	0.089	5.5	6.0	2.3
1965	Trix	6524	C	41.2	106.0	66	27	0.079	20.0	4.6	0.4
1966	Ida	6626	C	47.8	30.0	50	23	-	-	-	-
1967	Dinah	6734	B	33.9	79.0	52	21	-	-	-	-
1968	Mary	6804	B	27.0	267.5	47	-52	0.016	-11.5	-3.4	3.7
1969	Cora	6909	A	43.1	54.0	40	64	0.042	3.4	-1.8	-2.1
1970	Olga	7002	B	27.9	77.5	28	-26	0.099	7.2	0.0	-0.1
1970	Wilda	7009	A	47.7	56.0	26	47	0.072	5.9	2.4	-0.9
1970	Anita	7010	B	52.0	102.5	21	-30	0.062	3.7	5.0	4.1
1971	Olive	7119	A	38.1	71.0	27	36	0.068	3.5	1.4	-9.2
1971	Trix	7123	A	33.1	123.5	24	18	0.009	-0.8	-2.3	1.9
1972	Tess	7209	A	21.2	99.5	15	-63	0.031	-3.4	5.7	7.1
1972	Helen	7220	B	54.4	93.0	53	22	0.077	15.0	3.3	0.1
1974	Polly	7416	B	31.3	88.0	30	-35	0.093	9.3	3.2	3.2
1975	Rita	7506	B	31.6	90.0	23	24	0.028	3.5	2.0	0.9
1976	Fran	7617	A	42.4	81.0	19	27	0.074	12.7	3.4	2.4
1979	Oweb	7916	B	56.8	40.5	49	35	0.148	7.7	3.9	2.5
1979	Tip	7920	B	29.0	117.5	64	38	0.059	17.5	9.4	0.9
1980	Orchid	8013	A	26.9	273.0	76	6	0.010	-29.4	-6.4	1.2
1981	Ogden	8110	A	32.3	36.5	22	-42	0.092	3.2	2.0	-1.7
1981	Thad	8115	C	38.6	261.0	48	26	0.008	-4.8	10.2	-4.0
1982	Cecil	8210	C	23.2	102.0	72	4	0.018	4.4	-6.8	-2.6
1982	Ellis	8213	A	40.9	82.0	18	24	0.050	6.8	3.4	-3.8
1982	Judy	8218	C	36.2	122.5	34	29	0.122	18.4	6.4	-2.1
1982	Ken	8219	B	29.5	111.0	41	12	0.092	12.3	2.8	-4.2
1983	Abby	8305	C	20.0	88.5	29	11	0.029	1.8	-3.1	-5.7
1985	Irma	8506	C	30.4	106.0	81	51	0.015	11.3	2.3	-1.3
1985	Pat	8513	A	52.3	52.0	42	-6	0.079	5.0	2.7	0.7
1987	Kelly	8719	B	36.8	110.5	44	34	0.096	14.2	2.6	-2.2
1989	Roger	8917	B	25.4	108.0	38	24	0.035	15.1	-0.3	4.4
1990	Flo	9019	B	59.6	74.0	40	56	0.107	6.7	2.0	-4.6
1991	Kinna	9117	A	42.2	72.0	40	30	0.108	9.7	2.5	-1.7
1991	Mireille	9119	A	69.0	83.5	67	61	0.068	14.6	11.0	-4.5
1992	Janis	9210	A	50.9	83.0	38	38	0.073	9.8	-0.6	-1.8
1993	Yancy	9313	A	77.1	56.0	44	28	0.100	9.1	1.7	-8.5
1994	Orchid	9426	B	59.5	49.5	28	39	0.161	12.3	6.3	-5.9

Statistics as given by Mitsuta and Fujii (1986)

| Central pressure depth [hPa] | Speed of forward movement [km/h] | Direction of forward movement [deg] |

Radius of maximum cyclostrophic wind [km]
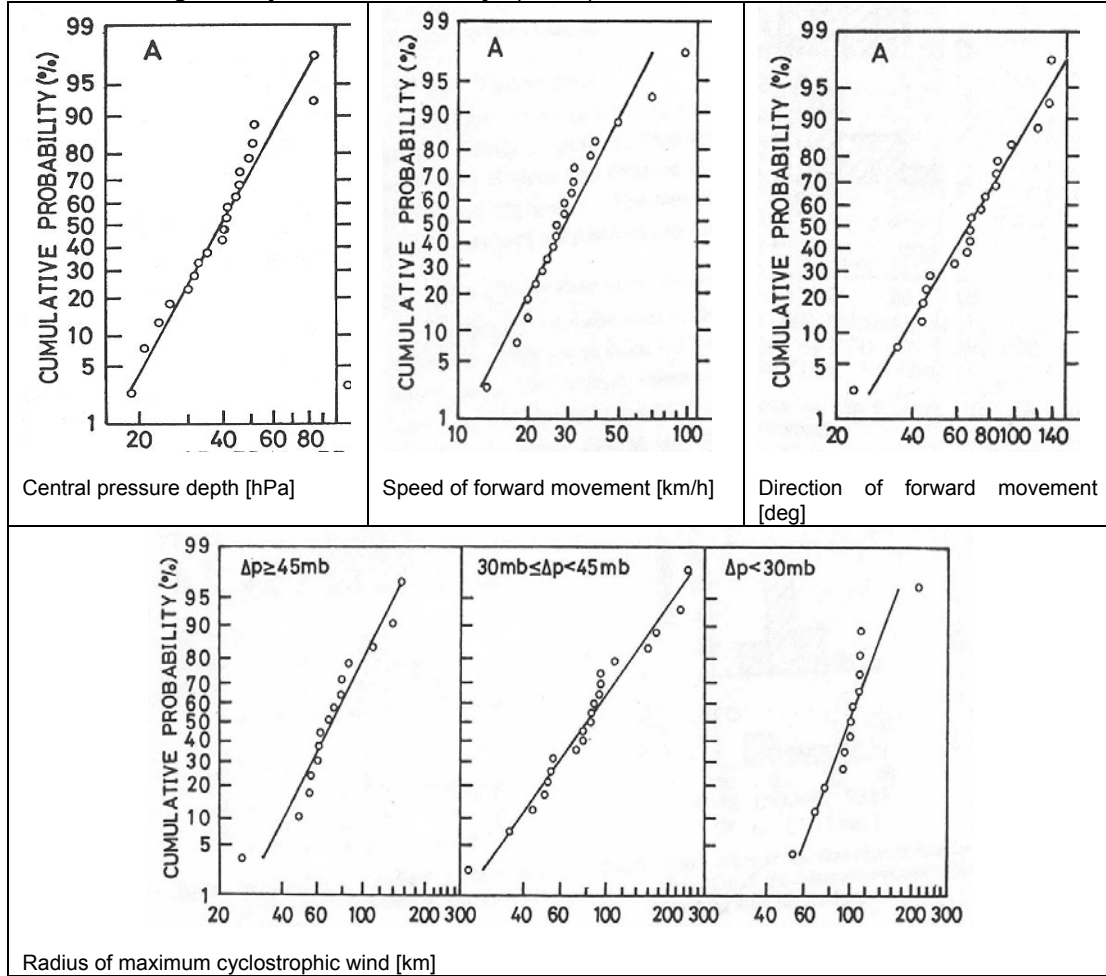
Lognormal distributions for different typhoon characteristics

Quantity	Dimension	Application	F(m-σ) Mean minus σ	F(m) Mean regr. line	F(m+σ) Mean plus σ
Δp	[hPa]	Area A	26 (1.42)	39 (1.59)	57 (1.76)
C_{fm}	[km/h]	Area A	19 (1.28)	30 (1.47)	46 (1.66)
θ	[deg]	Area A	43 (1.63)	67 (1.83)	105 (2.02)
R_m	[km]	0 < Δp < 30	74 (1.87)	100 (2.0)	136 (2.13)
		30< Δp < 45	45 (1.65)	81 (1.91)	146 (2.16)
		45< Δp	46 (1.67)	71 (1.85)	107 (2.03)

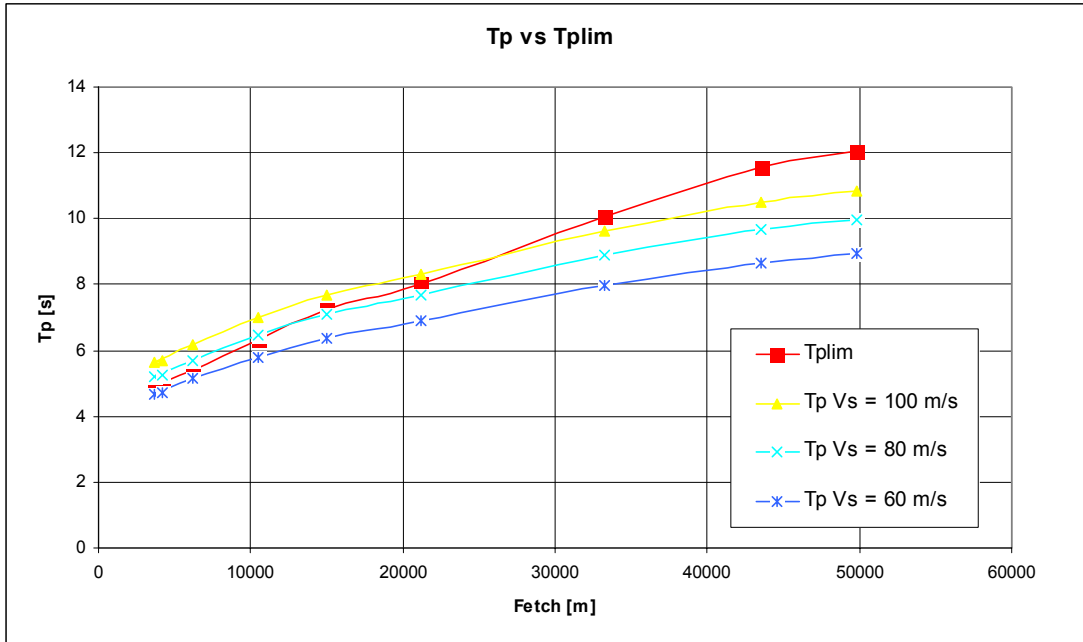# Appendix E   Limitation in wave height and wave period

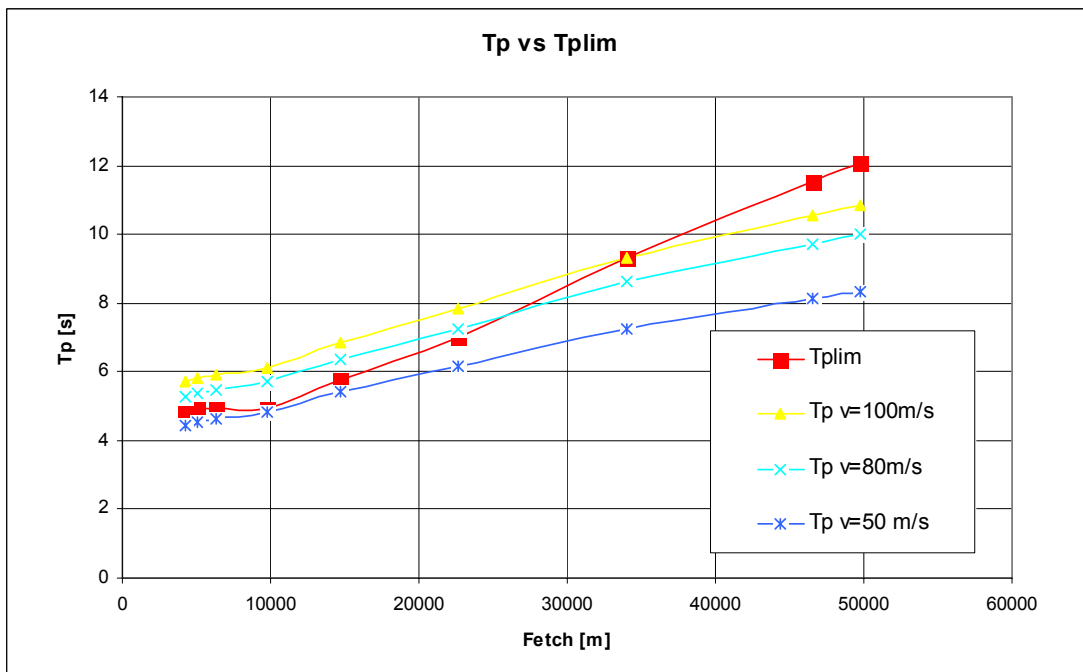Hs limit with Hs for fetches from east to west in southern direction
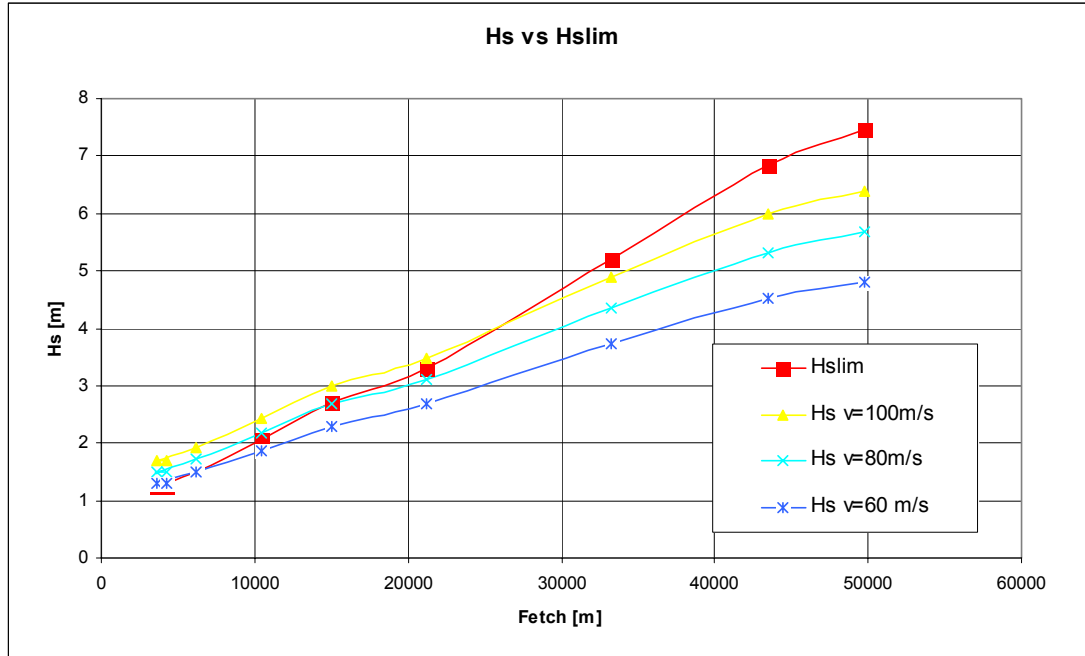
Hs limit with Hs for fetches from east to west in northern direction

Tp limit with Tp for fetches from east to west in southern direction

Tp limit with Tp for fetches from east to west in northern direction

The wave height and wave period are only limited in cases of abnormal high wind speeds. The limitation therefore does not affect the wave height and the wave period.

Appendix F　　　Duration or fetch limited model

Average of observed wave characteristics of four historical typhoons:

Typhoon	H_s [m]	T_p [s]
9117	1.87	5.9
9119	2.78	7.3
9210	2.01	5.9
9313	1.56	5.1
Average	2.06	6.05

Computation of wave group speed with average values of T_p and H_s

$$c_0 = \frac{g \cdot T}{2\pi} = \frac{9.81 m/s^s \cdot 6.05 s}{2\pi} = 9.4 m/s$$

$$L_0 = \frac{g \cdot T^2}{2\pi} = \frac{9.81 m/s^2 \cdot (6.05 s)^2}{2\pi} = 56 m$$

$$\frac{h}{L_0} = \frac{10m}{56m} = 0.18 \rightarrow \text{tanhkh=0.86} \rightarrow \text{n=0.69}$$

$$c_g = n \cdot c_0 = n \cdot c_0 \tanh kh = 0.69 \cdot 9.4 m/s \cdot 0.86 = 5.58 m/s \rightarrow 20 \text{km/h}$$

Always fetch limited if F_{max} already fetch limited instead of duration limited $F_{max} = 90 km$

Duration of wave before reaching shore: 4.5h. Typhoon induced intensified storms must a duration of at least:

$$C_{fm} = 30 km/h \cdot 4.5 \text{ hours} \rightarrow 135 km$$

The wind field around the centre is relatively smooth. The wind speed can be extimated correctly with the wind in one point and a duration long enough for fetch limited wave growth.

Spatial distribution of surface wind speed [m/s]
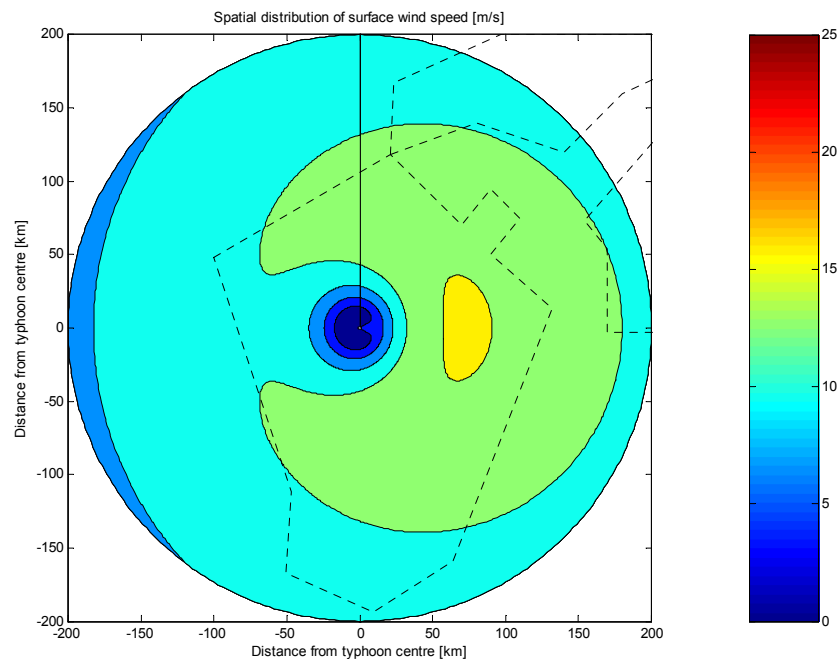
# Appendix G   Observed hydraulic variables

Storm surges

Date and time (JST)	JST	UTC	t rel. to time of landing	Storm surge	Date and time (JST)	JST	UTC	t rel. to time of landing	storm surge
yymmddhhmm	[h]	[h]	[h]	[m]	yymmddhhmm	[h]	[h]	[h]	[m]
Typhoon 7009					Typhoon 9117				
7008142200	22	13	0	0.47	9109140500	5	20	0.2	0.25
7008142300	23	14	1	0.56	9109140600	6	21	1.2	0.37
7008150000	0	15	2	0.68	9109140700	7	22	2.2	0.58
7008150100	1	16	3	0.81	9109140800	8	23	3.2	0.67
7008150200	2	17	4	0.98	9109140900	9	0	4.2	0.61
7008150300	3	18	5	1.11	9109141000	10	1	5.2	0.49
7008150400	4	19	6	1.09	9109141100	11	2	6.2	0.30
7008150500	5	20	7	0.91	9109141200	12	3	7.2	0.11
7008150600	6	21	8	0.57					
Typhoon 7617					Typhoon 9119				
7609130100	1	16	0	0.37	9109271600	16	7	0.2	1.14
7609130200	2	17	1	0.49	9109271700	17	8	1.2	1.42
7609130300	3	18	2	0.67	9109271800	18	9	2.2	1.45
7609130400	4	19	3	0.95	9109271900	19	10	3.2	1.19
7609130500	5	20	4	1.22	9109272000	20	11	4.2	0.86
7609130600	6	21	5	1.27	9109272100	21	12	5.2	0.57
7609130700	7	22	6	1.10	9109272200	22	13	6.2	0.35
7609130800	8	23	7	0.89	9109272300	23	14	7.2	0.19
7609130900	9	0	8	0.64					

Wave height and wave period

Typhoon number	Year Month Day	JST [hr]	UTC [hr]	Time after landing [hr]	H_s [m]	T_s [s]	T_p [s]
9117	19910914	6	21	1.2	1.70	5.0	5.6
		8	23	3.2	no data		
		10	1	5.2	1.87	5.3	5.9
		12	3	7.2	1.56	4.7	5.2
9119	19910927	16	7	0.2	2.78	6.6	7.3
		18	9	2.2	no data		
		20	11	4.2	no data		
		22	13	6.2	no data		
9210	19920808	8	23	1.4	no data		
		10	1	3.4	no data		
		12	3	5.4	1.88	5.9	6.6
		14	5	7.4	2.01	5.3	5.9
		16	7		no data		
9313	19930903	16	7	0.2	0.98	4.0	4.4
		18	9	2.2	1.16	3.9	4.3
		20	11	4.2	1.19	4.6	5.1
		22	13	6.2	1.20	5.0	5.6
		0	15	8.2	1.56	4.6	5.1
		2	17	10.2	0.83	3.7	4.1
		4	19		0.76	3.1	3.4
		6	21		0.71	3.2	3.6

Appendix H   Change in fetch and depth

Change in fetch length during historical typhoons due to changing wind directions
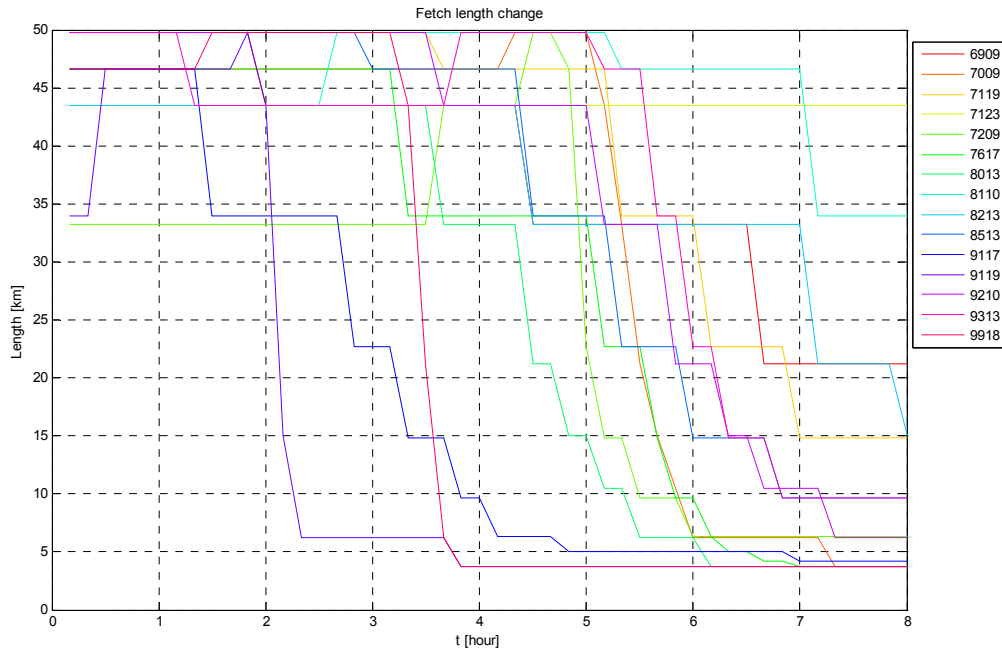
Change in water depth during historical typhoons due to changing wind directions
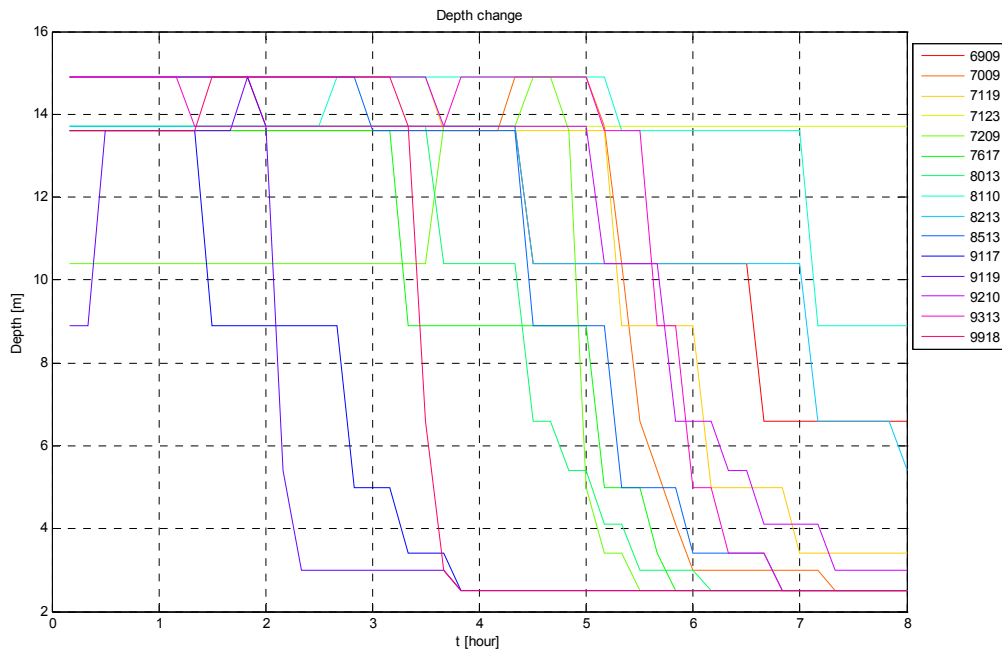
Appendix I   Number of years of simulation

The number of years of simulation to obtain stable results for low probabilities of exceedance is stated in the figures below:

10 years of simulations

100 years of simulations

1000 years of simulations
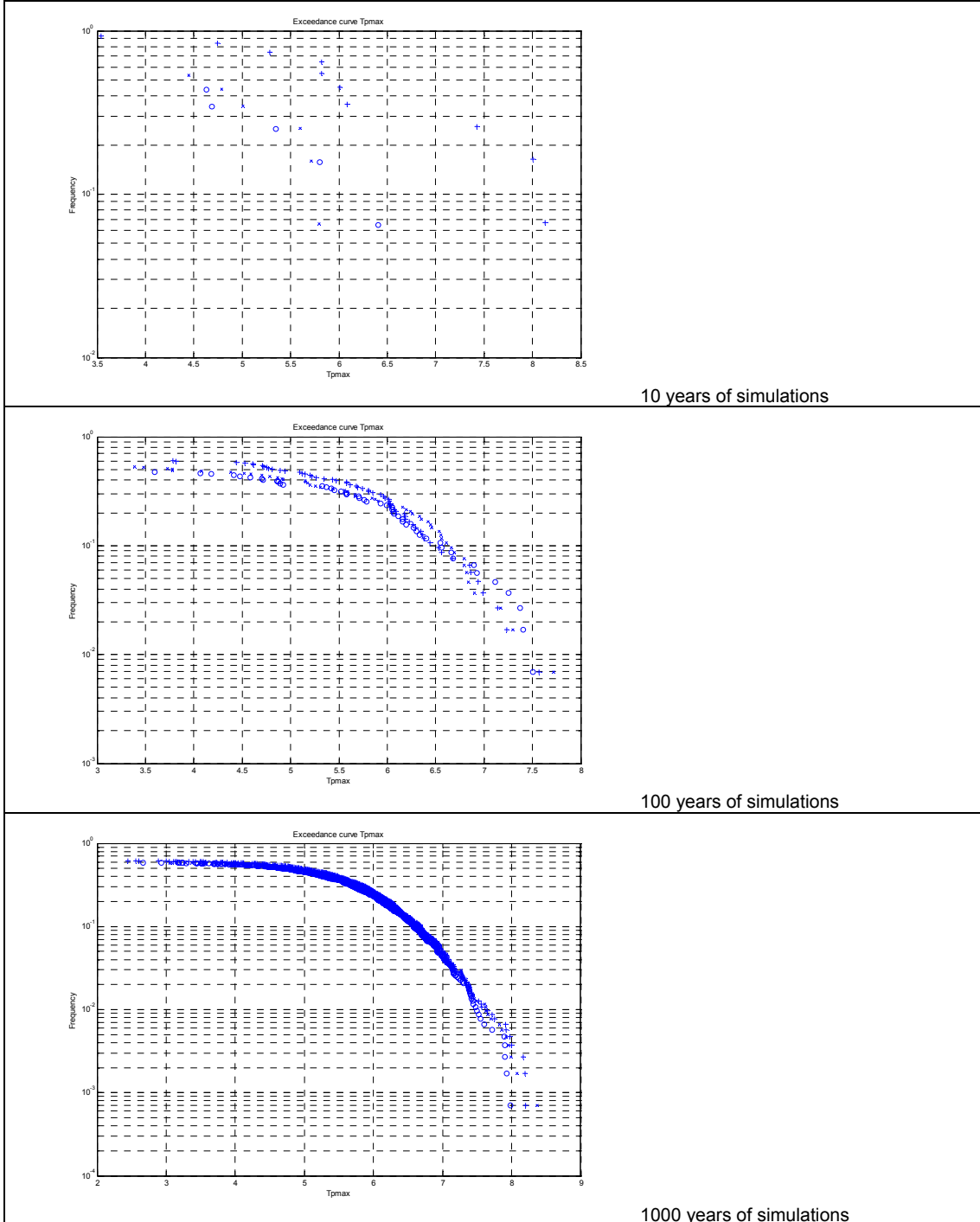
Appendix J   Typhoon tracks for 1000 simulations

Extreme values of hydraulic variables with accompanying typhoon tracks that have been determined with the input distributions of direction of forward movement and the uniform position of landing on the boundary in the direction of the typhoon.
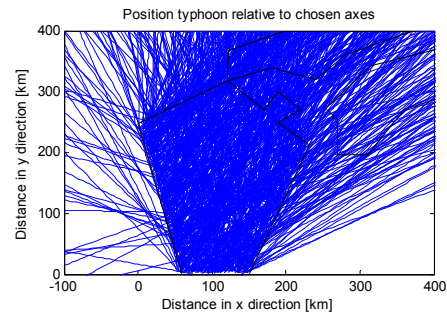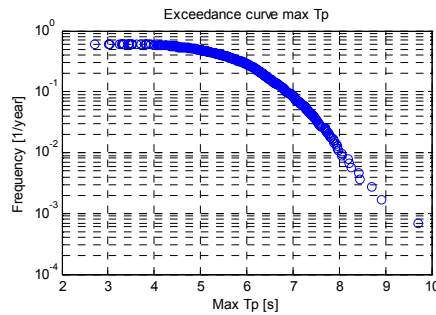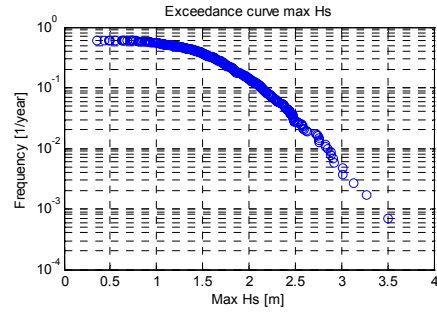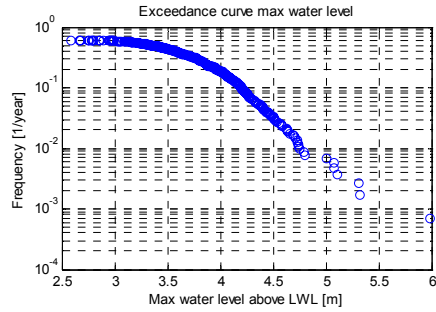
Appendix K   Relation pressure set-up and wind speed

The gradient wind speed is related to the central pressure depth:

$$V_{gr} :: c + \sqrt{c + c\Delta p}$$

$$V_{gr} - c :: \sqrt{c + c\Delta p}$$

$$(V_{gr} - c)^2 :: c + c\Delta p$$

$$V_{gr} - 2cV_{gr} + c^2 :: c + c\Delta p$$

$$V_{gr} - 2cV_{gr} + c^2 - c :: c\Delta p$$

$$\frac{V_{gr} - 2cV_{gr} + c^2 - c}{c} :: \Delta p$$

$$\Delta h_p = c_1 \cdot \Delta p \cdot (1 - e^{-r_m/r})$$

$$\Delta h_p :: aV_{gr}^2 + bV_{gr} + c$$

Since the gradient wind speed is related to the surface wind speed with a constant ratio, the following holds:

$$\Delta h_p :: aV_s^2 + bV_s + c$$

a, b and c are constants

Appendix L   Limitation in wave height

The limitation in wave height by the SMB formula is given below: